

Controls of vertical carbon stable isotope  
distribution in topsoil:  
temperature, precipitation and time

Dissertation

der Mathematisch-Naturwissenschaftlichen Fakultät  
der Eberhard Karls Universität Tübingen  
zur Erlangung des Grades eines  
Doktors der Naturwissenschaften  
(Dr. rer. nat.)

vorgelegt von  
Diplom-Geographin Melanie Brunn  
aus Bad Kreuznach

Tübingen  
2016

Gedruckt mit Genehmigung der Mathematisch-Naturwissenschaftlichen Fakultät der  
Eberhard Karls Universität Tübingen.

Tag der mündlichen Qualifikation:

17.02.2017

Dekan:

Prof. Dr. Wolfgang Rosenstiel

1. Berichterstatterin:

Prof. Dr. Yvonne Oelmann

2. Berichterstatterin:

Prof. Dr. Sandra Spielvogel

# Contents

Contents .....	I
Danksagung .....	IV
Summary.....	V
Zusammenfassung .....	VI
List of abbreviations .....	VII
List of tables .....	VIII
List of figures .....	IX
1 Summarizing overview .....	1
1.1 Introduction.....	1
1.2 Methods.....	6
1.2.1 Study sites .....	6
1.2.1.1 Rhineland-Palatinate, Germany.....	7
1.2.1.2 Black Forest, Germany .....	8
1.2.1.3 Haast, New Zealand.....	9
1.2.2 Sampling and sample preparation .....	10
1.2.3 Elemental and isotopic measurements .....	11
1.2.4 Calculations and statistical analysis.....	12
1.3 Results and discussion .....	13
1.3.1 Temperature and precipitation effects on $\delta^{13}\text{C}$ depth profiles in SOM under temperate beech forests (Chapter 2) .....	13
1.3.2 Three decades after afforestation are sufficient to yield decomposition-related vertical $\delta^{13}\text{C}$ depth profiles in soil (Chapter 3).....	14
1.3.3 Vertical distribution of carbon and nitrogen stable isotope ratios in topsoil across a temperate rainforest dune chronosequence in New Zealand (Chapter 4).....	15
1.3.4 Interaction of spatially independent data with vertical C stable isotope distribution .....	15
1.3.5 Error discussion .....	26
1.4 General conclusion.....	29
1.5 Author contribution.....	31
1.6 References .....	32
2 Temperature and precipitation effects on $\delta^{13}\text{C}$ depth profiles in SOM under temperate beech forests.....	37
2.1 Abstract .....	38
2.2 Introduction.....	39

---

2.3 Material and methods .....	41
2.3.1 Sampling sites .....	41
2.3.2 Sampling and sample preparation .....	43
2.3.3 Roots .....	44
2.3.4 Laboratory analysis .....	44
2.3.4.1 pH measurement .....	44
2.3.4.2 Elemental and isotopic measurements .....	44
2.3.5 Statistical analysis and calculation of beta values .....	45
2.4. Results .....	46
2.4.1 $\delta^{13}\text{C}$ depth profiles .....	46
2.4.2 Temperature and precipitation gradient .....	47
2.5 Discussion .....	50
2.5.1 Temperature impact on $\delta^{13}\text{C}$ depth profiles .....	51
2.5.2 Precipitation impact on $\delta^{13}\text{C}$ depth profiles .....	52
2.6 Conclusion .....	53
2.7 Acknowledgement.....	54
2.8 References .....	54
3 Three decades after afforestation are sufficient to yield decomposition-related vertical $\delta^{13}\text{C}$ depth profiles in soil .....	57
3.1 Abstract .....	58
3.2 Introduction .....	58
3.3 Material and methods .....	60
3.3.1 Sampling sites .....	60
3.3.2 Sampling and sample preparation .....	61
3.3.4 Laboratory analysis, statistics and calculations .....	61
3.3.4.1 pH measurement .....	61
3.3.4.2 Potential soil respiration .....	61
3.3.5 Elemental and isotopic measurements .....	62
3.3.6 Calculations and statistical analyses .....	63
3.4 Results .....	64
3.5 Discussion .....	67
3.6 Conclusion .....	70
3.7 Acknowledgement.....	71
3.8 References .....	71
3.9 Supplementary material .....	74
4 Vertical distribution of carbon and nitrogen stable isotope ratios in topsoil across a temperate rainforest dune chronosequence in New Zealand.....	75
4.1 Abstract .....	76
4.2 Introduction .....	76
4.3 Material and methods .....	80
4.3.1 Sampling site.....	80
4.3.2 Sampling and sample preparation .....	80

---

4.3.3 Laboratory analysis, calculations and statistics .....	81
4.3.3.1 Elemental and isotopic measurements.....	81
4.3.3.2 Calculations and statistical analysis.....	82
4.4 Results .....	83
4.4.1 Element concentrations, C: N ratios and isotopic signatures in litter, organic layer and mineral soil with proceeding pedogenesis .....	83
4.4.2 Vertical differences in $\delta^{13}\text{C}$ and $\delta^{15}\text{N}$ values and beta values with proceeding pedogenesis.....	87
4.5 Discussion .....	88
4.5.1 $\delta^{13}\text{C}$ and $\delta^{15}\text{N}$ values in litter with proceeding pedogenesis.....	88
4.5.2 Vertical patterns of $\delta^{13}\text{C}$ values with proceeding pedogenesis.....	91
4.5.3 Vertical patterns in $\delta^{15}\text{N}$ values with proceeding pedogenesis.....	93
4.6 Conclusion .....	95
4.7 Acknowledgment .....	96
4.8 Literature .....	96
4.9 Supplementary material .....	100

## Danksagung

Besonderer Dank gilt Frau Prof. Dr. Yvonne Oelmann, für die Ermöglichung dieser Arbeit, das Teilen ihres Wissens, ihre Geduld und ihr Vertrauen, für die Ermutigung zur Entwicklung eigener Ideen und die gegebene Freiheit, diese zu verwirklichen. Weiterer Dank gilt Frau Prof. Dr. Sandra Spielvogel für die Betreuung in Koblenz, die Realisierung interessanter Tagungsteilnahmen und die Begleitung dieser Arbeit. Ulli Bange und Sabine Flaiz möchte ich für ihren Einsatz im Labor danken. Ebenso auch allen anderen Mitarbeitern und wissenschaftlichen Hilfskräften für die produktive Zusammenarbeit und die Assistenz in Mainz, Koblenz, Tübingen, Hannover, in der Schweiz und in Neuseeland, ohne die diese Arbeit nicht möglich gewesen wäre. Hervorragend unterstützt bei den Probenahmen haben mich Karina Traub in den Rheinland-Pfälzischen Wäldern, sowie Prof. Dr. Leo Condrón und Dr. Andrew Wells, die die Begehung des Dünen-Sumpfgebietes in Neuseeland ermöglicht haben. Den Mitgliedern der Arbeitsgruppen in Koblenz und Tübingen danke ich für ihre Unterstützung bei Organisatorischem, ihrer Anteilnahme, ihrem offenen Ohr und die konstruktiven Gespräche. Besonders danke ich Marc Ruppenthal für den Wissensaustausch, Agnes Rehmus für die langjährige Freundschaft, Sophia Leimer für die Einladungen zu den informativen Kolloquien, Alevtina Evgrafova für die motivierenden Worte, Elisabeth Sorkau, Karla Dietrich, Jennifer Herschbach und Michaela Dippold unter anderem für die Gastlichkeit und Harald Neidhardt für die Bereitschaft und die schnelle Bearbeitung von Anliegen aller Art.

Diese Arbeit wäre nicht möglich gewesen ohne die Unterstützung meiner Eltern und meiner Familie, die immer an mich geglaubt haben. Meinem Mann gilt besonderer Dank für das entgegengebrachte Verständnis, die Reisebereitschaft und den fachlichen Austausch. Und auch meinen Kindern danke ich für die Möglichkeit, die Welt aus einer anderen Perspektive zu betrachten.

Dem Interdisziplinären Promotionszentrum und der Forschungsförderung des wissenschaftlichen Nachwuchses der Universität Koblenz-Landau danke ich für die Finanzierung wissenschaftlicher Hilfskräfte sowie nationaler und internationaler Tagungen. Diese Arbeit wurde finanziert durch ein Promotionsstipendium der Stipendienstiftung Rheinland-Pfalz und durch ein Stipendium des Deutschen Akademischen Austauschdienstes.

## Summary

A crucial ability to evaluate the effects of changes in land-use and global climate is the understanding of carbon (C) storage in soil. The decomposition of organic matter (OM) in soil presents a determining mechanism, due to the impact it has on whether soils function as a sink for C or fuel the atmosphere's carbon dioxide concentrations. The vertical distribution of C stable isotopes in topsoil serves as a powerful tool to investigate decomposition of OM in soil.

It is of particular interest how the decomposition of OM in soil relates to changing mean annual temperature (MAT) and mean annual precipitation (MAP). Therefore, I conducted a field study with comparable confounding variables and MAT or MAP, respectively as changing variable. Relations between the vertical decrease of C concentrations and the increase of  $\delta^{13}\text{C}$  values in soil profiles from litter to mineral soil at 10 cm depth served to approximate decomposition. In contrast to the general assumption of the Van't Hoff's kinetic theory, the results suggest a decline of decomposition with increasing MAT. Low soil moisture likely hampered microbial activity under elevated MAT. Approximated decomposition increased across the gradient of MAP. Selective sorption and the downward transport of hydrophilic,  $^{13}\text{C}$  enriched compounds with fluxes of soil solution might have dominated the development of  $\delta^{13}\text{C}$  depth profiles under high MAP.

The investigation of  $\delta^{13}\text{C}$  depth profiles during land-use change indicated that three decades following afforestation of former cropland are sufficient to develop  $\delta^{13}\text{C}$  depth profiles. On timescales of millennia, aged soils are supposed to sequester large amounts of C with an assumed decrease of decomposition. However,  $\delta^{13}\text{C}$  depth profiles suggested no constant decrease of OM decomposition during 2,870 years of ecosystem development and pedogenesis. Interestingly,  $\delta^{13}\text{C}$  depth profiles were related to the depth distribution of nitrogen stable isotopes, suggesting shared processes shaping  $\delta^{13}\text{C}$  and  $\delta^{15}\text{N}$  vertical depth profiles.

Carbon stable isotope distribution in topsoil significantly changed with MAT, MAP and over time. The findings of this work contribute to a better understanding of how decomposition responds to climate change and pedogenesis. In essence, the analysis of  $\delta^{13}\text{C}$  depth profiles in topsoil offers an alternative and reliable method to approximate decomposition of OM in soil.

## Zusammenfassung

Kohlenstoffspeicherung in Böden ist eine entscheidende Komponente zur Beurteilung der Folgen des globalen Klima- und Nutzungswandels. Umsatz von organischer Bodensubstanz (OBS) gilt dabei als wichtiger Mechanismus der Senken- oder Quellenfunktion von Böden für Kohlenstoff (C). Die vertikale Verteilung stabiler C Isotope ( $\delta^{13}\text{C}$ ) im Oberboden bietet ein Instrument zur Untersuchung des Umsatzes von OBS.

Es ist von besonderem Interesse, welchen Einfluss sich ändernde Jahresmitteltemperaturen (JMT) oder Jahresniederschlagssummen (JNS) auf Umsatz von OBS haben. Um dies zu untersuchen führte ich eine Feldstudie durch mit vergleichbaren Standortbedingungen, jedoch JMT beziehungsweise JNS als sich ändernde Variable. Zur Abschätzung des Umsatzes der OBS diente der Zusammenhang zwischen der vertikalen Abnahme von C Gehalten und der Zunahme von  $\delta^{13}\text{C}$  Werten in Profilen von der Streuauflage zum Mineralboden bei 10 cm Tiefe. Entgegen der generellen Annahme der kinetischen Theorie (Van 't Hoff) deuten die Ergebnisse auf eine Abnahme des Umsatzes mit zunehmender JMT hin. Niedrige Bodenfeuchte erschwerte wahrscheinlich die mikrobielle Aktivität unter höherer JMT. Der abgeschätzte Umsatz der OBS stieg entlang des Niederschlagsgradienten. Selektive Sorption und der abwärtsgerichtete Transport hydrophiler,  $^{13}\text{C}$  angereicherter Bestandteile mit der Bodenlösung könnten die Tiefenverteilung von  $\delta^{13}\text{C}$  unter hoher JNS dominiert haben.

Nach Aufforstung ehemaliger Ackerflächen zeigte sich, dass eine Zeit von drei Dekaden zur Entstehung von  $\delta^{13}\text{C}$  Tiefenprofilen ausreichen. Auf einer Zeitskala von Jahrtausenden wird angenommen, dass Böden große Mengen von Kohlenstoff speichern und eine Reduzierung des Umsatzes von OBS stattfindet. Die  $\delta^{13}\text{C}$  Tiefenverteilung deutet allerdings darauf hin, dass Umsatz der OBS mit der Zeit nicht kontinuierlich abnimmt. Interessanterweise zeigten sich Zusammenhänge zwischen  $\delta^{13}\text{C}$  Tiefenprofilen und der Tiefenverteilung von stabilen Stickstoffisotopen, was auf gemeinsame Prozesse zur Entwicklung von  $\delta^{13}\text{C}$  und  $\delta^{15}\text{N}$  Tiefenprofilen hindeutet.

Die Verteilung von  $\delta^{13}\text{C}$  Werten in Oberböden änderte sich signifikant mit JMT, JNS und der Zeit. Meine Ergebnisse können zu einem besseren Verständnis von Änderungen des Umsatzes der OBS während des Klimawandels und der Bodenbildung beitragen. Die Analyse von  $\delta^{13}\text{C}$  Tiefenprofilen scheint eine alternative und verlässliche Methode zur Abschätzung von Umsatz von OBS in Oberböden zu sein.



## List of abbreviations

AM	Arbuscular mycorrhiza
B.P.	Before present
beta/beta <sub>C</sub>	Absolute value of the linear regression slope between logarithmized C concentrations [ $\text{g}\cdot\text{C}\cdot\text{kg}^{-1}$ ] and $\delta^{13}\text{C}$ values. The term beta <sub>C</sub> was equally used. Both serve to approximate decomposition.
beta <sub>N</sub>	Absolute value of the linear regression slope between logarithmized N concentrations [ $10^{-1}\text{g}\cdot\text{N}\cdot\text{kg}^{-1}$ ] and $\delta^{15}\text{N}$ values.
<i>c.</i>	Around
C	Carbon
CO <sub>2</sub>	Carbon dioxide
DOC	Dissolved organic carbon
DOM	Dissolved organic matter
EM	Ectomycorrhiza
MAP	Mean annual precipitation [ $\text{mm yr}^{-1}$ ]
MAT	Mean annual temperature [ $^{\circ}\text{C}$ ]
N	Nitrogen
m.a.s.l.	Meters above sea level
OM	Organic matter
P	Phosphorus
RSD	Relative standard deviation
SD	Standard deviation
SE	Standard error
SOC	Soil organic carbon
SOM	Soil organic matter
<i> yrs</i>	Years

## List of tables

Table 1.1 Studies with location, mean annual temperature (MAT), mean annual precipitation (MAP), average beta value and the underlying sampling depth.....	18
Table 2.1 Selection criteria for all sampling sites across the temperature and precipitation gradient in Rhineland-Palatinate, Germany .....	42
Table 2.2 Sampling sites within the temperature and precipitation gradient with according MAT [°C] and MAP [mm·yr <sup>-1</sup> ]. MAP varied between 675 to 733 mm across the temperature gradient, while MAT varied between 7.94 to 9.07°C across the precipitation gradient.....	43
Table 2.3 Sampling sites with according site characteristics, mean root mass in g·roots·g <sup>-1</sup> finefraction, Oi horizon (litter) δ <sup>13</sup> C values and <sup>13</sup> C enrichment from top Oi horizon down to the mineral soil at 10 cm depth. Mean values with ±SE and <i>n</i> ..	47
Table 3.1 Mean ± SE values of parameters at sites of different land-use with letters representing significant differences between land-uses. <i>n</i> = 9, except litter δ <sup>13</sup> C values <i>n</i> = 6 owing to the missing organic layer at arable sites. ....	65
Table 3.2 Correlation coefficients between variables. Bold numbers represent significant relations with *, <i>P</i> ≤ 0.05; **, <i>P</i> ≤ 0.01; ***, <i>P</i> ≤ 0.001. <i>n</i> = 9, except litter δ <sup>13</sup> C values <i>n</i> = 6 owing to the missing organic layer on arable sites with 0 yrs of forest cover.....	67
Table 4.1 Sampling sites description with dune age [B.P.], dating method, depth of the organic horizons [cm] (= Oi, Oe and Oa horizons) with standard errors and letters across the Haast dune chronosequence, New Zealand.....	81
Table S4.1 Mean ± SE element concentrations and isotopic signatures in litter (Oi layer), organic layers (Oe and Oa layer) and in mineral soil of dune stages. Letters represent significant differences between dune stages. In case of homogeneous variances we used a post-hoc Tukey test. In case of heteroscedasticity, a Games-Howell test was conducted. <i>P</i> ≤ 0.05; <i>n</i> = 5.....	102
Table S4.2 Mean ± SE beta values and maximum isotopic difference as Δ <sup>13</sup> C or Δ <sup>15</sup> N in soil profiles of dune stages. Letters represent significant differences between dune stages. In case of homogeneous variances we used a post-hoc Tukey test. In case of heteroscedasticity, a Games-Howell test was conducted. <i>P</i> ≤ 0.05; <i>n</i> = 5.....	103

## List of figures

Figure 1.1 Conceptual figure showing general trends of decreasing C concentrations and increasing $\delta^{13}\text{C}$ values with soil depth (A & B). Beta values can be calculated from linear regression slopes by plotting $\delta^{13}\text{C}$ values against logarithmized C concentrations (C). Linear regression slopes were found to change with temperature, precipitation and time. Beta serves as approximation for decomposition of organic matter in topsoil.....	3
Figure 1.2 Map showing the distribution of sampling sites in the Black Forest, Germany. Agricultural sites were sampled at “Oberer Kurzbach”, “Stampfershof” and “Sumhof”, afforested sites at “Im Eulersbach”, “Eulersbacher Hof” and “Hunselhof” and continuously forested sites at “Sumhof”, “Im Eulersbach” and “Hunselhof” .....	9
Figure 1.3 Satellite image of the Haast dune chronosequence with sampled dune stages (0-10) that represent a soil age gradient from <i>c.</i> 120 – <i>c.</i> 2,870 yrs B.P. Included map of New Zealand shows the Haast chronosequence as study area (provided by Wells and Goff 2006).....	10
Figure 1.4 Division of the soil core (A) and soil core sectioned into 1-cm segments (B) to obtain stable isotope depth profiles in high resolution. Pictures took by A. Rehmus.....	11
Figure 1.5 Globally distributed study locations with mean beta values.....	17
Figure 1.6 Beta values in relation to mean annual temperature (MAT) of spatially independent data. * Data from Acton et al. 2013.....	20
Figure 1.7 Beta values in relation to mean annual temperature (MAT) separated into classes with different mean annual precipitation (MAP) with 1,000 mm yr <sup>-1</sup> (A) and 1,500 mm yr <sup>-1</sup> as class boundary. Insignificant relations were not depicted..	22
Figure 1.8 Beta values in relation to mean annual precipitation (MAP) of spatially independent data. * Data from Acton et al. 2013.....	23
Figure 1.9 Beta values in relation to MAP separated into MAT classes with 15°C MAT as class boundary. Insignificant linear relations were not depicted. ....	24
Figure 1.10 Beta values in relation to soil and ecosystem age with detailed figure showing soil and ecosystem or stand ages < 300 yrs. ....	25
Figure 2.1 Maps of the sampling sites with distribution of forest areas in Rhineland-Palatinate (A), the temperature gradient (B) and the precipitation gradient (C)...	41
Figure 2.2 Changes of the soil organic carbon content (SOC) [%] and the $\delta^{13}\text{C}$ values [ $\%_{\text{VPDB}}$ ] with depth of all sites. ....	46
Figure 2.3 Regressions between C content ( $\log_{10}(\text{g}\cdot\text{C}\cdot\text{kg}^{-1})$ ) and the corresponding $\delta^{13}\text{C}$ values [ $\%_{\text{VPDB}}$ ] for all sampling sites with 5 replicates each (A, B, C, D, E) and according linear regression line. * $P < 0.05$ ; ** $P < 0.01$ ; *** $P < 0.001$ . ....	48

- Figure 2.4 Beta values ( $|\delta^{13}\text{C}/\log_{10}(\text{g}\cdot\text{C}\cdot\text{kg}^{-1})|$ ) across the temperature gradient ( $^{\circ}\text{C}$  MAT) and the precipitation gradient ( $\text{mm}\cdot\text{yr}^{-1}$  MAP) with linear regression lines. \*\*\*  $P < 0.001$ . ..... 49
- Figure 2.5 C: N ratios of the Oi layer (upper circles) and the mineral soil (circles below) across the temperature gradient ( $^{\circ}\text{C}$  MAT) and the precipitation gradient ( $\text{mm}\cdot\text{yr}^{-1}$  MAP) with linear regression lines. \*\*\*  $P < 0.001$ . ..... 49
- Figure 3.1 Mean  $\pm$  SE changes of logarithmized C concentrations [ $\log_{10}(\text{g}\cdot\text{C}\cdot\text{kg}^{-1})$ ] with depth (a), of OM  $\delta^{13}\text{C}$  values [ $\text{‰}_{\text{VPDB}}$ ] with depth (b) and  $\log_{10}(\text{g}\cdot\text{C}\cdot\text{kg}^{-1})$  plotted against  $\delta^{13}\text{C}$  values (c) for sites under different land-use: arable sites (yellow), afforested sites (blue) and continuously forested sites (green).  $n = 3$  for each data point. Error bars represent two standard errors. .... 66
- Figure 3.2 Conceptual figure showing parameters that appeared to affect  $\delta^{13}\text{C}$  depth profiles for sites exposed to different land-use (arable sites, afforested sites, and continuously forested sites) in this study. Potential soil respiration,  $^{13}\text{C}$  enrichment, soil organic carbon (SOC) concentration and pH were determined in this study. Other parameters are based on literature data. .... 68
- Figure S3.1 Linear regressions between carbon concentrations [ $\log_{10}(\text{g}\cdot\text{C}\cdot\text{kg}^{-1})$ ] and corresponding  $\delta^{13}\text{C}$  values [ $\text{‰}_{\text{VPDB}}$ ] with linear regression lines and regression equation of arable sites, afforested sites and continuously forested sites. Plots in one line represent fourfold pseudoreplicates at one location. \*,  $P < 0.05$ ; \*\*,  $P < 0.01$ ; \*\*\*,  $P < 0.001$ . .... 74
- Figure 4.1 Mean  $\pm$  SE C (a) and N concentrations [ $\text{g}\cdot\text{kg}^{-1}$ ] (d) and  $\delta^{13}\text{C}$  [ $\text{‰}_{\text{VPDB}}$ ] and (b)  $\delta^{15}\text{N}$  values [ $\text{‰}_{\text{Air}}$ ] (e) with depth [cm] across all dune stages ( $n = 11$ , except the organic layer:  $n = 4$ ) showing a vertical decrease in C and N concentrations and an increase in  $\delta^{13}\text{C}$  and  $\delta^{15}\text{N}$  values. Figures on the right represent relations between  $\log_{10}(\text{g}\cdot\text{C}\cdot\text{kg}^{-1})$  and  $\delta^{13}\text{C}$  values (c) or  $\log_{10}(10^{-1}\cdot\text{g}\cdot\text{N}\cdot\text{kg}^{-1})$  and  $\delta^{15}\text{N}$  values (f) of which beta values can be derived. Litter layer (Oi layer) values depicted as triangles ( $n = 11$ ), organic layers (Oe and Oa layer) as squares ( $n = 4$ ). Organic layers occur from stage 7 on (soil age  $> 1,300$  yrs) and are not present in the stages before. Depths of litter and organic layers as mean  $\pm$  SE in cm. Error bars represent two standard errors. .... 84
- Figure 4.2 Mean  $\pm$  SE C (a) and N concentrations [ $\text{g}\cdot\text{kg}^{-1}$ ] (b) and C: N ratios (c) in litter (Oi horizon), organic layers (Oe and Oa horizons) and mineral soil as functions of site age in years before present [yrs B.P.]. Dotted lines depict significant linear trends across the overall chronosequence, while arrows depict linear trends during the early (stages 0-2), the intermediate (stages 3-6) or the late (stages 7-10) phase of ecosystem development. Numbers at the x axis represent the dune stages referring to Tab. 4.1. Error bars are two standard errors and represent variation on one dune with  $n = 5$ . .... 85
- Figure 4.3 Mean  $\pm$  SE  $\delta^{13}\text{C}$  [ $\text{‰}_{\text{VPDB}}$ ] (a) and  $\delta^{15}\text{N}$  [ $\text{‰}_{\text{Air}}$ ] values (b) in the litter layer (Oi horizon), the organic layers (Oe and Oa horizons) and in the mineral soil. Maximum isotopic difference from litter to mineral soil in  $^{13}\text{C}$  (c) and  $^{15}\text{N}$  (d) is given as  $\Delta^{13}\text{C}$  and  $\Delta^{15}\text{N}$ .  $\text{Beta}_{\text{C}}$  (c) and  $\text{beta}_{\text{N}}$  (d) values represent absolute values

of regression slopes between  $\log_{10}x$  element concentrations and isotopic signatures. All values as functions of site age in years before present [yrs B.P.]. Dotted lines depict significant linear trends across the overall chronosequence, while arrows depict linear trends during the early (stages 0-2), the intermediate (stages 3-6) or the late (stages 7-10) phase of ecosystem development. Numbers at the  $x$ -axis represent the dune stages referred to Tab. 4.1. Error bars are two standard errors and represent variation on one dune with  $n = 5$ . ..... 86

Figure S4.1 Linear regressions between logarithmized carbon concentrations  $\log_{10}$  ( $\text{g}\cdot\text{C}\cdot\text{kg}^{-1}$ ) and corresponding  $\delta^{13}\text{C}$  values [ $\text{‰}_{\text{VPDB}}$ ] for dune stages (0-10) with five replicates each (A-E) and linear regression lines including regression equation. No regression lines at sites with insignificant linear regressions. \*,  $P < 0.05$ ; \*\*,  $P < 0.01$ ; \*\*\*,  $P < 0.001$ . ..... 100

Figure S4.2 Linear regressions between logarithmized nitrogen concentrations  $\log_{10}$  ( $10^{-1}\cdot\text{g}\cdot\text{N}\cdot\text{kg}^{-1}$ ) and corresponding  $\delta^{15}\text{N}$  values [ $\text{‰}_{\text{Air}}$ ] for dune stages (0-10) with five replicates each (A-E) and linear regression lines including regression equation. No regression lines at sites with insignificant linear regressions. \*,  $P < 0.05$ ; \*\*,  $P < 0.01$ ; \*\*\*,  $P < 0.001$ . ..... 101

# 1 Summarizing overview

## 1.1 Introduction

The decomposition of organic matter (OM) in soil is crucial to sustain fertility of soils and to discuss mitigation strategies of the climate change (Lehmann and Kleber, 2015; Schmidt et al., 2011). Soils are able to store vast amounts of carbon (C) with particular importance of world forests soils (Dixon et al., 1994; Lal et al., 2007; Post and Kwon, 2000; Schlesinger, 1990; Wiesmeier et al., 2014). This soil C can be released to the atmosphere as CO<sub>2</sub> or stored, with decomposition as important mechanism to control the soil's source and sink function. Therefore, understanding C sequestration in soil to mitigate rising atmospheric CO<sub>2</sub> concentrations depends in part on our ability to investigate decomposition of OM.

Projections of the global climate predict a significant increase of temperature and greater variability of precipitation (Intergovernmental Panel on Climate Change, 2013). It has often been questioned how the predicted global warming will affect the decomposition of OM in soil (Amundson, 2001; Conant et al., 2011; Davidson and Janssens, 2006; Kirschbaum, 2000). According to the kinetic theory describing chemical reactions, reaction rates increase with increasing temperature (van't Hoff, 1898) which should accelerate the decomposition of OM in soil under increased temperatures. This relation has widely been observed across varieties of ecosystems (Davidson and Janssens, 2006; Kirschbaum, 2000). However, constraints remain for decreased microbial substrate accessibility, e.g. under hampered solute transport (Giardina and Ryan, 2000). At low soil moisture levels, decomposition of OM is therefore supposed to decline (Moyano et al., 2013; Townsend et al., 1995; Trumbore, 2009). In contrast, saturated conditions in soil under elevated soil moisture similarly inhibit microbial respiration and hamper decomposition (Moyano et al., 2013). Generally, adequate amounts of precipitation provide supply of sufficient pore water and fluxes of soil solution that maintain microbial activity and decomposition (Guggenberger and Kaiser, 2003; Kaiser and Kalbitz, 2012) leading to an increase of decomposition of OM under elevated temperature (Kirschbaum, 2000; Trumbore, 2009). Incubation studies or soil warming experiments allow for testing the response of soil to increased temperature. In contrast, not actively manipulated soil research at field sites with comparable environmental and soil conditions (temperature, precipitation, soil texture, mineralogy, vegetation etc.) consider

soil under steady state and may provide differing results compared to manipulated studies (Agren and Bosatta, 2002; Conant et al., 2011). Since manipulated experiments are supposed to address easily accessible C that can get rapidly lost (Agren and Bosatta, 2002), not actively manipulated studies probably include other processes linked to C accessibility in soil, such as transport and sorption.

Huge amounts of C are stored in topsoil (Scharlemann et al., 2014) and particularly the accumulation of thick organic layers with time is discussed to contribute to long-term C sequestration (Clemmensen et al., 2013; Clemmensen et al., 2015). Therefore, ecosystem dynamics experience growing attention in discussions of C sequestration (Schmidt et al., 2011). Long-term chronosequences serve as ideal sites to investigate C dynamics. Ecosystem and soil development across chronosequences can be defined in a progressive phase after initial disturbance, in a phase of maximal biomass in which the ecosystem stabilizes and in a retrogressive phase, where the ecosystem undergoes declines in productivity and nutrient cycling; trends that have been observed along chronosequences around the world (Peltzer et al., 2010; Wardle et al., 2004). Decomposition of OM in soil increases in progressive phases due to the accumulation of organic materials while at the later phases of long-term soil development, decomposition is supposed to decrease (Peltzer et al., 2010; Wardle et al., 2004). In particular, mycorrhizal fungi are considered to hamper decomposition at old sites and therefore, to contribute to C sequestration of soil (Clemmensen et al., 2015).

During the decomposition process, complex compounds are biochemically transformed. Greater transfer of the light isotope  $^{12}\text{C}$  and discrimination of the heavy isotope  $^{13}\text{C}$  during microbial metabolism result in enrichment of the remaining C pool (Lerch et al., 2011; Werth and Kuzyakov, 2010). The relation of  $^{13}\text{C}/^{12}\text{C}$  stable carbon isotopes in OM can therefore serve as indirect indicator of biogeochemical processes such as C decomposition. In soil profiles from litter to mineral soil, a vertical decrease of C associated with an enrichment of the heavier isotope  $^{13}\text{C}$  can be measured across varieties of ecosystems and environmental gradients (Acton et al., 2013; Boström et al., 2007; Ehleringer et al., 2000). The accumulation of  $^{13}\text{C}$  enriched compounds from microbial products or microbial cells itself (Diochon and Kellman, 2008; Lerch et al., 2011) are assumed to play a major role in this vertical increase of  $\delta^{13}\text{C}$  values. Therefore, the relation between vertical enrichment in  $^{13}\text{C}$  and C processing has been ascertained to approximate decomposition of OM in soil (Acton et al., 2013; Balesdent and Mariotti, 1996; Boström et al., 2007; Garten, 2006; Guillaume et al., 2015; Marty et al., 2015).

By plotting logarithmized ( $\log_{10}x$ ) element concentration in OM against its isotopic ratio, the slopes of the linear regression (indicated as beta values) can serve as proxy for decomposition (Fig. 1.1).

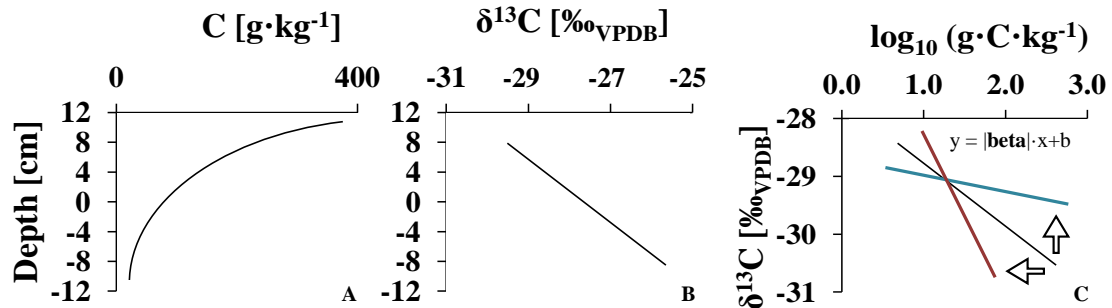


Figure 1.1 Conceptual figure showing general trends of decreasing C concentrations and increasing  $\delta^{13}\text{C}$  values with soil depth (A & B). Beta values can be calculated from linear regression slopes by plotting  $\delta^{13}\text{C}$  values against logarithmized C concentrations (C). Linear regression slopes were found to change with temperature, precipitation and time. Beta serves as approximation for decomposition of organic matter in topsoil.

In addition to microbial fractionation, other parameters are discussed to control the vertical C isotope distribution: i) the Suess effect, ii) root OM additions, iii) physico-chemical sorption of C and downward cycling of dissolved OM with soil solution. First, impacts of a continuous decrease of atmospheric  $\delta^{13}\text{C}\text{CO}_2$  by 1.5‰ during the last two centuries (Francey et al., 1999; Keeling et al., 2005) - known as the Suess effect - might contribute to the observed average vertical  $\delta^{13}\text{C}$  distribution. However, studies of  $\delta^{13}\text{C}$  depth profiles in archived and modern soils (Torn et al., 2002) or bare-fallow soil studies excluding vegetation inputs and therefore impacts of atmospheric changes (Balesdent and Mariotti, 1996) gave evidence that additional processes must contribute to the shifts of  $\delta^{13}\text{C}$  throughout the soil profile. Second, since roots are enriched in  $^{13}\text{C}$  by 1–2‰ compared to  $\delta^{13}\text{C}$  values of aboveground plant material (Badeck et al., 2005; Werth and Kuzyakov, 2010), their considerable presence in topsoil might explain another part of the difference in  $\delta^{13}\text{C}$  of OM with soil depth. Third, the vertical distribution of C stable isotopes is additionally attributed to the selective physico-chemical sorption characteristic of soils and therefore to soil texture (Kaiser et al., 2001; Kaiser and Kalbitz, 2012; Nakanishi et al., 2012). The idea behind this is that hydrophilic,  $^{13}\text{C}$  enriched decomposition products cycle down the soil profile with fluxes of dissolved organic carbon, while hydrophobic,  $^{13}\text{C}$  depleted compounds were sorbed (Nakanishi et



al., 2012). Thus, soils with finer texture develop greater isotopic differences between litter and mineral soil (Bird et al., 2003; Wynn et al., 2005).

Although temperature and precipitation effects on  $\delta^{13}\text{C}$  depth profiles were reported in several studies (Garten, 2006; Garten et al., 2000), such effects might be caused by factors that coincided with temperature/precipitation gradients which probably affected shifts of  $^{13}\text{C}$  distribution throughout the soil profile, e.g. soil texture, tree species, litter quantity and quality or site exposition. A field study was necessary along temperature and precipitation gradients with negligible variation in soil, vegetation and site characteristics but the examined parameter as changing variable, i.e. temperature during the determination of precipitation impacts and vice versa. In former studies on  $\delta^{13}\text{C}$  depth profiles, these factors were not considered systematically and therefore, environmental conditions excluding temperature and precipitation need to be comparable among sites.

During vegetation changes of ecosystems like the conversion from arable sites to forests, microbial processing and the impact of the Suess effect can profoundly change and therefore affect  $\delta^{13}\text{C}$  depth profiles. This might be attributed to shifted conditions for microbial activity and to time effects. For example, increased above- and below-ground biomass production and potential acidification induced by afforestation of arable sites can shift microbial community structures by promoting fungal abundance (Laganière et al., 2010; Pietri and Brookes, 2009), increase soil respiration (Hall and Silver, 2013) and increase dissolved organic matter production (Hansson et al., 2010) that are supposed to promote the development  $\delta^{13}\text{C}$  depth profiles (Kaiser and Kalbitz, 2012). While at arable sites, the removal of OM and disturbance through plowing may impede the development of  $\delta^{13}\text{C}$  depth profiles through hampered physical protection and aggregation of OM (Del Galdo et al., 2003; Six et al., 2002), afforested sites should experience a distinct vertical distribution of C stable isotopes. More pronounced  $\delta^{13}\text{C}$  depth profiles under afforested sites might be attributed to accumulated  $^{13}\text{C}$  enriched products originating from decomposition of OM, to greater OM inputs, to the Suess effect and to undisturbed transport and sorption processes within the soil column. At continuously forested sites, these parameters should be amplified and facilitate a greater isotopic difference in topsoil and therefore more distinct  $\delta^{13}\text{C}$  depth profiles. The land-use change from arable sites to afforestation can perfectly serve to test for the time required to develop decomposition-related  $\delta^{13}\text{C}$  depth profiles.

Under prolonged times of soil and ecosystem development, the retrogressive model suggests declines in ecosystem productivity, decomposition and nutrient cycling

(Peltzer et al., 2010; Wardle et al., 2004). Given a potential decline of microbial cycled products, the enrichment of  $^{13}\text{C}$  should decrease with proceeding time. In addition, shifts of nitrogen (N) stocks and cycling may influence the isotopic signatures of soils and plants (Martinelli et al. 1999). These shifts comprise N limited conditions during primary succession (Vitousek, 2004; Vitousek and Howarth, 1991) which may progress to phosphorus (P) limitation in extremely old and/or highly weathered soils (Vitousek and Farrington, 1997; Walker and Syers, 1976). According to positive relations between foliar N concentrations and  $\delta^{13}\text{C}$  values (Guehl et al., 1995; Körner and Diemer, 1987; Vitousek et al., 1990),  $\delta^{13}\text{C}$  values of litter should increase with increasing N and therefore with time across chronosequences. However, litter  $\delta^{13}\text{C}$  values in boreal forest chronosequences in Sweden increased with proceeding time (Hyodo et al., 2013; Hyodo and Wardle, 2009). Foliar morphological adaption to lower nutrient availability at late stages of pedogenesis, i.e. increased internal resistance of  $\text{CO}_2$  diffusion through the development of thicker and smaller leaves was supposed. This adaption is comparable to water stress effects on plants that equally reduces the stomatal conductance and results in higher  $\delta^{13}\text{C}$  values due to closed stomata (Farquhar et al., 1989). In addition to the widely observed vertical enrichment of  $^{13}\text{C}$  in soil profiles, a similar enrichment of  $^{15}\text{N}$  can develop in topsoil (Craine et al., 2015; Hobbie and Ouimette, 2009; Wallander et al., 2009). Likewise,  $\beta_{\text{N}}$  values can be calculated by means of linear regressions between logarithmized N concentrations and according  $\delta^{15}\text{N}$  values. Similar relations were compiled by Hobbie and Ouimette (2009) and the authors emphasized the importance of mycorrhizal fungi in controlling vertical  $\delta^{15}\text{N}$  depth trends. Fractionation against  $^{15}\text{N}$  during N transfer by mycorrhizal fungi to host plants is suggested, resulting in  $^{15}\text{N}$  depleted litter and  $^{15}\text{N}$  enriched OM in mineral soil (Hobbie and Ouimette, 2009). The vertical enrichment in  $^{15}\text{N}$  between litter and mineral soil was found to vary strongly, with ectomycorrhizal (EM) systems *c.* doubling the enrichment in  $^{15}\text{N}$  compared to systems dominated by arbuscular mycorrhiza (AM) (Hobbie and Ouimette, 2009). Mycorrhizal associations inconstantly shifted with time across chronosequences (Dickie et al., 2013) with strong host specificity (Martinez-Garcia et al., 2015). Due to shifts in mycorrhizal communities,  $\delta^{15}\text{N}$  values of litter and mineral soil OM could change with time and therefore affect  $\beta_{\text{N}}$  values, while beta values, as a measure of decomposition, could decrease in relation to the retrogressive model.

Former studies were lacking information on temperature or precipitation effects on  $\delta^{13}\text{C}$  depth profiles with MAT or MAP, respectively as sole changing variable under

field site conditions. In addition, the required time to develop distinct decomposition-related  $\delta^{13}\text{C}$  depth profiles needs to be clarified and the proceeding development during long-term pedogenesis. According to above mentioned possible impacts of temperature, precipitation and time on vertical C stable isotope distribution, I addressed the following research questions in this thesis:

- 1) How do temperature and precipitation affect vertical C stable isotope distribution under field site conditions and comparable environmental parameters (Chapter 2)?
- 2) Can distinct  $\delta^{13}\text{C}$  depth profiles be found a few decades following afforestation of former cropland (Chapter 3)?
- 3) How do  $\delta^{13}\text{C}$  and  $\delta^{15}\text{N}$  depth profiles develop during long-term ecosystem and soil formation (Chapter 4)?

First, I hypothesized that higher temperatures increase microbial activity and decomposition of OM in soil and thus, beta values. In addition, I hypothesized that increasing precipitation positively affects decomposition due to conditions favorable for microbial activity which enhances the downward transport of microbial cycled DOM and therefore, increases beta values. Second, I hypothesized that  $\delta^{13}\text{C}$  depth profiles do not develop under arable land but vertical changes emerge within decades under afforested cropland and become further amplified at continuously forested sites. Third, conforming to the retrogressive model which suggests declines in ecosystem productivity, decomposition and nutrient cycling (Peltzer et al., 2010), I hypothesized that beta values, as a measure of decomposition, decrease with proceeding time during long-term soil and ecosystem development. According to a possible shift in mycorrhizal communities with time, i.e. AM to EM due to host specificity inferred from shifts in tree species (Turner et al., 2012b), I additionally hypothesized that differences between  $\delta^{15}\text{N}$  values of litter and mineral soil OM increase with time, resulting in increasing  $\text{beta}_\text{N}$  values.

## 1.2 Methods

### 1.2.1 Study sites

To address my research questions, I chose three different study sites; (1) sites across a temperature and precipitation gradient in northern Rhineland-Palatinate, Germany, (2)

sites under different times of forest cover in the Black Forest, Germany and (3) sites across a long-term soil chronosequence at Haast, New Zealand. Due to regular intensive survey of environmental parameters and careful analysis of extensive geospatial data, exclusion of confounding variables affecting gradients of MAT or MAP can be assumed in forests of northern Rhineland-Palatinate. The widely distributed land-use change of afforestation of former cropland is exactly dated in the Black Forest (Germany). Therefore, the short-term establishment of vertical  $\delta^{13}\text{C}$  distribution can well be investigated here. Beside short-term soil and ecosystem development, also long-term changes can be determined across chronosequences, turning them into “natural experiments” investigating pedogenetic impacts on the vertical distribution of C stable isotopes (Laliberté et al., 2013; Lambers et al., 2008; Vitousek and Farrington, 1997; Walker and Syers, 1976). Intensive silvicultural use, strong human disturbance and high atmospheric N depositions found in Europe are neglectable in New Zealand. The humid temperate climate at New Zealand’s West coast in addition to its unique rainforest vegetation are supposed to provide new insights into C dynamics and the Haast chronosequence might complement information on long-term development of vertical C stable isotope distribution.

#### 1.2.1.1 Rhineland-Palatinate, Germany

With the objectives to ascertain climate effects on patterns of vertical  $\delta^{13}\text{C}$  values of soil organic matter (SOM) while minimizing the effect of confounding variables, I chose ten sites of mature beech (*Fagus sylvatica* L.) forest ecosystems under silvicultural use in Rhineland-Palatinate, Germany (Chapter 2; Fig. 2.1) (between 49°54’N and 50°46’N, 6°52’E and 7°57’E). Sites were located across gradients of MAT (7.9 to 9.7 °C mean annual temperature) and MAP (607 to 1085 mm mean annual precipitation) (German Weather Service). Due to my preselection, environmental characteristics other than climate and altitude (i.e., soil type = Cambisol, soil texture = clayloam, tree species = beech, stand age = 40-70 yrs and exposition = north) did not differ among sampling sites. ArcGIS Desktop (10) was used to select sampling sites out of extensive geodata sets provided by the Rhineland-Palatinate Forest Administration, the Rhineland-Palatinate Geological Survey and Mining Authority, the Rhineland-Palatinate Centre of Excellence for Climate Change Impacts and the German Weather Service.

Temperature and precipitation data were based on interpolated climate data (reference period 1971-2000) with a spatial resolution of 1x1 km (German Weather Service). Climate characteristics were selected in an orthogonal way that allowed for a separation

between temperature and precipitation effects i.e., differences in temperature under constant precipitation and vice versa. Across the temperature gradient, precipitation varied between 675 and 733 mm MAP, while MAT varied between 7.9 and 9.1°C MAT across the precipitation gradient.

The temperature gradient covaried with an altitudinal gradient with significant relation between both parameters ( $r = -0.92$ ;  $P < 0.001$ ). Altitude and temperature were not analyzed separately, so that a potential altitudinal effect forms part of the temperature gradient. The maximum difference in altitude in the study was 300 m and thus, small in comparison with literature on altitudinal effects on carbon isotope fractionation (Körner et al., 1991). Organic layer and mineral soil samples of 10 cm depth were collected in November and December 2011, shortly after the autumnal abscission of the leaves. At each site, five pseudoreplicated samples were taken.

#### 1.2.1.2 Black Forest, Germany

To address the question whether  $\delta^{13}\text{C}$  have developed already a few decades following afforestation of cropland, sites associated with different land-use forms and different times of forest cover (arable sites: 0 yrs, afforested sites: < 50 yrs and continuously forested sites: > 150 yrs) were chosen in the Black Forest, Germany (48°16'N, 8°15'E) (Fig. 1.2). This area in Southwestern Germany is prominent for afforestation of former cropland that became unprofitable and thus, land-use change has established as a widely distributed practice within the last century. Arable sites were regularly plowed until a depth of 20 cm and grown with potato, rye and oat in crop rotation, while dominating species at afforested sites was *Picea abies* (L.) Karst. (Norway spruce), cultivated c. 31 to 48 yr ago and followed crop rotation (potato, rye and oat). Continuously forested sites were grown with *Picea abies* (L.) Karst. and *Abies alba* Mill. (Silver fir) which have persisted for  $\geq 150$  yrs. Silvicultural practice at the afforested and the continuously forested sites was selection cutting according to the local "Plenterwald" system. All sites were continuously grown with C<sub>3</sub>-vegetation and not exceeding a distance of 20 km. Cambisols with gneiss and granite as bedrock were sampled within an altitudinal range between 385 and 680 meters above sea level. Mean annual temperature (1961-1990) at Wolfach was 9.4 °C with MAP of 1286 mm yr<sup>-1</sup> (German Weather Service). For each land-use type, soil cores were sampled in fourfold repetition at three different locations in October and November 2013, i.e. each type contains four pseudoreplicates (fourfold repetition at each site = variation at one site) multiplied by three (sampling at

three different locations) resulting in 12 profile samples for each land-use and a total of 36 profile samples.

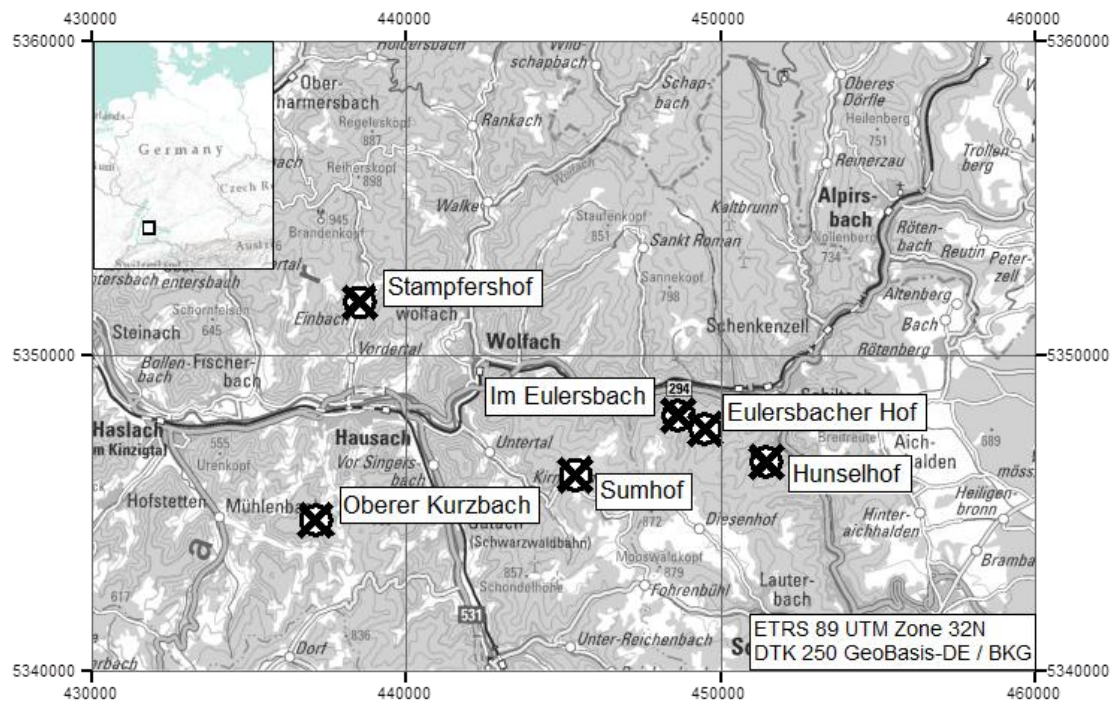


Figure 1.2 Map showing the distribution of sampling sites in the Black Forest, Germany. Agricultural sites were sampled at “Oberer Kurzbach”, “Stampfershof” and “Sumhof”, afforested sites at “Im Eulersbach”, “Eulersbacher Hof” and “Hunselhof” and continuously forested sites at “Sumhof”, “Im Eulersbach” and “Hunselhof”.

### 1.2.1.3 Haast, New Zealand

A total of 11 sites across a soil age gradient were chosen at the coastal foredune progradation dune ridge system located at the West Coast of New Zealand’s South Island (43°53’S, 169°3’E) to test for long-term effects of soil development on  $\delta^{13}\text{C}$  and  $\delta^{15}\text{N}$  depth profiles in topsoil (Fig. 1.3). This Haast dune chronosequence has formed under temperate humid climate (mean annual temperature = 11.3 °C, mean annual precipitation = 3455 mm) with parent material containing  $88.7 \pm 2.8\%$  sand,  $8.0 \pm 2.1\%$  silt and  $3.5 \pm 0.5\%$  clay (Turner et al., 2012a) and is exposed to negligible human disturbance and low atmospheric N deposition ( $0.9$  to  $1.5 \text{ kg N}\cdot\text{ha}^{-1}\cdot\text{yr}^{-1}$ ) (Galloway et al., 2004; Menge et al., 2011). Dune ridges form a slightly undulating topography (< 5 m to 20 m a.s.l.) with overall extension c. 5 km inland and soils developing from Arenosol to Podzol (Turner et al., 2012a). The whole formation covers a time of c. 6,000 yrs and was extensively described by Wells and Goff (2007) and Turner et al. (2012a). Five pseudoreplicated samples from litter, organic layers and mineral soil were sampled on

11 dune ridges (landward direction) in March 2013, resulting in 55 profiles covering a time span from *c.* 120 to *c.* 2,870 yrs (Chapter 4; Tab. 4.1).

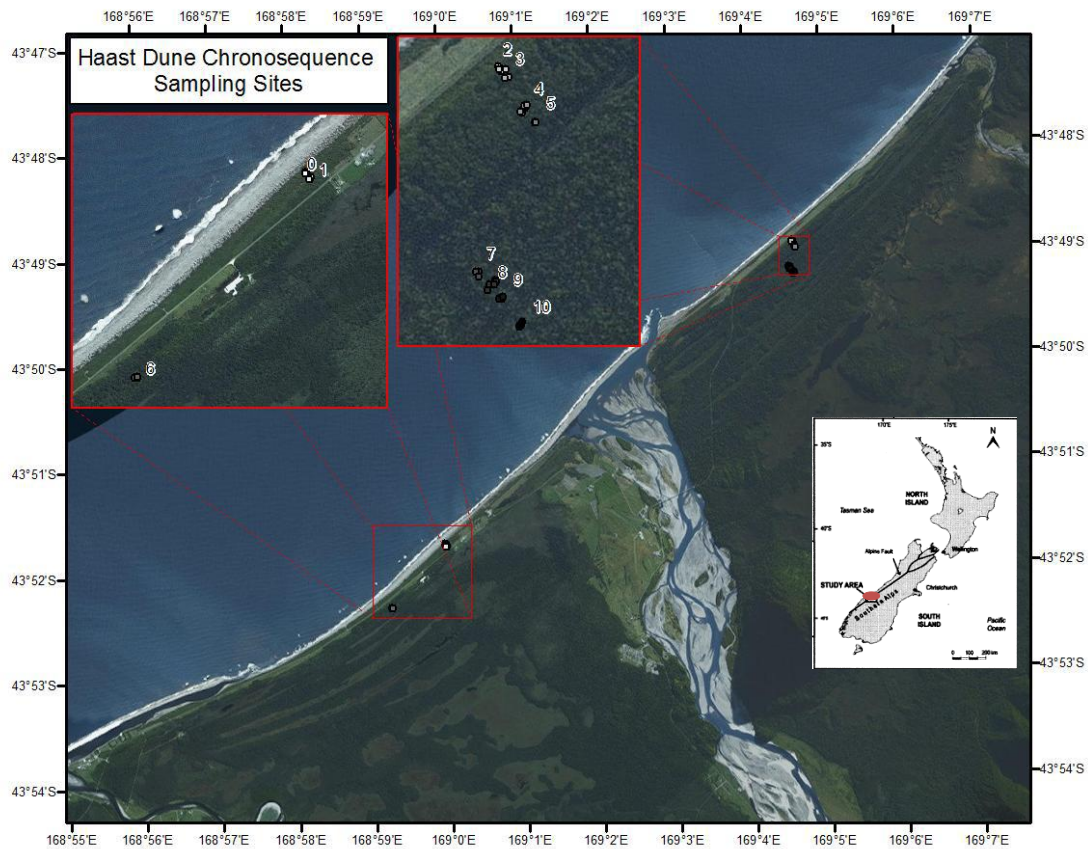


Figure 1.3 Satellite image of the Haast dune chronosequence with sampled dune stages (0-10) that represent a soil age gradient from *c.* 120 – *c.* 2,870 yrs B.P. Included map of New Zealand shows the Haast chronosequence as study area (provided by Wells and Goff 2006).

## 1.2.2 Sampling and sample preparation

At all study sites, soil samples were collected by a root auger (Eijkelkamp Agrisearch Equipment BV, Netherlands). Since the isotopic enrichment of  $^{13}\text{C}$  in OM throughout the soil is most pronounced in the upper centimeters of the soil profile (Accoe et al., 2003; Fang and Moncrieff, 2005; Kammer et al., 2012) soil cores were taken to a depth of 10 cm of the mineral soil. The soil cores with a diameter of 8 cm were cut into 1 cm sections (Fig. 1.4).

The organic layers were collected as Oi horizon (litter) and, if present, Oe and Oa horizon prior to cutting the mineral soil into sections. All samples were oven dried at 55°C or 60°C, respectively until weight constancy. The dried organic layer samples were ground in a shredder (Retsch SM 2000) resulting in a homogeneous mixture.



Dried mineral soil samples were sieved through a 2 mm sieve. To reduce impacts of “fresh” belowground C input, roots were removed by a pair of tweezers. Thereafter, these aliquots and those of the shredded organic layer samples were ground and homogenized with a Planetary Ball Mill PM 200 (Retsch, Germany).



Figure 1.4 Division of the soil core (A) and soil core sectioned into 1-cm segments (B) to obtain stable isotope depth profiles in high resolution. Pictures took by A. Rehmus.

### 1.2.3 Elemental and isotopic measurements

Carbon and nitrogen concentrations were analyzed with an Elemental Analyzer (Isotope Cube, Elementar, Hanau, Germany). Since all soil samples were free of carbonate (verified by means of hydrochloric acid addition to finely ground mineral soil samples) and acidic ( $\text{pH} \leq 4.5$ ), measured total C concentration equals the organic C concentration. Stable isotope ratios were analyzed by coupled isotope ratio mass spectrometry (IRMS) (Isoprime 100, Isoprime, Manchester, England). Results are given in delta notation as  $\delta^{13}\text{C}$  [ $\text{‰}_{\text{VPDB}}$ ] for C and  $\delta^{15}\text{N}$  [ $\text{‰}_{\text{Air}}$ ] for N stable isotopes (Eq. 1.1):

$$[1.1] \quad \delta^{13}\text{C}, \delta^{15}\text{N} = \left[ \frac{(R_{\text{sample}} - R_{\text{standard}})}{R_{\text{standard}}} \right] \times 1000$$

, where R represents the  $^{13}\text{C}/^{12}\text{C}$  or the  $^{15}\text{N}/^{14}\text{N}$  ratio, respectively. Data across the temperature and precipitation gradient (Chapter 2) were measured in Mainz, Germany with IAEA-CH-6 and IAEA-CH-7 for normalization of measured  $\delta^{13}\text{C}$  values to the VPDB scale. Data of the Black Forest (Chapter 3) were measured in Bern, Switzerland with



IAEA-CH-6, IAEA-CH-7 and EMA-P2 used for normalization. Data across the Haast chronosequence (Chapter 4) were measured in Hannover, Germany with IAEA-CH-3, IAEA-CH-6 and IAEA-600 for normalization of measured  $\delta^{13}\text{C}$  values (in ‰<sub>VPDB</sub>) and USGS25, IAEA-N-1 and IAEA-N-2 for normalization of measured  $\delta^{15}\text{N}$  values (in ‰<sub>Air</sub>). Long-term measurement accuracy of all IRMS analyses based on routine measurements of interspersed standard samples in each run during the measurement period was less than  $\pm 0.3\text{‰}$  for  $\delta^{13}\text{C}$  and  $\pm 0.2\text{‰}$  for  $\delta^{15}\text{N}$ .

#### 1.2.4 Calculations and statistical analysis

According to Garten (2006), linear regression analyses determined the patterns of isotopic changes within soil profiles. Therefore,  $\log_{10}x$ -transformed C concentrations [ $\log_{10}(\text{g}\cdot\text{C}\cdot\text{kg}^{-1})$ ] (= x) were regressed against their C stable isotope value [ $\delta^{13}\text{C}$ ] (= y) of the depth intervals (organic layers and mineral soil). The absolute values of the slopes were termed beta. In a similar way, I plotted  $\log_{10}x$ -transformed N concentrations [ $\log_{10}(10^{-1}\text{g}\cdot\text{N}\cdot\text{kg}^{-1})$ ] (= x) against  $\delta^{15}\text{N}$  values (=y) to obtain  $\text{beta}_\text{N}$  values (Chapter 4). Different units for the logarithmized C and N concentrations resulted in positive values on the x-axis (Chapter 4). To my knowledge,  $\text{beta}_\text{N}$  values have never been calculated before.

In addition to beta values, vertical isotopic differences were used to describe vertical changes in C ( $\Delta^{13}\text{C}$ ) and N stable isotopes ( $\Delta^{15}\text{N}$ ) from litter to mineral soil (Chapter 3 and 4). There was spatial variation in the depth and thickness of soil horizons between sites, e.g. a soil horizon at 10 cm soil depth of a given location does correspond to a slightly deeper or shallower depth as compared to the neighboring sampling site. I tried to account for this by using maximum difference in profiles instead of the difference between the litter layer and mineral soil at 10 cm soil depth to best represent the vertical changes in  $\delta^{13}\text{C}$  and  $\delta^{15}\text{N}$  values (Chapter 4).

One-way ANOVA post-hoc tests were applied to detect significant differences between beta values. In case of homogeneous variances I used a post-hoc Tukey test. In case of heteroscedasticity, a Games-Howell test was conducted. In addition to this, matched pairs t-tests (in case of homogeneity of variances) or Welch's t tests (in case of heteroscedasticity) for the comparison of beta values, proportions of explained variations and  $\Delta^{13}\text{C}$  or  $\Delta^{15}\text{N}$  values were applied. The level of significance was set to  $P \leq$

0.05 in all tests. Probability of fit to normal distribution was tested by Kolmogorov-Smirnov tests (Chapter 2, 3 and 4).

Autocorrelation of data was tested by the Durbin-Watson Test and reconciled with critical values for the Durbin-Watson Test provided by Savin and White (1977). Only non-autocorrelated data were evaluated (Chapter 4).

## 1.3 Results and discussion

### 1.3.1 Temperature and precipitation effects on $\delta^{13}\text{C}$ depth profiles in SOM under temperate beech forests (Chapter 2)

From litter down to the mineral soil at 10 cm depth, soil organic carbon (SOC) content decreased ( $47.5 \pm \text{SE } 0.1\%$  to  $2.5 \pm 0.1\%$ ) while  $\delta^{13}\text{C}$  values increased ( $-29.4 \pm 0.1\%$  to  $-26.1 \pm 0.1\%$ ) (Chapter 2; Fig. 2.2). Litter of sites under higher MAP or lower MAT had lower  $\delta^{13}\text{C}$  values. This is in line with literature data on climate driven plant physiological processes. Beta values ranged between 0.6 and 4.5 (range of  $r$  from -0.7 to -1.0;  $P < 0.01$ ). Due to an assumed decay continuum and similar variations of  $\delta^{13}\text{C}$  values in litter and at 10 cm depth, I conclude that effects on isotopic composition in the Oi layer continue vertically and therefore,  $\delta^{13}\text{C}$  values in litter do not solely control beta values. Beta values decreased with increasing MAT ( $r = -0.83$ ;  $P < 0.05$ ). Reduced soil moisture and therefore both, reduced microbial activity and reduced downward transport of microbial cycled DOM ( $=^{13}\text{C}$  enriched) might be responsible for less pronounced  $\delta^{13}\text{C}$  depth profiles in case of high temperatures. Greater C: N ratios (lower degradability) of litter under higher temperatures likely contributed to these depth trends. Beta values increased with increasing MAP ( $r = 0.73$ ;  $P < 0.05$ ). I found decreasing C: N ratios in the mineral soil with increasing MAP suggesting higher decomposition. Exclusion of the organic layers from linear regressions indicated a stronger impact of MAP on the development of  $\delta^{13}\text{C}$  depth profiles.

The results suggest temperature and precipitation effects on  $\delta^{13}\text{C}$  depth profiles and indicate stronger  $^{13}\text{C}$  enrichment under lower MAT and higher MAP. This was against my hypotheses assuming accelerated decomposition under higher temperatures and increased decomposition under higher precipitation. Time series of vertical  $\delta^{13}\text{C}$  depth profiles might provide insights into climate change effects. So far, it remained unclear

how fast  $\delta^{13}\text{C}$  depth profiles develop. Therefore, I chose a second approach in order to test for the temporal aspects of the vertical  $^{13}\text{C}$  enrichment.

### 1.3.2 Three decades after afforestation are sufficient to yield decomposition-related vertical $\delta^{13}\text{C}$ depth profiles in soil (Chapter 3)

Since many parameters affecting  $\delta^{13}\text{C}$  depth patterns can change fast and strongly during land-use changes, vegetation conversions provide valuable insights into C dynamics in soil. During land-use changes from cropland over afforested cropland to continuously forested sites in the Black Forest, Germany, C accumulated with increasing time of forest cover while  $\delta^{13}\text{C}$  depth profiles developed within decades. Carbon concentration of mineral soil and approximated decomposition were positively related, suggesting that C accumulation is not necessarily coupled with reduced decomposition. The Suess effect, increased belowground biomass production and related greater dissolved organic matter production as well as lower pH values may have accounted for greater isotopic differences in topsoil and increased potential soil respiration at afforested sites, leading to greater transport of  $^{13}\text{C}$  enriched microbial products. These parameters appeared to become further amplified at continuously forested sites. In contrast, soils under agricultural use showed near zero vertical enrichment in  $^{13}\text{C}$  but low measured potential soil respiration fits well to trends of increasing decomposition with time of forest cover. In line with my hypothesis, the results suggest a hampered applicability of vertical C stable isotope distribution to approximate low decomposition in soil. Respiration was related to vertical C stable isotope patterns and therefore, seems to contribute to shape  $\delta^{13}\text{C}$  depth profiles. In total, the data revealed that short timescales of 30 yrs are sufficient to develop distinct  $\delta^{13}\text{C}$  depth profiles in topsoil.

With proceeding time of ecosystem and soil development, the decomposition-related distribution of C stable isotopes in soil profiles may be subject to change. Therefore, a long-term soil chronosequence was chosen to test for relations to vertical  $\delta^{15}\text{N}$  distribution and the development of  $\delta^{13}\text{C}$  depth profiles during millennia.

### 1.3.3 Vertical distribution of carbon and nitrogen stable isotope ratios in topsoil across a temperate rainforest dune chronosequence in New Zealand (Chapter 4)

Chronosequences can provide valuable insights into C and N dynamics across natural gradients with C and N stable isotopes serving as powerful tool investigating these dynamics. During 2,870  *yrs* of soil and ecosystem development across the Haast chronosequence, decreasing  $\delta^{13}\text{C}$  values of litter with age suggested a physiological response of plants to decreased litter N concentrations. A decrease of litter  $\delta^{15}\text{N}$  in the early succession stages and a second decline after 1,300  *yrs* indicated reduced  $\text{N}_2$  fixation. Beta values calculated from linear regressions between logarithmized C concentrations and  $\delta^{13}\text{C}$  values ( $\text{beta}_\text{C}$ ) increased during early ecosystem development and at old sites while they were lowest at the intermediate stages (1,500  *yrs*) (Chapter 4; Fig. 4.3), which suggests decomposition did not decrease constantly with time.  $\text{beta}_\text{N}$  values describing the relation between the vertical distribution of N concentrations and  $\delta^{15}\text{N}$  values were lowest at the youngest site and increased within the first 200  *yrs*, likely because litter as the uppermost part of the vertical depth profile reflected an increased supply of N depleted in  $^{15}\text{N}$  provided by fungi. I found relations between  $\text{beta}_\text{C}$  and  $\text{beta}_\text{N}$  values suggesting that there might be shared processes shaping  $\delta^{13}\text{C}$  and  $\delta^{15}\text{N}$  vertical depth profiles, e.g. microbial cycling, transport or sorption. The rather fluctuating patterns of beta and  $\text{beta}_\text{N}$  values falsify my third hypothesis assuming a continuous decrease of beta and an increase of  $\text{beta}_\text{N}$  values within times of millennia. Therefore, my results demand a reconsideration of OM decomposition during long-term soil and ecosystem development in temperate rainforest dune systems and a possible transferability to other studies.

### 1.3.4 Interaction of spatially independent data with vertical C stable isotope distribution

Investigating impacts of climatic parameters on the vertical distribution of C stable isotopes in topsoil was addressed in the study across the temperature and precipitation gradient in northern Rhineland-Palatinate, Germany (Chapter 2). However, interpretation of the temperature impact was restricted by low soil moisture levels at warm sites. My study was designed to keep MAP (and other parameters like soil texture, tree species, exposition etc.) comparable across the temperature gradient, resulting in missing information on temperature effects on beta values under changed soil texture or changed

vegetation. To test whether temperature impacts on beta values can be observed independently of site property restrictions set across the MAT and MAP gradient in Rhineland-Palatinate, I extended data from my studies with other literature data of global distribution (Tab. 1.1). By including spatially independent data, I aimed to: (i) expand the temperature range and (ii) to vary the underlying parameters like soil moisture contents by changing MAP of sites. In the same way, I used data from these studies to extend the precipitation gradient in order to test for precipitation impacts on the vertical distribution of C stable isotopes in topsoil by adding literature data. Similarly, I aimed to expand the precipitation gradient and to vary the underlying parameters to better conclude temperature and precipitation effects on beta values.

Since I observed effects of time on the development of  $\delta^{13}\text{C}$  depth profiles, i.e. of forest cover (Chapter 3) and of soil and ecosystem development (Chapter 4), I embedded the observed beta values into spatially independent literature data from Diochon et al. (2009) with the objective to assess effects of soil and ecosystem age on beta values.

#### *Data collection*

Results from a total of 22 globally distributed studies constantly grown with  $\text{C}_3$  vegetation were included in the analysis of temperature and precipitation impacts (Fig. 1.5 and Tab. 1.1). MAT ranged between  $5.5^\circ\text{C}$  and  $27^\circ\text{C}$  and MAP between 687 mm and 4,065 mm.

Due to strong variations in MAP, data from Brunn et al. (2014) (Chapter 2) were averaged and divided into beta values from sites with low MAP ( $< 1,000$  mm) and sites with high MAP ( $\geq 1,000$  mm). Results from the Black Forest (Chapter 3) and from the Haast chronosequence (Brunn et al., 2016) (Chapter 4) were incorporated as one single average beta value each. From all other studies, I used the absolute values of the given beta value, so that higher beta values approximate high decomposition of OM in soil and vice versa. All 12 studies incorporated in the meta-analysis by Acton et al. (2013) were included in this thesis with 13 data points (Tab. 1.1). Another 13 data points are based on my studies and literature data not investigated in the meta-analysis by Acton et al. (2013).

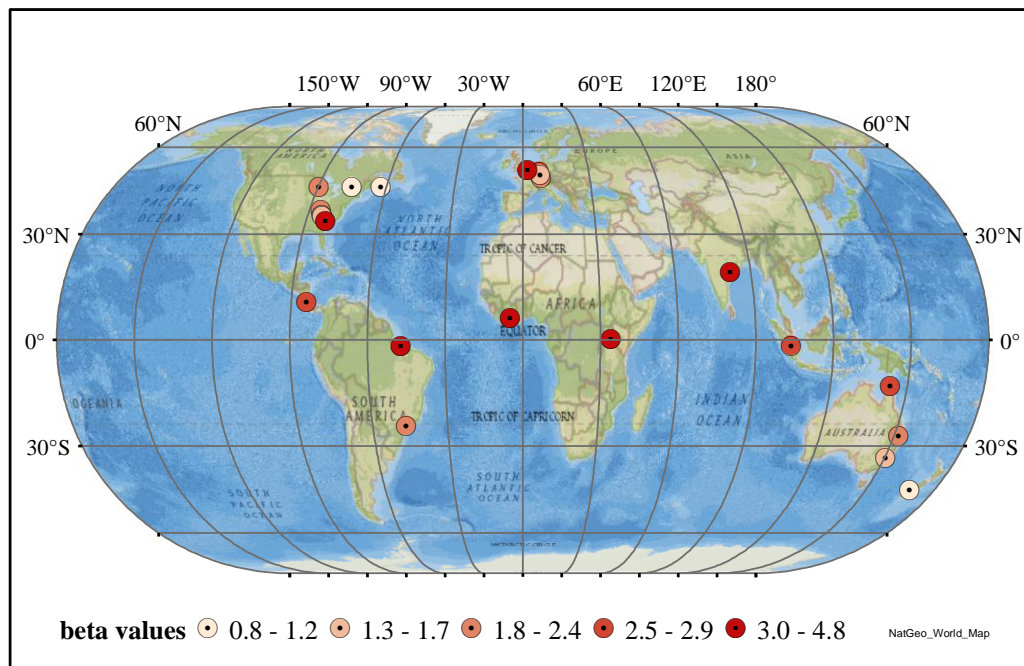


Figure 1.5 Globally distributed study locations with mean beta values.

However, I combined beta values by building means of data sampled in Kentucky by Acton et al. (2013) and by Campbell et al. (2009). The data provided by Garten et al. (2000) varied strongly in MAT and were therefore separated and averaged to obtain two mean beta values, one from sites with  $\text{MAT} \geq 10^\circ\text{C}$ , and one from sites with  $\text{MAT} < 10^\circ\text{C}$ . In a similar way, I included two beta values from Garten (2006) by building means of sites with  $\text{MAT} \geq 10^\circ\text{C}$  and of sites with  $\text{MAT} < 10^\circ\text{C}$ . Data from Gregorich et al. (1995), Nadelhoffer and Fry (1988), Richter et al. (1999), Richards et al. (2007), Desjardins et al. (1994) and Martin et al. (1990) were included as given by Acton et al. (2013). I calculated beta values by Diochon et al. (2009) to separate the data into an age gradient across their investigated chronosequence. However, only one mean beta value was included into the investigation of temperature and precipitation impacts. Since linear regression slopes were calculated from Rayleigh distillation in Wynn et al. (2005), I multiplied the given Rayleigh fractionation factor by  $2.3 = \ln(10)$ , based on differences between plotting  $\delta^{13}\text{C}$  values against  $\ln$ -transformed (natural logarithm) or  $\log_{10}$ -transformed (decadal logarithm) C concentrations. A similar relation between the Rayleigh fractionation factor and beta was observed by Garten (2006). Accordingly, I added data by Accoe et al. (2003) and by Laskar et al. (2016) which I both multiplied by 2.3.

In addition, beta values from Guillaume et al. (2015), Powers and Schlesinger (2002), Lins et al. (2016), Krull et al. (2002) and unpublished data provided by Rehmus et al. collected in forests of Southern Rhineland-Palatinate (Germany) were added with one average beta value each. With aim to investigate time effects on beta values I included studies by Brunn et al. (2014), Brunn et al. (2016), unpublished data from the Black Forest (Chapter 3) and by Diochon et al. (2009).

Table 1.1 Studies with location, mean annual temperature (MAT), mean annual precipitation (MAP), average beta value and the underlying sampling depth

Study	Location	MAT [°C]	MAP [mm yr <sup>-1</sup> ]	beta	Sampling depth [cm]
Accoe et al. 2003	Belgium	10.1	755	3.9	40
Acton et al. 2013*	Blue Mountains, SE Australia	11.8	1,076	1.3	50
	Letcher County, Kentucky, USA	12.0	1,085	1.4	50
Brunn et al. 2014 (Chapter 2)	Rhineland-Palatine, Germany	8.9	687	2.1	10
		8.1	1,061	3.5	10
Brunn submitted (Chapter 3)	Black Forest, Germany	9.4	1,286	2.1	10
Brunn et al. 2016 (Chapter 4)	Haast, New Zealand	11.3	3,455	1.2	10
Campbell et al (2009)*	Eastern Kentucky, USA	13.1	1,220	2.0	40
Desjardins et al. 1994*	Capito Poço, Para, Brazil	26.7	2,500	4.3	40
Diochon et al. 2009*	Liscomb Game Sanctuary, Nova Scotia, Canada	5.8	1,300	1.1	50
Garten et al. 2000*	Southern Appalachian Mountains, USA	11.6	1,500.0	2.1	40
		6.3	1,500.0	1.2	40
Garten 2006	Great Smoky Mountains National Park, USA	11.2	1,658	2.0	30
Powers & Schlesinger 2002	Sarapiquí, Costa Rica	24.6	4,065	2.9	100
Gregorich et al. 1995*	Eastern Ontario, Canada	5.5	975	0.8	70
Guillaume et al. 2015	Jambi Province, Sumatra, Indonesia	27.0	2,224	2.8	100
Krull et al. 2002	Kakamega Forest, Kenya	25	2,040	3.9	74
Laskar et al. 2016	Kangar Valley National Park, Central India	25.7	1,533	4.8	110/170
Lins et al. 2016	Serra do Mar State Park, Sao Paulo, Brazil	18.6	2,836	2.2	100
Martin et al. 1990*	Lamto, Ivory Coast	27.0	1,300	4.7	120
Nadelhoffer & Frey 1988*	Wisconsin; USA	7.0	950	2.2	20
Rehmus et al. unpublished	Rhineland-Palatinate, Germany	8.0	994	1.4	10
Richards 2007*	Yarraman State Forest, Australia	17.1	3,000	2.4	100
Richter et al 1999*	Calhoun Experimental Forest, South Carolina, USA	17.0	1,250	3.7	60
Wynn et al. 2005*	Iron Range National Park, Australia	25.5	2,159	2.7	100

Sampling depth of all studies varied considerably between 10 and 170 cm with mean sampling depth of  $56 \pm 7$  cm and relative standard deviation (RSD) of 68%. The variation of beta values was smaller with RSD = 48%, suggesting that variation of the sampled soil depth is not transferred to beta values. Beta values represent the relation between C concentrations and  $\delta^{13}\text{C}$  values and therefore reduce effects of the sampled soil depth. In addition, great differences in C concentrations with depth converge by logarithmizing C concentrations which again reduces differences of C concentrations between litter and mineral soil and therefore sampled soil depth. Although sampling depth and beta values were linearly related ( $r = 0.47$ ;  $P = 0.015$ ), this relation might not

only be an effect of sampling depth, but the fact that soils were sampled deeper at tropical warm sites with deeply developed soils and a high decomposition of OM that is supposed to increase the vertical  $^{13}\text{C}$  enrichment.

All beta values ( $n = 26$ ) were compiled to perform linear regression analysis in order to investigate the relationship between beta and MAT or beta and MAP. Control of precipitation effects across the temperature gradient was tested by classification of the data into beta values from studies with  $\text{MAP} \leq 1,000$  mm and with  $\text{MAP} > 1,000$  mm and into sites  $\leq 1,500$  mm and sites  $> 1,500$  mm MAP. According to the average MAT of  $14.6 \pm 1.5^\circ\text{C}$  of all studies, I classified beta values across the precipitation gradient into sites  $\geq 15^\circ\text{C}$  and  $< 15^\circ\text{C}$  MAT. To assess the impact of time on beta values, data points ( $n = 29$ ) were tested for linear relations with an age gradient spanning from 1 to 2,870 yrs B.P. The level of significance was set to  $P \leq 0.05$ . Probability of fit to normal distribution was tested by Kolmogorov–Smirnov tests.

### *Results and Discussion*

**Temperature:** If environmental parameters and precipitation were kept constant, beta values decreased across the temperature gradient (Chapter 2). However, these results were obtained under low levels of precipitation (675–733 mm MAP) that were supposed to affect beta values by constraining the decomposition process by reducing soil moisture. No effects of temperature on  $\delta^{13}\text{C}$  values in topsoil vegetation were observed across a transect of 400 mm  $\text{yr}^{-1}$  MAP in China (Jia et al., 2016) and in alpine grasslands on the Tibetan Plateau (Yang et al., 2015). Missing temperature impacts might similarly be based on reduced microbial activity. In addition, a potential reduction of the downward flux of  $^{13}\text{C}$  enriched materials could be hampered under dry conditions and result in lower beta values of sites with low MAP. At dry sites with  $\text{MAP} < 1000$  mm, beta values of compiled studies showed no linear trend with MAT (Fig. 1.7 A). However, sites with  $\text{MAT} < 5.5^\circ\text{C}$  and  $\text{MAP} < 687$  mm were not covered in this thesis.

In contrast to these findings, beta values increased significantly with increasing MAT ( $r = 0.7$ ;  $P < 0.001$ ) if spatially independent data from different climatic zones are compiled (Fig. 1.6). Mean beta value of these 22 studies was  $2.3 \pm 0.2$  and residuals of the linear regression were normally distributed. This result of steeper regression slopes between logarithmized C concentrations and  $\delta^{13}\text{C}$  values of depth profiles under higher MAT is in line with Acton et al. (2013) and supports the general assumption of increasing decomposition with increasing temperature (Amundson, 2001; Jobbagy and Jackson, 2000; Kirschbaum, 2000; Trumbore, 2009). Separating data points from Acton



et al. (2013) and others results in a slightly steeper regression line with higher significance ( $y = 0.1x + 0.3$ ;  $r = 0.87$ ;  $P < 0.001$ ) compared to linear regression build up of own and literature data not analyzed by Acton et al. (2013) ( $y = 0.1x + 1.4$ ;  $r = 0.56$ ;  $P = 0.045$ ). The coefficient of correlation of meta-analysis by Acton et al. (2013) was 1.4 times higher compared to the coefficient of correlation of beta values regressed against MAT of all compiled studies. However, the trend of increasing beta values with increasing MAT significantly persists despite this added data (Fig. 1.6). In addition, strong effects of MAT on beta values dominate soil moisture affected results observed across the temperature gradient in Rhineland-Palatinate, Germany (Chapter 2).

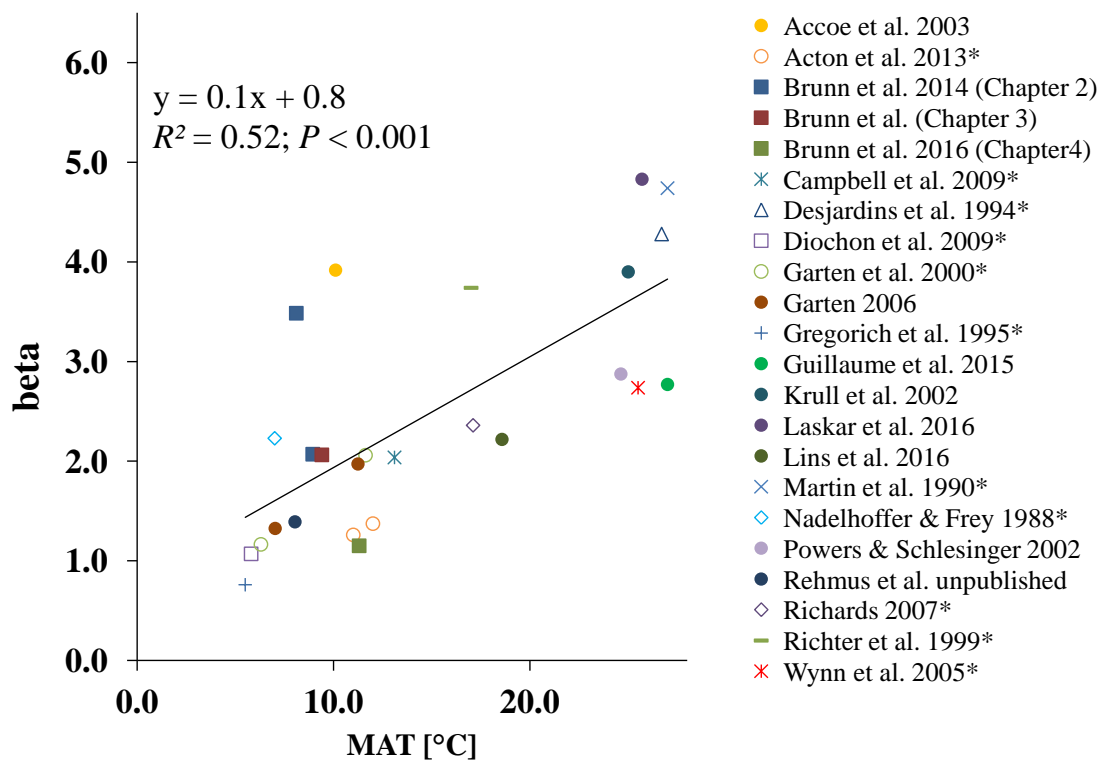


Figure 1.6 Beta values in relation to mean annual temperature (MAT) of spatially independent data. \* Data from Acton et al. 2013.

Positive differences from predicted beta values calculated with the linear regression equation with values  $\geq$  two-times the standard deviation stem from studies by Brunn et al. (2014) and Accoe et al. (2003), both not considered in the study by Acton et al. (2013) and therefore contribute to explain the lower coefficient of correlation in this thesis. The beta value included from Accoe et al. (2003) is derived from  $\delta^{13}\text{C}$  depth distribution of Belgian grassland soils. Data from the Black Forest (Chapter 3) are partly

based on cropland sites, similarly to data by Richards et al. (2007) who compared pasture with forest sites. However, the included beta value was an average value for each study. Clearcut and post-clearcut sites were investigated by Diochon et al. (2009) and similarly included with one average value. Yet, vegetation and/or land-use type may affect beta values which need further consideration that is not addressed in the investigation of MAT and MAP effects, since forest was the underlying vegetation type of all other investigated beta values. The second data point with strong deviation from its predicted value originates from German forest sites in northern Rhineland-Palatinate. These sites exposed to average MAP of 1,060 mm yr<sup>-1</sup> and MAT of 8.1°C MAT were characterized by increased beta values compared to sites of similar MAT. Likewise, beta values were slightly but not significantly higher in the precipitation class > 1,000 mm yr<sup>-1</sup> and in the precipitation class > 1,500 mm yr<sup>-1</sup>, respectively, suggesting greater decomposition under higher MAP. Alternatively, transport of hydrophilic, <sup>13</sup>C enriched products might be enhanced in soil profiles exposed to higher MAP (Nakanishi et al., 2012). On a global scale, a high number of sampling sites located in the Tropics with high decomposition of OM in soil might raise beta values under high MAT. Yet, it appeared that approximated decomposition increases more strongly with increasing temperature under dryer conditions, represented by steeper regression lines of beta values at sites ≤ 1,500 mm MAP with increasing MAT (Fig. 1.7 B). A more dense survey of beta values of savanna sites with high MAT and low MAP would give better insights here. Martin et al. (1990) observed <sup>13</sup>C depth distribution in savanna soils and their beta values fits well to tropical sites with much higher MAP, suggesting that MAP is compared to effects of MAT of minor importance in affecting beta values. However, literature data combined with own data suggest a strong positive relation between beta values and MAT which is well in line with the assumption that higher temperatures increase the decomposition of OM in soil.

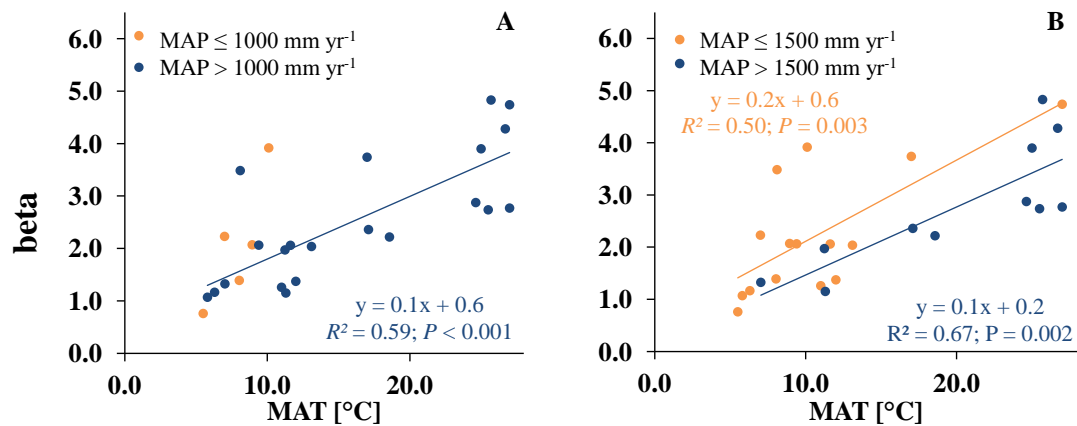


Figure 1.7 Beta values in relation to mean annual temperature (MAT) separated into classes with different mean annual precipitation (MAP) with 1,000 mm yr<sup>-1</sup> (A) and 1,500 mm yr<sup>-1</sup> as class boundary. Insignificant relations were not depicted.

Precipitation: Keeping temperature and environmental parameters (soil texture, tree species) comparable (between 7.9 and 9.1°C MAT), I found beta strongly and positively related to MAP (Chapter 2). In contrast, compiled literature data showed no linear trend of beta values and MAP (Fig. 1.8). It remains challenging whether other sites would feature corresponding results if soil and vegetation characteristics in addition to MAT were kept comparable with precipitation as sole changing variable. Compiled studies often capture MAP effects by varying altitude and therefore MAT with considerable reductions on decomposition of OM in soil. Under comparable site conditions and exclusion of anaerobic situations but MAP as changing variable, I assume a dominating mechanistic influence on  $\delta^{13}\text{C}$  depth profile development. I speculate that  $^{13}\text{C}$  enriched products were shifted down the soil profile with fluxes of dissolved organic matter, conforming to the stripping idea in soil columns (Kaiser and Kalbitz, 2012), leading to greater isotopic differences between litter and mineral soil and therefore beta values at sites with higher MAP. This process might only sustain under sufficient supply of microbial recycled products that might not be available if MAT goes below the temperature needed to maintain the decomposition of OM. At sites in northern Rhineland-Palatinate, Germany, exceptionally high beta values suggest that the vertical transport of hydrophilic  $^{13}\text{C}$  might have dominated the impact of decomposition on beta. Fine soil texture with increased selective sorption characteristics may have contributed to results of greater isotopic enrichment of  $^{13}\text{C}$  in depth profiles.

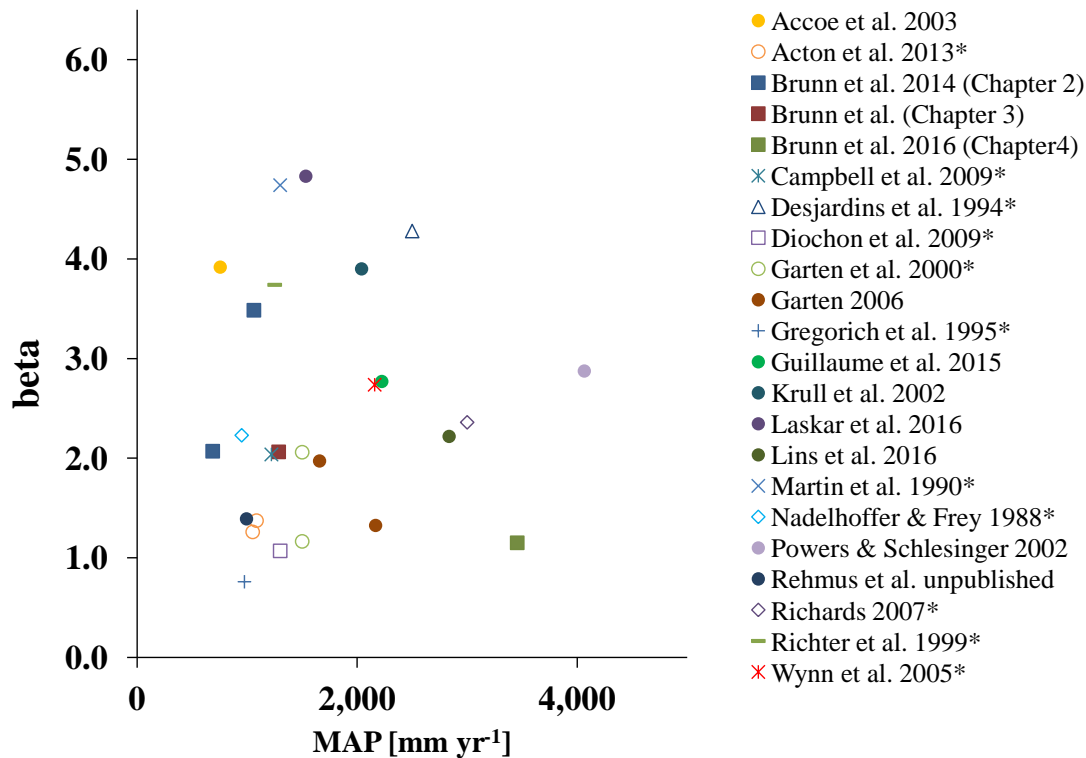


Figure 1.8 Beta values in relation to mean annual precipitation (MAP) of spatially independent data. \* Data from Acton et al. 2013.

The assumption of hampered decomposition under increased MAP (Amundson, 2001) cannot be shown with global data. Yet, if beta values are separated into data with MAT > 15°C, beta values decrease with increasing precipitation (Fig. 1.9), conforming to literature findings (Amundson, 2001; Meier and Leuschner, 2010). Results of lowest beta values under high MAP and temperatures > 15°C might be based on water-saturated soil conditions resulting in low vertical enrichment of <sup>13</sup>C by low microbial decomposition (Krüger et al., 2014). Both, relatively low beta values given in the study of Lins et al. (2016) who calculated beta without the litter layer and data by Richards et al. (2007) with sites of highly variable precipitation might additionally have affected this negative linear trend. In either case, increasing beta with increasing MAP as found in Rhineland-Palatinate sites could not be shown. Neither do beta values show increasing trends with MAP if MAT is kept constant.

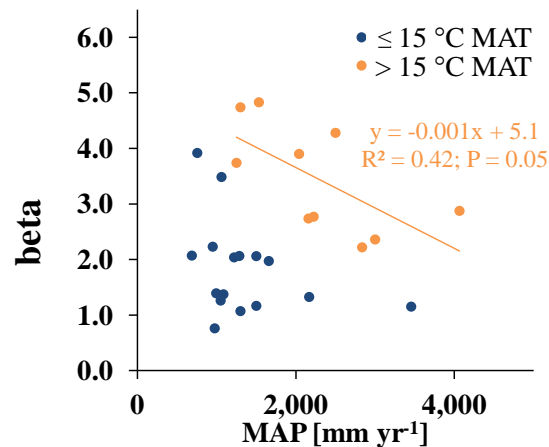


Figure 1.9 Beta values in relation to MAP separated into MAT classes with 15°C MAT as class boundary. Insignificant linear relations were not depicted.

Multiple regression analysis indicated that 64% of beta values can be explained by MAT and by MAP. Although sampling sites differed in many parameters, e.g. in altitude, in soil texture, in vegetation, in litter quality and quantity, in climatic zones and therefore in distribution of precipitation throughout the year, radiation and evapotranspiration, sampling method and the underlying laboratory of measurement, MAT appeared to explain a high percentage of beta values compiled from these apparently different studies. An even better prediction of beta values might be achieved if above mentioned parameters were included.

Age: No linear trend of beta values across an age gradient of soil and ecosystem development was observed (Fig 1.10). In contrast, I found that potential soil respiration and  $\delta^{13}\text{C}$  shaping processes like the Suess effect, organic matter input (above- and belowground), and fungal: bacterial ratios might be higher only three decades following afforestation. This time was sufficient to detect a significant vertical C stable isotope distribution used for the calculation of beta values.

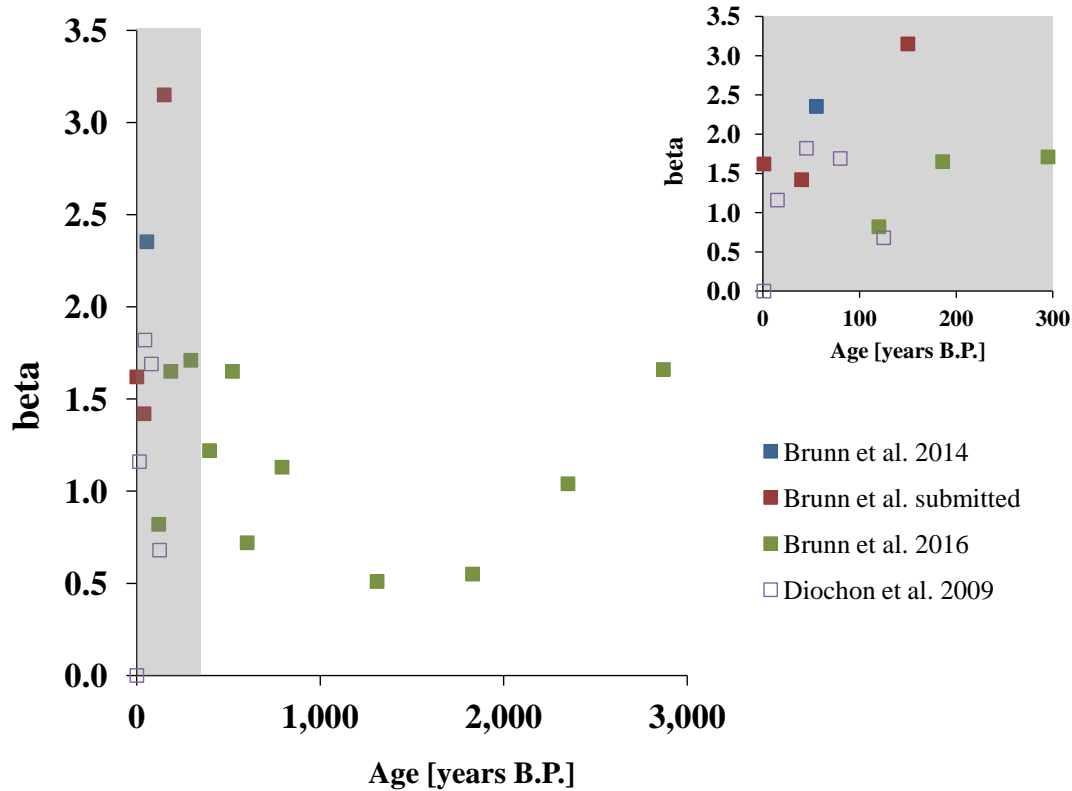


Figure 1.10 Beta values in relation to soil and ecosystem age with detailed figure showing soil and ecosystem or stand ages < 300 yrs.

Similarly, Diochon et al. (2009) observed increasing beta values during forest development with development of distinct  $\delta^{13}\text{C}$  depth profiles 15 yrs post-clearcut. However, results of increased beta values in continuous forest sites were not found in their study. Diochon et al. (2009) found lower beta values in the continuous forest which is in line with assumptions that C is more stabilized at older forest sites (Six et al., 2002). Beta values developed in a similar way at the long-term Haast chronosequence in New Zealand (Chapter 4), with increasing beta values during early ecosystem development in the first 300 yrs but a decline of beta values in the phase of maximal biomass. It seems that beta values increase during early ecosystem development, although more data are needed to underpin this assumption. In particular, including more data from long-term soil chronosequences might sustain trends of beta values during soil and ecosystem development and would clarify the impact of fungi, mycorrhiza, vegetation type, the organic layer and proposed ecosystem phases (Peltzer et al., 2010; Wardle et al., 2004) on beta values. Particularly MAT and MAP could significantly affect the dimension and the timescale needed to increase beta values in early progressive phases.

### *Conclusion*

Decomposition of OM in soil approximated via  $\delta^{13}\text{C}$  depth profiles (= beta) showed effects of temperature, precipitation and time along global gradients. While there was a positive relation between decomposition and MAT according to the kinetic theory, MAP seems to play a minor role in affecting decomposition of OM compared to MAT. However, under specific conditions, MAP significantly affects  $\delta^{13}\text{C}$  distribution and therefore beta values. This was given under saturated soil conditions that reduced decomposition under high MAP and when confounding variables (MAT, soil texture, vegetation) were excluded. In the latter, increased  $^{13}\text{C}$  transport via DOM fluxes likely dominated. Further studies are needed covering areas with comparable confounding variables but changing MAP, e.g. at windward and leeward sides. However, keeping input quality and quantity comparable remains challenging within not manipulated field site studies. Effects of time on beta values appeared to be ecosystem specific, but with an increase of decomposition during early ecosystem development and measureable  $\delta^{13}\text{C}$  depth profiles after three decades. Thus, with the prerequisite of a dominance of C processing over selective sorption in the soil column, beta values represent a reliable approximation of decomposition of OM of soils under steady state.

### 1.3.5 Error discussion

Possible bias may have arisen during following procedures: i) sampling site selection, ii) sample collection, iii) sample preparation, iv) isotopic analysis and v) application of the sampling design. In addition, vi) the approach using beta values as approximation for decomposition of OM in soil may be questioned.

First, extensive spatial geodata sets served to select sampling sites across the temperature and precipitation gradient (Chapter 2). Forest spatial geodata relied on frequent survey by forest officials. Climate spatial geodata were interpolated to a resolution of  $1 \times 1$  km and therefore, subject to generalization. Therefore, in situ MAT and MAP values might slightly deviate from spatial geodata. In addition, the selected temperature gradient covaried with an altitudinal gradient. I did not vary altitude and temperature separately, so that a potential altitudinal effect formed part of the temperature gradient. However, the maximum difference in altitude in the study was 300 m and thus, small in comparison with literature on altitudinal effects on carbon isotope fractionation (Körner et al., 1991).

Second, the high percentage of coarse fractions or thick roots at some sampling sites restricted the sampling of the entire soil depth profiles at certain sites. As extensively discussed in section 1.3.4, the calculation of beta values reduces variations of the sampled soil depth. This reduction is caused by: i) transformation of “depth” into C concentrations and by ii) using logarithmized values of C concentrations. The latter compresses the variations of C. To overcome variations of sampling depth and thickness of soil horizons between sampling sites, I related maximum isotopic difference in profiles to beta values to additionally represent vertical changes.

Third, great amounts of roots or fungi might affect beta values by “fresh C” inputs into mineral soil and by changing  $\delta^{13}\text{C}$  values. In preliminary studies in northern Rhineland-Palatinate, I tested the impact of fine roots on  $\delta^{13}\text{C}$  depth profiles. In four out of five soil profiles,  $\delta^{13}\text{C}$  depth profiles containing fine roots were less steep compared to  $\delta^{13}\text{C}$  depth profiles without fine roots (Chow-test,  $F(2,16)$  = range between 6.1 to 224.3,  $p \leq 0.01$ ). In addition to this, I analyzed the vertical change of  $\delta^{13}\text{C}$  values of removed roots at two selected sites ( $n = 93$  samples). The difference between roots of each depth and the respective Oi horizon ranged between  $-0.1$  to  $+3.2\text{‰}$  and thus, was not consistent across the depth profiles. On average, OM of soil was by  $2.7 \pm 0.5\text{‰}$  enriched in  $^{13}\text{C}$  compared to the Oi horizon (Wilcoxon signed-rank test,  $Z(93) = -12.0$ ,  $p < 0.001$ ) while roots were by  $1.1 \pm 1.1\text{‰}$   $^{13}\text{C}$  enriched compared to the Oi horizon (Wilcoxon signed-rank test,  $Z(93) = -6.5$ ,  $p < 0.001$ ). These results suggest that roots contribute to shape vertical  $\delta^{13}\text{C}$  depth distribution, although they are insufficient to explain entire  $^{13}\text{C}$  enrichment. I accounted for this by a careful removal of all visible roots by a pair of tweezers. However, in systems where fungi are abundant, removal of roots is supposed to affect the vertical isotopic changes in depth profiles by changing the ratio between soils to fungal litter. Since fungi were found to be  $^{13}\text{C}$  depleted (Kohl et al., 2015) their contribution could lower  $\delta^{13}\text{C}$  values in mineral soil samples and therefore the isotopic difference between litter and mineral soil OM. I assume that fungi were abundant at least at some stages across the Haast chronosequence and therefore, I discussed and took into account that the sample preparation might have an impact on  $\delta^{13}\text{C}$  depth profiles (Chapter 4).

Fourth, since all soil samples were free of carbonate (verified by means of hydrochloric acid addition to finely ground mineral soil samples) and acidic ( $\text{pH} \leq 4.5$ ), measured total C concentration equals the organic C concentration. The isotopic analysis of the samples was performed in different laboratories, each with slightly different



methods of isotopic determination. Data across the temperature and precipitation gradient (Chapter 2) were measured in Mainz, Germany with IAEA-CH-6 and IAEA-CH-7 for normalization of measured  $\delta^{13}\text{C}$  values to the VPDB scale. Data of the Black Forest (Chapter 3) were measured in Bern, Switzerland with IAEA-CH-6, IAEA-CH-7 and EMA-P2 used for normalization. Data across the Haast chronosequence (Chapter 4) were measured in Hannover, Germany with IAEA-CH-3, IAEA-CH-6 and IAEA-600 for normalization of measured  $\delta^{13}\text{C}$  values (in ‰<sub>VPDB</sub>) and USGS25, IAEA-N-1 and IAEA-N-2 for normalization of measured  $\delta^{15}\text{N}$  values (in ‰<sub>Air</sub>). Long-term measurement accuracy of all IRMS analyses based on routine measurements of interspersed standard samples in each run during the measurement period was less than  $\pm 0.3\text{‰}$  for  $\delta^{13}\text{C}$  and  $\pm 0.2\text{‰}$  for  $\delta^{15}\text{N}$ . This analytical uncertainty is less than the expected natural variability. In addition, analytical uncertainties can be neglected if comparing data sets within one study or if beta values are compared.

Fifth, the studies at Rhineland-Palatinate, Germany (Chapter 2) and at Haast, New Zealand (Chapter 4) contain no real replications. I used pseudoreplicates to describe impacts of parameters on vertical C stable isotope distribution. Data of both studies therefore rather represent location differences than treatment effects and provide limited transferability (Hurlbert, 1984). However, replication of sites across chronosequences is not possible, because comparable sites are not available (Diochon et al., 2009) and therefore, results involve dynamics within this investigated system. I tried to account on the use of pseudoreplicated samples by extending my results with spatially independent data (Chapter. 1.3.5).

Sixth, although beta values seem to be robust on variations of depth, the development of thick organic layers at aged soils across the Haast chronosequence (Chapter 4) may have hampered the accuracy of beta values to approximate decomposition of OM in soil. Including the organic layer (Oe and Oa layer) with high C concentrations but strong  $^{13}\text{C}$  enrichment into linear regressions between  $\log_{10}(\text{g}\cdot\text{C}\cdot\text{kg}^{-1})$  and  $\delta^{13}\text{C}$  values of aged soils results in less steep regression lines, visible in diverging  $\Delta^{13}\text{C}$  and beta values (Chapter 4; Fig. 4.3). In addition, due to its strong depletion in  $^{13}\text{C}$ , data from litter layers (Oi layers) strongly deviated from their predicted values at aged soils (Fig. S4.1). Despite the normal distribution of residuals, litter layers steepened regression lines. Similar effects of the litter layer were found under continuously forested sites in the Black Forest, Germany (Chapter 3). However, these statistical deviations of litter layer data should not account assuming a decay continuum from litter to mineral soil.

## 1.4 General conclusion

In line with results across varieties of ecosystems and environmental gradients, organic matter C stable isotope ratios significantly increased with soil depth. However, variation of vertical C stable isotope distribution occurred depending on temperature, precipitation and time. According to the questions raised in the introduction, my results allow to draw the following general conclusions. In addition they allow providing an outlook for using organic matter C stable isotopes as proxy for decomposition.

1. How do temperature and precipitation affect vertical C stable isotope distribution under field site conditions and comparable environmental parameters (Chapter 2)?

Vertical  $\delta^{13}\text{C}$  values showed distinct patterns depending on variations of MAT and MAP. Given the relation between the vertical distribution of  $\delta^{13}\text{C}$  values in topsoil and the approximation of decomposition of OM (= beta values), my results suggest decreasing decomposition with increasing MAT. This was against my hypothesis assuming accelerated decomposition under higher temperatures and contrasts results from globally independent data which rely on general assumptions of the kinetic theory. Lower microbial activity linked with decreased substrate accessibility due to low soil moisture levels serve to discuss effects of MAT on vertical C stable isotope distribution. In line with my hypothesis, I observed increasing decomposition with increasing MAP. However, selective sorption and the downward transport of hydrophilic,  $^{13}\text{C}$  enriched compounds with fluxes of soil solution might have dominated the development of  $\delta^{13}\text{C}$  depth profiles under high MAP. Higher numbers of cross site studies with comparable confounding variables are necessary to test how microbial decomposition of OM and selective sorption interact and how these processes affect  $\delta^{13}\text{C}$  depth profiles.

2. Can distinct  $\delta^{13}\text{C}$  depth profiles be found a few decades following afforestation of former cropland (Chapter 3)?

Examining the impact of time on the development of vertical C stable isotope distribution in topsoil, I found a few decades following afforestation of former cropland sufficient to develop distinct  $\delta^{13}\text{C}$  depth profiles. In line with my hypothesis, vertical C stable isotope distribution suggests limited applicability to approximate low de-

composition in soil, but an increase of approximated decomposition with time of forest cover.

3. How do  $\delta^{13}\text{C}$  and  $\delta^{15}\text{N}$  depth profiles develop during long-term ecosystem and soil formation (Chapter 4)?

At timescales of millennia, I found variable trends for  $\delta^{13}\text{C}$  and  $\delta^{15}\text{N}$  depth profiles with time and no constant decrease of beta values. The rather fluctuating behavior of beta and  $\beta_{\text{N}}$  values falsifies my third hypothesis assuming a continuous decrease of beta and an increase of  $\beta_{\text{N}}$  values during millennia. Beta values increased during early ecosystem development and at old sites, while they were lowest at the intermediate stages (1,500 *yr*s) across the Haast dune chronosequence under temperate rainforest. Increasing beta values during the early phase of ecosystem development suggest enhanced decomposition, probably stimulated through plant communities containing low abundances of woody species, while fungal colonization in accumulated organic layers likely decreased beta values at the intermediate stages. I could not clarify one main process responsible for increasing beta values at the late stages of the chronosequence. Increasing decomposition related to the canopy opening after the collapse of first generation trees was discussed which however, contradicts decreasing N availability observed across the chronosequence. A separation from aboveground input from input in soil serves as another explanation. However, the latter assumption raises doubt relating to the existence of a decomposition continuum in soil profiles. Increasing manganese concentrations of litter as a measure of greater litter decomposition status rather suggest that litter processes are transferred down in soil profiles. This strengthens the robustness of beta values to approximate decomposition. Interestingly, relations between  $\delta^{13}\text{C}$  and  $\delta^{15}\text{N}$  depth profiles reveal shared processes shaping depth distribution of stable isotopes of C and N, e.g. microbial cycling, transport or sorption and therefore, the interplay with other nutrients suggests processes relevant for  $\delta^{13}\text{C}$  depth distribution.

The analysis of vertical C stable isotope distribution appeared to provide an easily applicable approach to approximate decomposition under field conditions. Further manipulative experiments together with a better understanding of fractionation processes in the plant-soil-continuum could considerably improve predictions of beta values as proxy for decomposition of OM and its relation to turnover times and decomposition rates. Shifts of microbial community structures with particular role of mycorrhiza in

temperate systems, the role of thick organic layers at old sites, the physical accessibility of C and fractionation during transport mechanisms should need closer consideration on their impact on  $\delta^{13}\text{C}$  depth profiles. Beta values describe progressive processes of C availability and accessibility in combination with the downward shift of OM. Clarifying how microbial decomposition of OM and selective sorption of OM interact and how these processes affect the isotopic signature of bulk SOM at different climate regimes and differently aged soils are great challenges. Labeling studies under field site conditions together with compound specific analysis might gain better insights. In addition, many open questions remained on processes affecting isotopic signatures of litter that forms the uppermost part of depth profiles. For example, the (physiological and morphological) response of plants to nutrient limitation of aged soils including the consequences on their isotopic signatures in addition to shifts in function and species composition of  $\text{N}_2$  fixers need to be studied.

A fast development of  $\delta^{13}\text{C}$  depth profiles within decades was measured and therefore, it remains uncertain whether beta values are able to evaluate long-term C storage reaching centuries. However, analyzing vertical  $\delta^{13}\text{C}$  distribution in topsoil provides a chance to overcome the measurement of C in soils with much faster turnover of months, as it is addressed in short-term manipulated experiments. Hence, with the prerequisite of a dominance of C processing over selective sorption in the soil column, beta values suggest to be a reliable approximation of decomposition of OM under steady state, and therefore, the distribution of C stable isotopes in topsoil may contribute to evaluate the source-/sink functions of soils for C.

## 1.5 Author contribution

### List of Publications

1. Temperature and precipitation effects on  $\delta^{13}\text{C}$  depth profiles in SOM under temperate beech forests (Chapter 2)
2. Three decades after afforestation are sufficient to yield decomposition-related vertical  $\delta^{13}\text{C}$  depth profiles in soil (Chapter 3)
3. Vertical distribution of carbon and nitrogen stable isotope ratios in topsoil across a temperate rainforest dune chronosequence in New Zealand (Chapter 4)

**Declaration of the author's contribution according to the § 5 Abs. 2 No 8 of the PromO of the Faculty of Science, Eberhard Karls - Universität Tübingen**

Nr.	Chapter in this thesis	Accepted for publication [yes/no]	Number of all authors	Position of the candidate in list of authors	Scientific ideas of candidate [%]	Data generation by candidate [%]	Analysis and interpretation by candidate [%]	Paper writing by candidate [%]
1	2	yes	4	1	25	90	70	70
2	3	no	3	1	10	0	20	70
3	4	yes	5	1	40	90	70	70

## 1.6 References

- Accoe, F., Boeckx, P., Van Cleemput, O., Hofman, G., 2003. Relationship between soil organic C degradability and the evolution of the delta C-13 signature in profiles under permanent grassland. *Rapid Communications in Mass Spectrometry* 17, 2591-2596.
- Acton, P., Fox, J., Campbell, E., Rowe, H., Wilkinson, M., 2013. Carbon isotopes for estimating soil decomposition and physical mixing in well-drained forest soils. *Journal of Geophysical Research-Biogeosciences* 118, 1532-1545.
- Agren, G.I., Bosatta, E., 2002. Reconciling differences in predictions of temperature response of soil organic matter. *Soil Biology & Biochemistry* 34, 129-132.
- Amundson, R., 2001. The carbon budget in soils. *Annual Review of Earth and Planetary Sciences* 29, 535-562.
- Badeck, F.W., Tcherkez, G., Nogues, S., Piel, C., Ghashghaie, J., 2005. Post-photosynthetic fractionation of stable carbon isotopes between plant organs - a widespread phenomenon. *Rapid Communications in Mass Spectrometry* 19, 1381-1391.
- Balesdent, J., Mariotti, A., 1996. Measurement of soil organic matter turnover using <sup>13</sup>C natural abundance, In: Boutton, T.W.Y., S. I. (Ed.), *Mass spectrometry of soils*, New York, pp. 83-111
- Bird, M., Kracht, O., Derrien, D., Zhou, Y., 2003. The effect of soil texture and roots on the stable carbon isotope composition of soil organic carbon. *Australian Journal of Soil Research* 41, 77-94.
- Boström, B., Comstedt, D., Ekblad, A., 2007. Isotope fractionation and C-13 enrichment in soil profiles during the decomposition of soil organic matter. *Oecologia* 153, 89-98.
- Brunn, M., Condron, L., Wells, A., Spielvogel, S., Oelmann, Y., 2016. Vertical distribution of carbon and nitrogen stable isotope ratios in topsoil across a temperate rainforest dune chronosequence in New Zealand. *Biogeochemistry*, 1-15.
- Brunn, M., Spielvogel, S., Sauer, T., Oelmann, Y., 2014. Temperature and precipitation effects on delta C-13 depth profiles in SOM under temperate beech forests. *Geoderma* 235, 146-153.
- Campbell, J.E., Fox, J.F., Davis, C.M., Rowe, H.D., Thompson, N., 2009. Carbon and Nitrogen Isotopic Measurements from Southern Appalachian Soils: Assessing Soil Carbon Sequestration under Climate and Land-Use Variation. *Journal of Environmental Engineering-Asce* 135, 439-448.
- Clemmensen, K.E., Bahr, A., Ovaskainen, O., Dahlberg, A., Ekblad, A., Wallander, H., Stenlid, J., Finlay, R.D., Wardle, D.A., Lindahl, B.D., 2013. Roots and Associated Fungi Drive Long-Term Carbon Sequestration in Boreal Forest. *Science* 339, 1615-1618.
- Clemmensen, K.E., Finlay, R.D., Dahlberg, A., Stenlid, J., Wardle, D.A., Lindahl, B.D., 2015. Carbon sequestration is related to mycorrhizal fungal community shifts during long-term succession in boreal forests. *New Phytologist* 205, 1525-1536.
- Conant, R.T., Ryan, M.G., Agren, G.I., Birge, H.E., Davidson, E.A., Eliasson, P.E., Evans, S.E., Frey, S.D., Giardina, C.P., Hopkins, F.M., Hyvonen, R., Kirschbaum, M.U.F., Lavelle, J.M., Leifeld, J., Parton, W.J., Steinweg, J.M., Wallenstein, M.D., Wetterstedt, J.A.M., Bradford, M.A., 2011. Temperature and soil organic matter decomposition rates - synthesis of current knowledge and a way forward. *Global Change Biology* 17, 3392-3404.
- Craine, J.M., Brookshire, E.N.J., Cramer, M.D., Hasselquist, N.J., Koba, K., Marin-Spiotta, E., Wang, L.X., 2015. Ecological interpretations of nitrogen isotope ratios of terrestrial plants and soils. *Plant and Soil* 396, 1-26.
- Davidson, E.A., Janssens, I.A., 2006. Temperature sensitivity of soil carbon decomposition and feedbacks to climate change. *Nature* 440, 165-173.

- Del Galdo, I., Six, J., Peressotti, A., Cotrufo, M.F., 2003. Assessing the impact of land-use change on soil C sequestration in agricultural soils by means of organic matter fractionation and stable C isotopes. *Global Change Biology* 9, 1204-1213.
- Desjardins, T., Andreux, F., Volkoff, B., Cerri, C.C., 1994. Organic carbon and  $^{13}\text{C}$  contents in soils and soil size-fractions, and their changes due to deforestation and pasture installation in eastern Amazonia. *Geoderma* 61, 103-118.
- Dickie, I.A., Martinez-Garcia, L.B., Koele, N., Grelet, G.A., Tylianakis, J.M., Peltzer, D.A., Richardson, S.J., 2013. Mycorrhizas and mycorrhizal fungal communities throughout ecosystem development. *Plant and Soil* 367, 11-39.
- Diochon, A., Kellman, L., 2008. Natural abundance measurements of  $(^{13}\text{C})$  indicate increased deep soil carbon mineralization after forest disturbance. *Geophysical Research Letters* 35, 1-5.
- Diochon, A., Kellman, L., Beltrami, H., 2009. Looking deeper: An investigation of soil carbon losses following harvesting from a managed northeastern red spruce (*Picea rubens* Sarg.) forest chronosequence. *Forest Ecology and Management* 257, 413-420.
- Dixon, R.K., Brown, S., Houghton, R.A., Solomon, A.M., Trexler, M.C., Wisniewski, J., 1994. Carbon pools and flux of global forest ecosystems. *Science* 263, 185-190.
- Ehleringer, J.R., Buchmann, N., Flanagan, L.B., 2000. Carbon isotope ratios in belowground carbon cycle processes. *Ecological Applications* 10, 412-422.
- Fang, C.M., Moncrieff, J.B., 2005. The variation of soil microbial respiration with depth in relation to soil carbon composition. *Plant and Soil* 268, 243-253.
- Farquhar, G.D., Ehleringer, J.R., Hubick, K.T., 1989. Carbon isotope discrimination and photosynthesis. *Annual Review of Plant Physiology and Plant Molecular Biology* 40, 503-537.
- Francey, R.J., Allison, C.E., Etheridge, D.M., Trudinger, C.M., Enting, I.G., Leuenberger, M., Langenfelds, R.L., Michel, E., Steele, L.P., 1999. A 1000-year high precision record of delta C-13 in atmospheric CO<sub>2</sub>. *Tellus Series B-Chemical and Physical Meteorology* 51, 170-193.
- Galloway, J.N., Dentener, F.J., Capone, D.G., Boyer, E.W., Howarth, R.W., Seitzinger, S.P., Asner, G.P., Cleveland, C.C., Green, P.A., Holland, E.A., Karl, D.M., Michaels, A.F., Porter, J.H., Townsend, A.R., Vorosmarty, C.J., 2004. Nitrogen cycles: past, present, and future. *Biogeochemistry* 70, 153-226.
- Garten, C.T., 2006. Relationships among forest soil C isotopic composition, partitioning, and turnover times. *Canadian Journal of Forest Research-Revue Canadienne De Recherche Forestiere* 36, 2157-2167.
- Garten, C.T., Cooper, L.W., Post, W.M., Hanson, P.J., 2000. Climate controls on forest soil C isotope ratios in the Southern Appalachian Mountains. *Ecology* 81, 1108-1119.
- Giardina, C.P., Ryan, M.G., 2000. Evidence that decomposition rates of organic carbon in mineral soil do not vary with temperature. *Nature* 404, 858-861.
- Gregorich, E.G., Ellert, B.H., Monreal, C.M., 1995. Turnover of soil organic-matter and storage of corn residue carbon estimated from natural  $^{13}\text{C}$  abundance. *Canadian Journal of Soil Science* 75, 161-167.
- Guehl, J.M., Fort, C., Ferhi, A., 1995. Differential response of leaf conductance, carbon isotope discrimination and water-use efficiency to nitrogen deficiency in maritime pine and pedunculate oak plants. *New Phytologist* 131, 149-157.
- Guggenberger, G., Kaiser, K., 2003. Dissolved organic matter in soil: challenging the paradigm of sorptive preservation. *Geoderma* 113, 293-310.
- Guillaume, T., Damris, M., Kuzyakov, Y., 2015. Losses of soil carbon by converting tropical forest to plantations: erosion and decomposition estimated by delta C-13. *Global Change Biology* 21, 3548-3560.
- Hall, S.J., Silver, W.L., 2013. Iron oxidation stimulates organic matter decomposition in humid tropical forest soils. *Global Change Biology* 19, 2804-2813.
- Hansson, K., Kleja, D.B., Kalbitz, K., Larsson, H., 2010. Amounts of carbon mineralised and leached as DOC during decomposition of Norway spruce needles and fine roots. *Soil Biology & Biochemistry* 42, 178-185.
- Hobbie, E.A., Ouimette, A.P., 2009. Controls of nitrogen isotope patterns in soil profiles. *Biogeochemistry* 95, 355-371.
- Hurlbert, S.H., 1984. Pseudoreplication and the Design of Ecological Field Experiments. *Ecological Monographs* 54, 187-211.
- Hyodo, F., Kusaka, S., Wardle, D.A., Nilsson, M.C., 2013. Changes in stable nitrogen and carbon isotope ratios of plants and soil across a boreal forest fire chronosequence. *Plant and Soil* 367, 111-119.
- Hyodo, F., Wardle, D.A., 2009. Effect of ecosystem retrogression on stable nitrogen and carbon isotopes of plants, soils and consumer organisms in boreal forest islands. *Rapid Communications in Mass Spectrometry* 23, 1892-1898.

- Intergovernmental Panel on Climate Change, I., 2013. *Climate Change 2013: The Physical Science Basis. Summary for Policymakers*, 33.
- Jia, Y., Wang, G., Tan, Q., Chen, Z., 2016. Temperature exerts no influence on organic matter  $\delta^{13}\text{C}$  of surface soil along the 400 mm isopleth of mean annual precipitation in China. *Biogeosciences* 13, 5057-5064.
- Jobby, E.G., Jackson, R.B., 2000. The vertical distribution of soil organic carbon and its relation to climate and vegetation. *Ecological Applications* 10, 423-436.
- Kaiser, K., Guggenberger, G., Zech, W., 2001. Isotopic fractionation of dissolved organic carbon in shallow forest soils as affected by sorption. *European Journal of Soil Science* 52, 585-597.
- Kaiser, K., Kalbitz, K., 2012. Cycling downwards - dissolved organic matter in soils. *Soil Biology & Biochemistry* 52, 29-32.
- Kammer, A., Schmidt, M.W.I., Hagedorn, F., 2012. Decomposition pathways of C-13-depleted leaf litter in forest soils of the Swiss Jura. *Biogeochemistry* 108, 395-411.
- Keeling, C.D., Piper, S.C., Bacastow, R.B., Wahlen, M., Whorf, T.P., Heimann, M., Meijer, H.A., 2005. Atmospheric CO<sub>2</sub> and (CO<sub>2</sub>)-C-13 exchange with the terrestrial biosphere and oceans from 1978 to 2000: Observations and carbon cycle implications, In: Ehleringer, J.R., Cerling, T.E., Dearing, M.D. (Eds.), *Ecological Studies*. Springer, 233 Spring Street, New York, Ny 10013, United States, pp. 83-113.
- Kirschbaum, M.U.F., 2000. Will changes in soil organic carbon act as a positive or negative feedback on global warming? *Biogeochemistry* 48, 21-51.
- Körner, C., Diemer, M., 1987. In situ photosynthetic responses to light, temperature and carbon dioxide in herbaceous plants from low and high altitude. *Functional Ecology* 1, 179-194.
- Körner, C., Farquhar, G.D., Wong, S.C., 1991. Carbon isotope discrimination by plants follows latitudinal and altitudinal trends. *Oecologia* 88, 30-40.
- Krüger, J.P., Leifeld, J., Alewell, C., 2014. Degradation changes stable carbon isotope depth profiles in peatlands. *Biogeosciences* 11, 3369-3380.
- Krull, E.S., Bestland, E.A., Gates, W.P., 2002. Soil organic matter decomposition and turnover in a tropical Ultisol: Evidence from  $\delta^{13}\text{C}$ ,  $\delta^{15}\text{N}$  and geochemistry. *Radiocarbon* 44, 93-112.
- Laganière, J., Angers, D.A., Paré, D., 2010. Carbon accumulation in agricultural soils after afforestation: a meta-analysis. *Global Change Biology* 16, 439-453.
- Lal, R., Follett, F., Stewart, B.A., Kimble, J.M., 2007. Soil carbon sequestration to mitigate climate change and advance food security. *Soil Science* 172, 943-956.
- Laliberté, E., Grace, J.B., Huston, M.A., Lambers, H., Teste, F.P., Turner, B.L., Wardle, D.A., 2013. How does pedogenesis drive plant diversity? *Trends in Ecology & Evolution* 28, 331-340.
- Lambers, H., Raven, J.A., Shaver, G.R., Smith, S.E., 2008. Plant nutrient-acquisition strategies change with soil age. *Trends in Ecology & Evolution* 23, 95-103.
- Laskar, A.H., Yadava, M.G., Ramesh, R., 2016. Stable and radioactive carbon in forest soils of Chhattisgarh, Central India: Implications for tropical soil carbon dynamics and stable carbon isotope evolution. *Journal of Asian Earth Sciences* 123, 47-57.
- Lehmann, J., Kleber, M., 2015. The contentious nature of soil organic matter. *Nature* 528, 60-68.
- Lerch, T.Z., Nunan, N., Dignac, M.F., Chenu, C., Mariotti, A., 2011. Variations in microbial isotopic fractionation during soil organic matter decomposition. *Biogeochemistry* 106, 5-21.
- Lins, S.R.M., Della Coletta, L., Ravagnani, E.D., Gragnani, J.G., Mazzi, E.A., Martinelli, L.A., 2016. Stable carbon composition of vegetation and soils across an altitudinal range in the coastal Atlantic Forest of Brazil. *Trees-Structure and Function* 30, 1315-1329.
- Martin, A., Mariotti, A., Balesdent, J., Lavelle, P., Vuattoux, R., 1990. Estimate of organic matter turnover rate in a Savanna soil by  $^{13}\text{C}$  natural abundance measurements. *Soil Biology & Biochemistry* 22, 517-523.
- Martinez-Garcia, L.B., Richardson, S.J., Tylianakis, J.M., Peltzer, D.A., Dickie, I.A., 2015. Host identity is a dominant driver of mycorrhizal fungal community composition during ecosystem development. *New Phytologist* 205, 1565-1576.
- Marty, C., Houle, D., Gagnon, C., 2015. Effect of the Relative Abundance of Conifers Versus Hardwoods on Soil  $\delta^{13}\text{C}$  Enrichment with Soil Depth in Eastern Canadian forests. *Ecosystems* 18, 629-642.
- Meier, I.C., Leuschner, C., 2010. Variation of soil and biomass carbon pools in beech forests across a precipitation gradient. *Global Change Biology* 16, 1035-1045.
- Menge, D.N.L., Baisden, W.T., Richardson, S.J., Peltzer, D.A., Barbour, M.M., 2011. Declining foliar and litter  $\delta^{15}\text{N}$  diverge from soil, epiphyte and input  $\delta^{15}\text{N}$  along a 120 000 yr temperate rainforest chronosequence. *New Phytologist* 190, 941-952.
- Moyano, F.E., Manzoni, S., Chenu, C., 2013. Responses of soil heterotrophic respiration to moisture availability: An exploration of processes and models. *Soil Biology & Biochemistry* 59, 72-85.

- Nadelhoffer, K.F., Fry, B., 1988. Controls on natural N-15 and C-13 abundances in forest soil organic-matter. *Soil Science Society of America Journal* 52, 1633-1640.
- Nakanishi, T., Atarashi-Andoh, M., Koarashi, J., Saito-Kokubun, Y., Hirai, K., 2012. Carbon isotopes of water-extractable organic carbon in a depth profile of forest soil imply a dynamic relationship with soil carbon. *European Journal of Soil Science* 63, 495-500.
- Peltzer, D.A., Wardle, D.A., Allison, V.J., Baisden, W.T., Bardgett, R.D., Chadwick, O.A., Condon, L.M., Parfitt, R.L., Porder, S., Richardson, S.J., Turner, B.L., Vitousek, P.M., Walker, J., Walker, L.R., 2010. Understanding ecosystem retrogression. *Ecological Monographs* 80, 509-529.
- Pietri, J.C.A., Brookes, P.C., 2009. Substrate inputs and pH as factors controlling microbial biomass, activity and community structure in an arable soil. *Soil Biology & Biochemistry* 41, 1396-1405.
- Post, W.M., Kwon, K.C., 2000. Soil carbon sequestration and land-use change: processes and potential. *Global Change Biology* 6, 317-327.
- Powers, J.S., Schlesinger, W.H., 2002. Geographic and vertical patterns of stable carbon isotopes in tropical rain forest soils of Costa Rica. *Geoderma* 109, 141-160.
- Richards, A.E., Dalal, R.C., Schmidt, S., 2007. Soil carbon turnover and sequestration in native subtropical tree plantations. *Soil Biology & Biochemistry* 39, 2078-2090.
- Richter, D.D., Markewitz, D., Trumbore, S.E., Wells, C.G., 1999. Rapid accumulation and turnover of soil carbon in a re-establishing forest. *Nature* 400, 56-58.
- Savin, N.E., White, K.J., 1977. Durbin-Watson Test for serial correlation with extreme sample sizes or many regressors. *Econometrica* 45, 1989-1996.
- Scharlemann, J.P.W., Tanner, E.V.J., Hiederer, R., Kapos, V., 2014. Global soil carbon: understanding and managing the largest terrestrial carbon pool. *Carbon Management* 5, 81-91.
- Schlesinger, W.H., 1990. Evidence from chronosequence studies for a low carbon-storage potential of soils. *Nature* 348, 232-234.
- Schmidt, M.W.I., Torn, M.S., Abiven, S., Dittmar, T., Guggenberger, G., Janssens, I.A., Kleber, M., Kögel-Knabner, I., Lehmann, J., Manning, D.A.C., Nannipieri, P., Rasse, D.P., Weiner, S., Trumbore, S.E., 2011. Persistence of soil organic matter as an ecosystem property. *Nature* 478, 49-56.
- Six, J., Callewaert, P., Lenders, S., De Gryze, S., Morris, S.J., Gregorich, E.G., Paul, E.A., Paustian, K., 2002. Measuring and understanding carbon storage in afforested soils by physical fractionation. *Soil Science Society of America Journal* 66, 1981-1987.
- Torn, M.S., Lapenis, A.G., Timofeev, A., Fischer, M.L., Babikov, B.V., Harden, J.W., 2002. Organic carbon and carbon isotopes in modern and 100-year-old-soil archives of the Russian steppe. *Global Change Biology* 8, 941-953.
- Townsend, A.R., Vitousek, P.M., Trumbore, S.E., 1995. Soil organic-matter dynamics along gradients in temperature and land-use on the island of Hawaii. *Ecology* 76, 721-733.
- Trumbore, S., 2009. Radiocarbon and Soil Carbon Dynamics, *Annual Review of Earth and Planetary Sciences*. Annual Reviews, Palo Alto, pp. 47-66.
- Turner, B.L., Condon, L.M., Wells, A., Andersen, K.M., 2012a. Soil nutrient dynamics during podzol development under lowland temperate rain forest in New Zealand. *Catena* 97, 50-62.
- Turner, B.L., Wells, A., Andersen, K.M., Condon, L.M., 2012b. Patterns of tree community composition along a coastal dune chronosequence in lowland temperate rain forest in New Zealand. *Plant Ecology* 213, 1525-1541.
- van't Hoff, J.H., 1898. *Lectures on Theoretical and Physical Chemistry*. Chemical Dynamics, Edward Arnold, London. Part 1.
- Vitousek, P., 2004. Nutrient cycling and limitation: Hawai'i as a model system. Princeton University Press, i-xx, 1-223 pp.
- Vitousek, P.M., Farrington, H., 1997. Nutrient limitation and soil development: Experimental test of a biogeochemical theory. *Biogeochemistry* 37, 63-75.
- Vitousek, P.M., Field, C.B., Matson, P.A., 1990. Variation in foliar  $\delta^{13}\text{C}$  in Hawaiian *Metrosideros* polymorpha: a case of internal resistance? *Oecologia* 84, 362-370.
- Vitousek, P.M., Howarth, R.W., 1991. Nitrogen limitation on land and in the sea: How it can occur? *Biogeochemistry* 13, 87-115.
- Walker, T.W., Syers, J.K., 1976. The fate of phosphorus during pedogenesis. *Geoderma* 15, 1-19.
- Wallander, H., Morth, C.M., Giesler, R., 2009. Increasing abundance of soil fungi is a driver for N-15 enrichment in soil profiles along a chronosequence undergoing isostatic rebound in northern Sweden. *Oecologia* 160, 87-96.
- Wardle, D.A., Walker, L.R., Bardgett, R.D., 2004. Ecosystem properties and forest decline in contrasting long-term chronosequences. *Science* 305, 509-513.
- Wells, A., Goff, J., 2007. Coastal dunes in Westland, New Zealand, provide a record of paleoseismic activity on the Alpine fault. *Geology* 35, 731-734.



- 
- Werth, M., Kuzyakov, Y., 2010. C-13 fractionation at the root-microorganisms-soil interface: A review and outlook for partitioning studies. *Soil Biology & Biochemistry* 42, 1372-1384.
- Wiesmeier, M., Hubner, R., Sporlein, P., Geuss, U., Hangen, E., Reischl, A., Schilling, B., von Lutzow, M., Kogel-Knabner, I., 2014. Carbon sequestration potential of soils in southeast Germany derived from stable soil organic carbon saturation. *Global Change Biology* 20, 653-665.
- Wynn, J.G., Bird, M.I., Wong, V.N.L., 2005. Rayleigh distillation and the depth profile of C-13/C-12 ratios of soil organic carbon from soils of disparate texture in Iron Range National Park, Far North Queensland, Australia. *Geochimica Et Cosmochimica Acta* 69, 1961-1973.
- Yang, Y.H., Ji, C.J., Chen, L.Y., Ding, J.Z., Cheng, X.L., Robinson, D., 2015. Edaphic rather than climatic controls over C-13 enrichment between soil and vegetation in alpine grasslands on the Tibetan Plateau. *Functional Ecology* 29, 839-848.

## 2 Temperature and precipitation effects on $\delta^{13}\text{C}$ depth profiles in SOM under temperate beech forests

Melanie Brunn<sup>1</sup>, Sandra Spielvogel<sup>1</sup>, Tilmann Sauer<sup>2</sup>, Yvonne Oelmann<sup>3</sup>

<sup>1</sup>Institute for Integrated Natural Sciences, University of Koblenz-Landau, Universitätsstraße 1, 56070 Koblenz, Germany

<sup>2</sup>Rhineland-Palatinate Centre of Excellence for Climate Change Impacts, Hauptstraße 16, 67705 Trippstadt, Germany

<sup>3</sup>Geoecology, University of Tübingen, Rümelinstraße 19-23, 72070 Tübingen, Germany

Geoderma 235–236 (2014) 146–153 (accepted 08.07.2014)

<http://dx.doi.org/10.1016/j.geoderma.2014.07.007>

## 2.1 Abstract

Enrichment of  $^{13}\text{C}$  in SOM with soil depth is related to interacting processes influenced by temperature and precipitation. Our objectives were to derive climate effects on patterns of vertical  $\delta^{13}\text{C}$  values of soil organic matter (SOM) while minimizing the effect of confounding variables.

We investigated vertical changes in  $\delta^{13}\text{C}$  values of SOM in 1-cm depth intervals in silvicultural mature beech (*Fagus sylvatica* L.) forest ecosystems in northern Rhineland-Palatinate across gradients of MAT (7.9 to 9.7°C mean annual temperature) and MAP (607 to 1085 mm mean annual precipitation) in winter 2011. Forest stands ( $n = 10$ ) were chosen based on data sets provided by the Rhineland-Palatinate Forest Administration so that variations in these gradients occurred while other environmental factors like physico-chemical soil properties, tree species, stand age, exposition and precipitation (for the temperature gradient) or temperature (for the precipitation gradient) did not differ among study sites.

From litter down to the mineral soil at 10 cm depth, soil organic carbon (SOC) content decreased ( $47.5 \pm \text{SE } 0.1\%$  to  $2.5 \pm 0.1\%$ ) while the  $\delta^{13}\text{C}$  values increased ( $-29.4 \pm 0.1\text{‰}$  to  $-26.1 \pm 0.1\text{‰}$ ). Litter of sites under higher MAP/ lower MAT had lower  $\delta^{13}\text{C}$  values which was in line with literature data on climate driven plant physiological process. To compare the dimension of the vertical  $^{13}\text{C}$  enrichment,  $\delta^{13}\text{C}$  values were regressed linearly against log-transformed carbon contents yielding absolute values of these slopes (beta). Beta values ranged between 0.6 and 4.5 (range of  $r$  from -0.7 to -1.0;  $p < 0.01$ ). Due to an assumed decay continuum and similar variations of  $\delta^{13}\text{C}$  values in litter and in 10 cm depth, we conclude that effects on isotope composition in the Oi layer continue vertically and therefore,  $\delta^{13}\text{C}$  values in litter do not solely control beta values. Beta values decreased with increasing MAT ( $r = -0.83$ ;  $p < 0.05$ ). Reduced soil moisture and therefore both, reduced microbial activity and reduced downward transport of microbial cycled DOM ( $= ^{13}\text{C}$  enriched) might be responsible for less pronounced  $\delta^{13}\text{C}$  depth profiles in case of high temperatures. Greater C:N ratios (lower degradability) of the litter under higher temperatures likely contributed to these depth trends. Beta values increased with increasing MAP ( $r = 0.73$ ;  $p < 0.05$ ). We found decreasing C:N ratios in the mineral soil that possibly indicates higher decomposition under higher precipitation. Exclusion of the organic layers from linear regressions indicated a stronger impact of MAP on the development of  $\delta^{13}\text{C}$  depth profiles.

Our results confirm temperature and precipitation effects on  $\delta^{13}\text{C}$  depth profiles and indicate stronger  $^{13}\text{C}$  enrichment under lower MAT/higher MAP. Therefore, time series of vertical  $\delta^{13}\text{C}$  depth profiles might provide insights into climate change effects.

## 2.2 Introduction

Stable carbon isotopes have been used to describe SOM dynamics (Accoe et al., 2003; Balesdent and Mariotti, 1996; Garten et al., 2000). With increasing soil depth the SOM becomes enriched in  $^{13}\text{C}$  leading to less negative  $\delta^{13}\text{C}$  values in deeper parts of the mineral soil (Boström et al., 2007; Ehleringer et al., 2000; Nadelhoffer and Fry, 1988b). Several processes might cause these  $\delta^{13}\text{C}$  depth changes. First, the Suess effect i.e., the depletion of  $^{13}\text{C}$  in the atmosphere due to combustion of fossil fuel, might lead to an accumulation of  $^{13}\text{C}$  depleted organic material in the surface layers of the soil (Friedli et al. 1986, Boström et al. 2007). However, studies of  $\delta^{13}\text{C}$  depth profiles in archived and modern soils (Torn et al., 2002) or bare-fallow soil studies (Balesdent and Mariotti, 1996) gave evidence that additional processes must contribute to the shifts of  $^{13}\text{C}$  throughout the soil profile. Second, roots are enriched in  $^{13}\text{C}$  by 1-2‰ compared to  $\delta^{13}\text{C}$  values of aboveground plant material (Badeck et al., 2005; Bird et al., 2003; Werth and Kuzyakov, 2010). The considerable presence of roots (from trees and herbaceous plants) in the upper soil might therefore explain another part of the differences in  $\delta^{13}\text{C}$  of SOM with soil depth. Third, isotopic fractionation during microbial metabolism of SOM with respiration of lighter compounds (Lerch et al., 2011; Werth and Kuzyakov, 2010; Wynn et al., 2005) and fourth, the downward cycling of hydrophilic,  $^{13}\text{C}$  enriched decomposition products (Dümig et al., 2013; Nakanishi et al., 2012) with dissolved organic carbon (DOC) fluxes and the selective physico-chemical sorption of hydrophobic,  $^{13}\text{C}$  depleted compounds likely contribute to establish the vertical  $\delta^{13}\text{C}$  depth trends (Dümig et al., 2013; Kaiser and Kalbitz, 2012; Nakanishi et al., 2012). However, to date, neither the mechanisms nor the dynamics are completely understood.

Several authors reported on the relationship between decomposition of SOM and  $\delta^{13}\text{C}$  depth profiles in soils (Acton et al., 2013; Ehleringer et al., 2000; Garten, 2006; Garten et al., 2000; Nadelhoffer and Fry, 1988b; Powers and Schlesinger, 2002). In the studies of Garten (2006) or Acton et al. (2013), rates of changes in  $\delta^{13}\text{C}$  throughout soil profile were interrelated to isotopic fractionation during decomposition and a relationship between  $^{13}\text{C}$  enrichment and C turnover verified by laboratory incubation meas-

measurements of soil C mineralization (Garten, 2006) and by carbon isotope mass balance modeling and meta-analysis (Acton et al., 2013). In these studies, the regression between log-transformed carbon contents (= soil depth) and  $\delta^{13}\text{C}$  values were established and slopes of the linear regressions (= beta values) were used to describe shifts of  $^{13}\text{C}$  throughout the soil profiles, while beta values served as proxy for C turnover. Except for the Suess effect all other processes potentially explaining the depth profile of  $\delta^{13}\text{C}$  values (see preceding paragraph) are affected by many environmental conditions including climate. Although temperature and precipitation effects on  $\delta^{13}\text{C}$  depth profiles were reported in several studies (Garten, 2006, 2011; Garten et al., 2000), such effects might be caused by factors that coincided with temperature/precipitation gradients and thus, influenced shifts of  $^{13}\text{C}$  throughout soil profile in the above-mentioned studies: (i) soil texture, (ii) tree species, (iii) litter quantity and quality or (iv) site exposition. A field study is necessary along temperature and precipitation gradients with negligible variation in soil, vegetation and site characteristics. Since in former studies on  $\delta^{13}\text{C}$  depth profiles these factors were not considered systematically, environmental conditions excluding temperature and precipitation need to be comparable among sites.

The relationship between temperature and reaction rates as well as biological processes established by Van't Hoff (1884) generally indicates an accelerated turnover of soil organic matter (SOM). On the other hand, soil moisture which is controlled by both, temperature and precipitation, might influence microbial activity (Davidson and Janssens, 2006; Giardina and Ryan, 2000; Goebel et al., 2011; Moyano et al., 2013). Because experimental field or laboratory studies have restricted predictive power for temperature and precipitation effects under real field conditions (Borken et al., 2006; Kirschbaum, 2000; Schindlbacher et al., 2012; Unger et al., 2010), studies along natural gradients are useful (Meier and Leuschner, 2010; Scharnweber et al., 2011; Wang et al., 2013).

In our study, we therefore selected forest sites with comparable environmental characteristics and soil properties across a temperature (7.9 to 9.7°C MAT) and a precipitation gradient (607 to 1085 mm MAP) under beech (*Fagus sylvatica* L.) forests in northern Rhineland-Palatinate. In high resolution we analyzed the organic layers and the upper mineral soil. Our objective was to assess temperature and precipitation effects on  $\delta^{13}\text{C}$  depth profiles. According to former studies (Acton et al., 2013; Garten, 2006; Powers and Schlesinger, 2002), the degree of  $^{13}\text{C}$  enrichment in SOM was described by beta values ( $(\delta^{13}\text{C}/\log(\text{g C kg}^{-1}))$ ) i.e., the absolute values of the slopes of the linear re-

gressions between log-transformed carbon contents (= soil depth) and  $\delta^{13}\text{C}$  values. We hypothesized that (i) higher temperatures increase microbial activity and decomposition of SOM and thus, beta values and (ii) increasing precipitation positively affects decomposition in soil due to conditions favorable for microbial activity and enhances the downward transport of microbial cycled DOM and therefore, increases beta values.

## 2.3 Material and methods

### 2.3.1 Sampling sites

Sampling sites were located across temperature and precipitation gradients in mature beech (*Fagus sylvatica* L.) forest ecosystems under silvicultural use in Rhineland-Palatinate (Fig. 2.1). ArcGIS Desktop (10) was used to select sampling sites out of the extensive geodata sets provided by the Rhineland-Palatinate Forest Administration, the Rhineland-Palatinate Geological Survey and Mining Authority, the Rhineland-Palatinate Centre of Excellence for Climate Change Impacts and the German Weather Service. Environmental characteristics other than climate and altitude (i.e., soil type, soil texture, tree species, stand age and exposition) did not differ among sampling sites (Tab. 2.1).

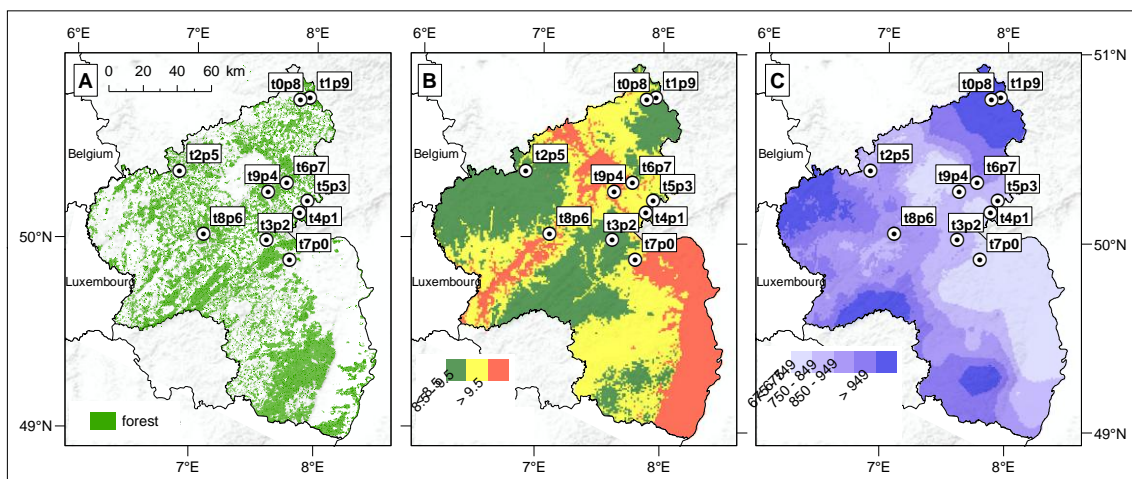


Figure 2.1 Maps of the sampling sites with distribution of forest areas in Rhineland-Palatinate (A), the temperature gradient (B) and the precipitation gradient (C).

In general, the selection of sites was different to the random approach commonly used. Due to our preselection, temperature (and altitude) and moisture are the only variables that differ across our study sites and therefore, site-effect is reduced which does minimize the need for replicates but does restrict the transferability to other site conditions.

Table 2.1 Selection criteria for all sampling sites across the temperature and precipitation gradient in Rhineland-Palatinate, Germany

<b>Environmental Characteristic</b>	<b>Value</b>	
<b>Soil</b>	Soil type	Cambisol
	Soil texture	Clayloam (20-30% clay; 50-65% silt) with siliceous sandstone as detritus (Lower Devonian)
	Bedrock	Deep argillaceous schist (Lower Devonian)
	Soil physical properties	Oven-dry-density $\leq 1.2 \text{ gcm}^{-3}$ ; free of carbonate
<b>Forest site</b>	Dominant tree species	<i>Fagus sylvatica</i> L.
	Tree species mixture	Monocultures (< 10 % other tree species)
	Stand age	40-70 years (sites t2p5 = 90 years and t3p2 = 25 years)
	Potential natural vegetation	Luzulo-Fagetum; Hordelymo-Fagetum
<b>Site properties</b>	Slope	0-26°
	Exposition	Northeast, north or northwest
	Altitude	140-440 m.a.s.l.(mean altitude = $323 \pm 31$ m)

Temperature and precipitation data is based on interpolated climate data (reference period 1971-2000) with a spatial resolution of 1x1 km (German Weather Service). Climate characteristics were selected in an orthogonal way that allowed for a separation between temperature and precipitation effects i.e., differences in temperature under constant precipitation and vice versa (Tab. 2.2). We aggregated the data of the precipitation gradient with sites < 8.5°C MAT and gradient with sites MAT 8.5 to 9.5°C to investigate precipitation effect on beta values and on C:N ratios.

The temperature gradient covaried with an altitudinal gradient. Altitude and temperature were related significantly ( $y = -0.01x + 10.51^{***}$ ;  $r = -0.92$ ). We did not vary altitude and temperature separately, so that a potential altitudinal effect forms part of our temperature gradient. The maximum difference in altitude in our study was 300 m and thus, small in comparison with literature on altitudinal effects on carbon isotope fractionation (Körner et al., 1991).

Table 2.2 Sampling sites within the temperature and precipitation gradient with according MAT [ $^{\circ}\text{C}$ ] and MAP [ $\text{mm}\cdot\text{yr}^{-1}$ ]. MAP varied between 675 to 733 mm across the temperature gradient, while MAT varied between 7.94 to 9.07 $^{\circ}\text{C}$  across the precipitation gradient.

		Precipitation gradient $\rightarrow$			
		< 675	675-749	750-849	$\geq 950$
Temperature gradient $\rightarrow$	$\geq 9.5$		t8p6; t9p4		
	8.5-9.5	t4p1; t7p0	t5p3	t6p7	
	< 8.5		t2p5; t3p2		t0p8; t1p9

### 2.3.2 Sampling and sample preparation

Organic matter and soil samples were collected at ten forest sites in November and December 2011, shortly after the autumnal abscission of the leaves. At each sampling site, five replicates were taken.

Soil samples were collected by a root auger (Eijkelkamp Agrisearch Equipment BV, Netherlands). Since the  $^{13}\text{C}$  enrichment throughout the soil is most pronounced in the upper centimeters of the soil profile (Accoe et al., 2003; Fang and Moncrieff, 2005; Kammer et al., 2012) soil cores were taken to a depth of 10 cm of the mineral soil. The soil cores with a diameter of 8 cm were cut into 1 cm sections and each stored separately in plastic bags.

The organic layers were collected as Oi (litter), Oe and Oa horizon prior to cutting the mineral soil into sections. The high percentage of the coarse fractions in soil at some forest sites restricted the depth which could be sampled resulting in a sampling depth of 7 cm at site t7p0 D, 8 cm at site t5p3 C and 9 cm for two replicates of the site t8p6 (A and B) and at the sites t1p9 D, t2p5 C, t3p2 E and t7p0 D.

All samples were oven dried at 55 $^{\circ}\text{C}$  until weight constancy. The dried organic layer samples were ground in a shredder (Retsch SM 2000) resulting in a homogeneous mixture. Dried mineral soil samples were sieved through a 2 mm sieve. Thereafter, these aliquots and those of the shredded organic layer samples were ground and homogenized with a Planetary Ball Mill PM 200 (Retsch, Germany).



### 2.3.3 Roots

To keep the root impact in our study as small as possible we i) chose forest sites with potential natural vegetation with negligible understory vegetation (Hordelymo- or Luzulo-Fagetum) and ii) removed all visible roots of each mineral soil sample by a pair of tweezers.

In preliminary studies (unpublished), we tested the impact of fine root removal on  $\delta^{13}\text{C}$  depth profiles. In 4 out of 5 soil profiles,  $\delta^{13}\text{C}$  depth profiles containing fine roots were less steep compared to  $\delta^{13}\text{C}$  depth profiles without fine roots (Chow-test,  $F(2,16)$  = range between 6.1 to 224.3,  $p \leq 0.01$ ). In addition to this, we analyzed the vertical change of  $\delta^{13}\text{C}$  values of removed roots at two selected sites ( $n = 93$  samples). The difference between roots of each depth and the respective Oi horizon ranged between  $-0.1$  to  $+3.2\text{‰}$  and thus, was not consistent across the depth profiles. On average, SOM was by  $2.7 \pm 0.5\text{‰}$  enriched in  $^{13}\text{C}$  compared to the Oi horizon (Wilcoxon signed-rank test,  $Z(93) = -12.0$ ,  $p < 0.001$ ) while roots were only by  $1.1 \pm 1.1\text{‰}$   $^{13}\text{C}$  enriched compared to the Oi horizon (Wilcoxon signed-rank test,  $Z(93) = -6.5$ ,  $p < 0.001$ ). Due to the results of these preliminary studies, we deduce that the contribution of roots to the  $\delta^{13}\text{C}$  depth profile is insufficient to explain entire  $^{13}\text{C}$  enrichment in SOM.

### 2.3.4 Laboratory analysis

#### 2.3.4.1 pH measurement

According to DIN 19684, 12.5 ml of 0.01 N  $\text{CaCl}_2$  solution was added to 5 g of a mixed soil sample of each soil core and stirred 5 minutes. The suspension was allowed to settle for one hour and then stirred up again. Afterwards, pH was measured with an HI 1292 electrode (HANNA instruments, Germany).

#### 2.3.4.2 Elemental and isotopic measurements

Carbon and nitrogen contents (w/%) were determined with an Elemental Analyzer (Vario EL III, Elementar). Since all soil samples were strongly acidic (pH 3.6 to pH 4.5) and free of carbonate (Tab. 3), the measured total C content was equivalent to the organic C content. Stable C isotope ratios were analyzed by a coupled isotope ratio mass spectrometry (IRMS) (Isoprime, GV Instruments, UK). Results are given in delta notation as  $\delta^{13}\text{C}$  in  $\text{‰}_{\text{VPDB}}$  (Eq.2.1):

$$[2.1] \quad \delta^{13}\text{C} = \left[ \frac{(R_{\text{sample}} - R_{\text{standard}})}{R_{\text{standard}}} \right] \times 1000$$

where R is the  $^{13}\text{C}/^{12}\text{C}$  ratio. We used IAEA-CH-6 and IAEA-CH-7 for normalization of measured  $\delta^{13}\text{C}$  values to the VPDB scale. Long-term measurement accuracy of IRMS analyses based on routine measurements of interspersed standard samples in each run (total number of standard replicates for this study:  $n = 100$ ) of sulfanilic acid (Merck KGaA, Germany) during the measurement period was  $\pm 0.3\%$ . We regularly evaluated the EA-IRMS system for nonlinearity and measurement drift and found that both did not affect the measurements beyond the general long-term measurement accuracy of  $0.3\%$ .

### 2.3.5 Statistical analysis and calculation of beta values

The  $\delta^{13}\text{C}$  depth profile approach is based on the vertical decrease of C content similarly to the SOC decay in soil as an approximation of the depth increments (Garten et al., 2000). Beta values were derived from the slopes of the linear regressions (Eq. 2.2)

$$[2.2] \quad \text{beta}_{yx} = \left| \frac{\sum_{i=1}^n ((x_i - \bar{x}) \times (y_i - \bar{y}))}{\sum_{i=1}^n (x_i - \bar{x})^2} \right|$$

between log-transformed C contents ( $\log(\text{g C kg}^{-1})$ ) ( $= x$ ) and their respective  $\delta^{13}\text{C}$  values ( $\text{‰}_{\text{VPDB}}$ ) ( $= y$ ) of the depth intervals (organic layers and of the mineral soil). We refer to the absolute value of the slope of the linear regression equation as beta values. Since environmental characteristics and soil properties, except climate and altitude were held constant, these beta values represent the climate dependent change in the  $\delta^{13}\text{C}$  values from fresh litter input to older SOM for every tenfold increase in the SOC content and, these beta values can be considered as indicative of isotopic fractionation during decomposition combined with physical processes in soil (Acton et al., 2013; Garten, 2006).

We employed linear regression analyses to quantify the influence of climatic parameters (MAT and MAP). The level of significance was set at  $p \leq 0.05$  in all tests. The prerequisite of normal distribution was verified by a Kolmogorov-Smirnov test.

## 2.4. Results

### 2.4.1 $\delta^{13}\text{C}$ depth profiles

With increasing soil depth the mean SOC content decreased from  $47.5 \pm \text{SD } 1.1\%$  to  $2.5 \pm 0.8\%$  while the mean  $\delta^{13}\text{C}$  values increased from  $-29.4 \pm 0.8\text{‰}$  to  $-26.1 \pm 0.6\text{‰}$  (Fig. 2.2). The vertical depth increase coincided with a decrease in the C content ( $y = 3.17x + 24.36^{***}$ ;  $r = 0.81$ ). In 26% of the profiles in our study, C contents of single increments ( $n = 16$ ) throughout the soil profile deviated marginally from trends of decreasing values with soil depth.

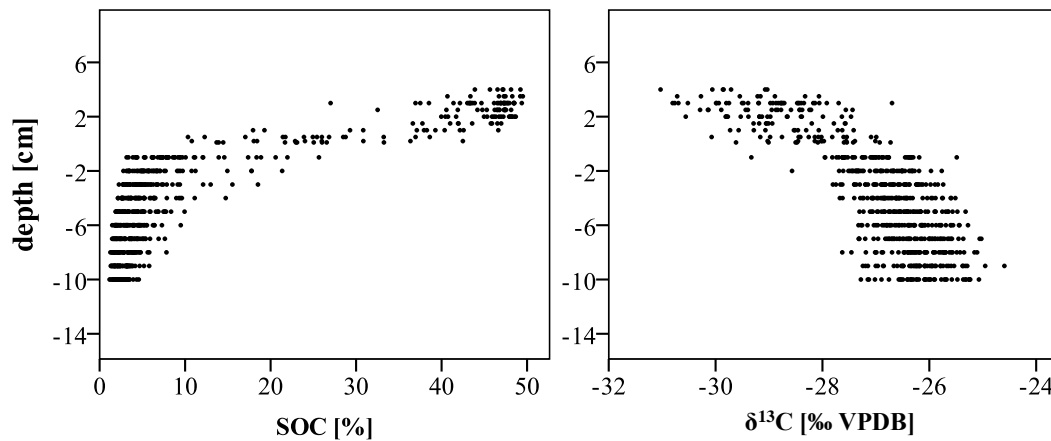


Figure 2.2 Changes of the soil organic carbon content (SOC) [%] and the  $\delta^{13}\text{C}$  values [ $\text{‰}_{\text{VPDB}}$ ] with depth of all sites.

The relative standard deviation ( $\% \text{RSD} = \text{relative standard deviation calculated by dividing the standard deviation by the mean}$ ) of  $\delta^{13}\text{C}$  values in the litter ( $\text{RSD} = 2.7\%$ ) was nearly comparable to the RSD of  $\delta^{13}\text{C}$  values in the mineral soil at 10 cm depth ( $\text{RSD} = 2.2\%$ ). The mean  $^{13}\text{C}$  enrichment i.e., the difference between  $\delta^{13}\text{C}$  values of the Oi horizon and  $\delta^{13}\text{C}$  values of SOM in 10 cm soil depth was  $3.4 \pm \text{SE } 0.2\text{‰}$  (Tab. 2.3). The logarithm of C contents was related closely to the change in  $\delta^{13}\text{C}$  values from the organic layers down to 10 cm of the mineral soil. Linear regressions between the log transformed C contents ( $\log(\text{g C kg}^{-1})$ ) and the corresponding  $\delta^{13}\text{C}$  values ( $\text{‰}_{\text{VPDB}}$ ) were highly significant ( $P \leq 0.008$ ) throughout all sampling sites with  $r$  ranging between  $-0.69$  and  $-0.99$  (Fig. 2.3). The variation of beta values among the five replicates within one forest site was low with RSD ranging between 9% (sites t3p2 and t4p1) and 33% (site t9p4). Beta values were most pronounced if the organic horizons were included

into the linear regressions, resulting in steeper regression slopes (higher beta values) in soil profiles containing the organic horizons compared to regressions in the mineral soil only ( $\beta_{\text{MineralSoil}}$ ) ( $\beta = 2.4 \pm 0.1$ ;  $\beta_{\text{MineralSoil}} = 2.0 \pm 0.2$ ).

#### 2.4.2 Temperature and precipitation gradient

The litter layer (Oi horizon) of the warmer sites tended to have higher  $\delta^{13}\text{C}$  values (Tab. 2.3) and its  $\delta^{13}\text{C}$  values were positively related to MAT ( $y = 0.65x - 34.89^{**}$ ;  $r = 0.59$ ). Site t8p6 B had an exceptionally high  $\delta^{13}\text{C}$  value in the Oi horizon that deviates from other Oi  $\delta^{13}\text{C}$  values and that was higher than  $\delta^{13}\text{C}$  values from deeper soil depth (Fig. 2.3). We found a weak negative relation between altitude and litter  $\delta^{13}\text{C}$  values with  $y = -0.003x - 28.31^{**}$ ;  $r = -0.39$ . Mean root: finefraction mass ratio of the removed roots ranged between  $0.004 \text{ g g}^{-1}$  (site t8p6) and  $0.02 \text{ g g}^{-1}$  (site t1p9) (Tab. 2.3) and no impact of MAT or MAP was found.

Table 2.3 Sampling sites with according site characteristics, mean root mass in  $\text{g} \cdot \text{roots} \cdot \text{g}^{-1}_{\text{finefraction}}$ , Oi horizon (litter)  $\delta^{13}\text{C}$  values and  $^{13}\text{C}$  enrichment from top Oi horizon down to the mineral soil at 10 cm depth. Mean values with  $\pm\text{SE}$  and  $n$ .

Site	MAT [°C]	MAP [mmyr <sup>-1</sup> ]	Altitude [m.a.s.l.]	pH	Mean root mass [gg <sup>-1</sup> ]	Litter $\delta^{13}\text{C}$ [‰ VPDB]	Mean $^{13}\text{C}$ enrichment [‰ VPDB]
<b>t0p8</b>	7.94	1037	385	3.6	0.01±0.00; n=50	-30.7±0.1; n=5	5.2±0.2; n=5
<b>t1p9</b>	8.28	1085	386	3.9	0.02±0.00; n=49	-29.4±0.3; n=5	3.3±0.3; n=4
<b>t2p5</b>	8.30	704	440	4.2	0.01±0.00; n=49	-29.4±0.1; n=5	3.5±0.2; n=4
<b>t3p2</b>	8.34	675	425	4.5	0.01±0.00; n=49	-29.7±0.2; n=5	3.7±0.2; n=4
<b>t4p1</b>	8.76	643	342	4.0	0.01±0.00; n=50	-29.3±0.3; n=5	3.3±0.2; n=5
<b>t5p3</b>	8.81	681	367	4.0	0.01±0.00; n=48	-29.0±0.2; n=5	2.4±0.1; n=4
<b>t6p7</b>	8.96	766	277	4.4	0.00±0.00; n=50	-29.3±0.2; n=5	3.8±0.3; n=5
<b>t7p0</b>	9.07	607	245	4.5	0.01±0.00; n=46	-29.6±0.2; n=5	3.1±0.2; n=3
<b>t8p6</b>	9.52	733	225	3.9	0.00±0.00; n=48	-28.3±0.4; n=5	3.3±0.3; n=3
<b>t9p4</b>	9.73	683	140	4.5	0.01±0.00; n=50	-28.9±0.4; n=5	2.1±0.3; n=5

Beta values decreased with increasing temperature (Fig. 2.4). The highest mean beta value of  $4.0 \pm 0.2$  was found at site t0p8, the forest site with the lowest MAT. The lowest mean beta value of  $0.9 \pm 0.1$  was observed at site t9p4, the site with the highest MAT (Fig. 2.3).

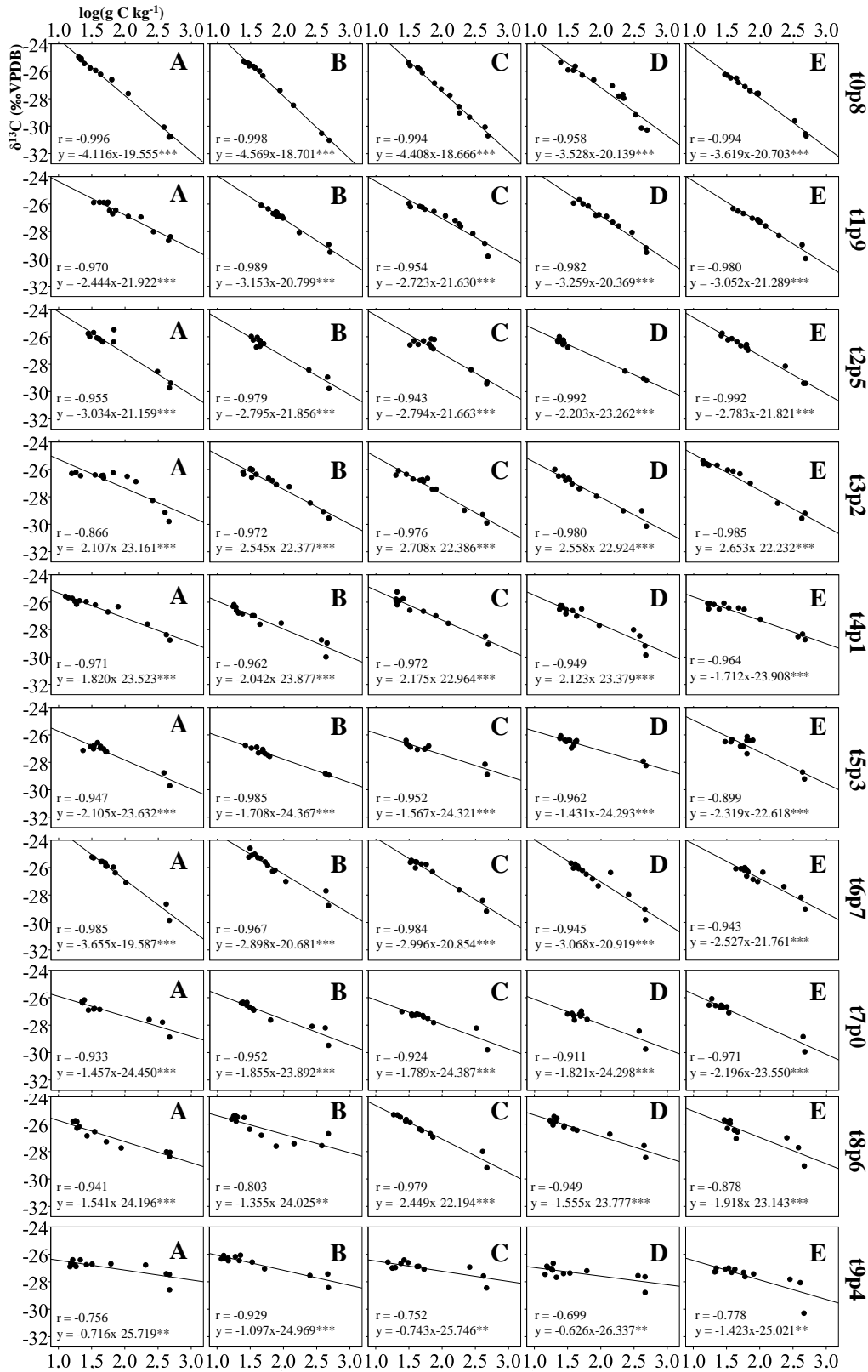


Figure 2.3 Regressions between C content ( $\log_{10}(\text{g C kg}^{-1})$ ) and the corresponding  $\delta^{13}\text{C}$  values [% $\text{VPDB}$ ] for all sampling sites with 5 replicates each (A, B, C, D, E) and according linear regression line. \* $P < 0.05$ ; \*\* $P < 0.01$ ; \*\*\* $P < 0.001$ .

We found an increase of C: N ratios with increasing temperature in the Oi horizon (Fig. 2.5). The C: N ratios of the mineral soil were not related to the MAT.  $\delta^{13}\text{C}$  values in the Oi horizon were weakly related to MAP ( $y = -0.001x - 28.41^{**}$ ;  $r = -0.40$ ) i.e., the litter  $\delta^{13}\text{C}$  values decreased with increasing precipitation. Beta values were positively related to MAP (Fig. 2.4). The C: N ratios of the mineral soil decreased with increasing MAP, whereas we found no significant change of the C:N ratios with increasing precipitation in the Oi horizon (Fig. 2.5).

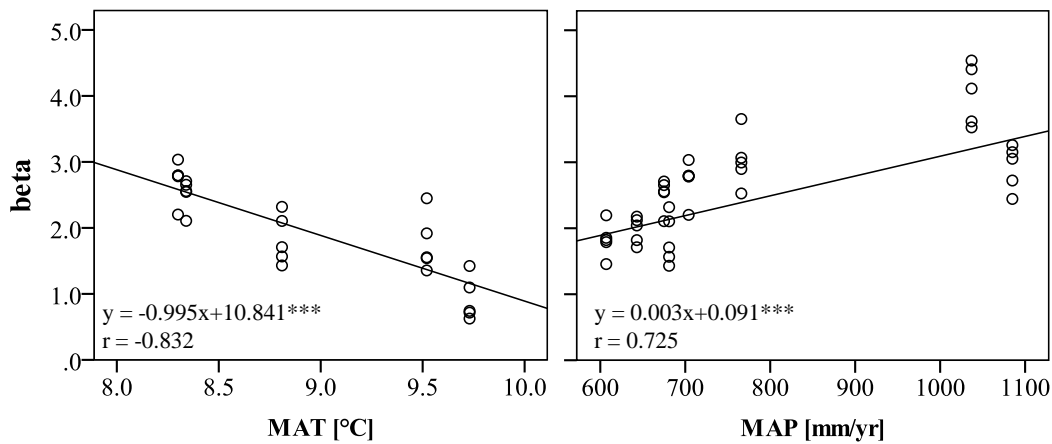


Figure 2.4 Beta values ( $[\delta^{13}\text{C}/\log_{10}(\text{g}\cdot\text{C}\cdot\text{kg}^{-1})]$ ) across the temperature gradient ( $^{\circ}\text{C}$  MAT) and the precipitation gradient ( $\text{mm}\cdot\text{yr}^{-1}$  MAP) with linear regression lines. \*\*\*  $P < 0.001$ .

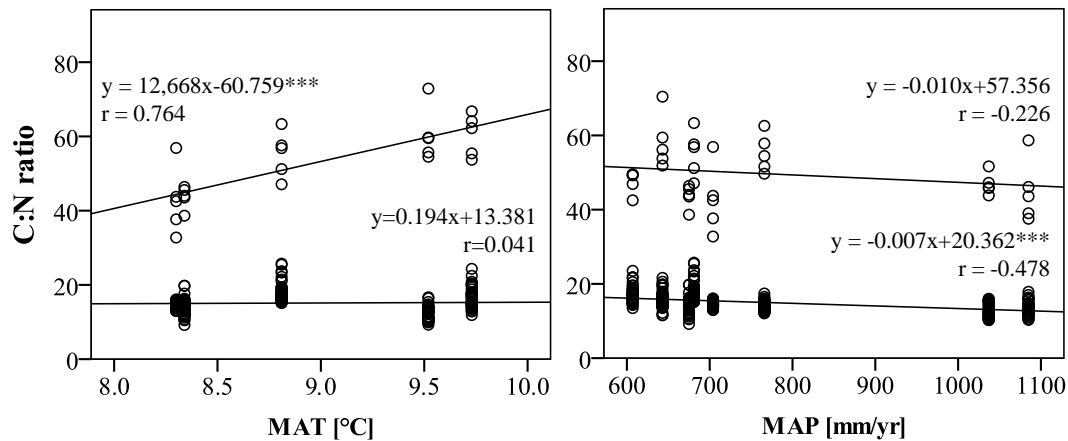


Figure 2.5 C: N ratios of the Oi layer (upper circles) and the mineral soil (circles below) across the temperature gradient ( $^{\circ}\text{C}$  MAT) and the precipitation gradient ( $\text{mm}\cdot\text{yr}^{-1}$  MAP) with linear regression lines. \*\*\*  $P < 0.001$ .

If the organic horizons were excluded from the linear regressions between  $\delta^{13}\text{C}$  and  $\log C$  contents, no significant relation was found for  $\beta_{\text{MineralSoil}}$  and MAT ( $y = -0.060x + 2.149$ ;  $r = -0.027$ ) but for  $\beta_{\text{MineralSoil}}$  and MAP ( $y = 0.003x - 0.06^{**}$ ;  $r = 0.46$ ).

## 2.5 Discussion

Our results confirm the widely reported enrichment of  $^{13}\text{C}$  in SOM with increasing soil depth (Accoe et al., 2003; Boström et al., 2007; Dümig et al., 2013; Garten, 2006; Nadelhoffer and Fry, 1988b). Measured mean  $^{13}\text{C}$  enrichment (3.4‰) nearly doubled the historic change of  $\delta^{13}\text{C}$  in the atmosphere (around 1.8‰) (Francey et al., 1999; Keeling et al., 2005). This is according to former investigations (Balesdent et al., 1993; Ehleringer et al., 2000; Garten et al., 2000; Torn et al., 2002; Werth and Kuzyakov, 2010; Wynn et al., 2005) and discloses that in addition to the Suess effect other processes must contribute to the shifts of  $^{13}\text{C}$  throughout the soil profile. While there might be a systematic influence of the Suess effect for all of our study sites, we can exclude a temperature/moisture-dependent Suess effect for our sites with a maximum distance of less than 100 km. To minimize the well known root impact on  $\delta^{13}\text{C}$  values throughout soil profile we i) chose northern exposed forest sites with potential natural vegetation with negligible understory vegetation and ii) removed all visible roots before analysis. In a preliminary study, the comparison of  $\delta^{13}\text{C}$  values of Oi horizon, roots and SOM suggested that roots were unlikely to entirely explain the vertical  $^{13}\text{C}$  changes in SOM.

To compare the dimension of vertical  $\delta^{13}\text{C}$  changes in SOM in high spatial resolution, we used the widely accepted (Campbell et al., 2009; Ehleringer et al., 2000; Garten, 2006; Garten et al., 2000; Nadelhoffer and Fry, 1988b; Powers and Schlesinger, 2002) relationship between SOM decay and vertical  $^{13}\text{C}$  enrichment by using beta values. The average beta values in our study were higher than values observed along an elevation gradient in temperate Southern Appalachian Mountains, USA (Garten, 2006; Garten et al., 2000) and lower than beta values observed in tropical Costa Rica (Powers and Schlesinger, 2002). In total, the range of beta values between 0.6 and 4.5 exceeded the range of beta values in the above mentioned studies. However, heterogeneous species (Brüggemann et al., 2011; Garten and Taylor, 1992), decomposition state of the litter (Kammer et al., 2012), soil texture differences (Bird et al., 2003; Wynn et al., 2005) or the different sampling methods within and among the studies might result in

specific beta values at different forest sites and therefore, lead to variations in beta values that hampers the comparability.

Yet, the impact of the Oi horizon  $\delta^{13}\text{C}$  values on beta is not fully understood. The initial substance should not affect the dimension of beta values within the decay continuum, as it has already been proposed by Garten et al. (2000) and is confirmed by comparable variations of  $\delta^{13}\text{C}$  values in the litter and in the mineral soil at 10 cm depth in our study. On the other hand, if we extended our approach to greater soil depths ( $> 10$  cm) and a specific steady-state  $\delta^{13}\text{C}$  value in greater soil depth existed,  $\delta^{13}\text{C}$  values in the litter would affect the slopes of the linear regressions used for beta. If the organic horizon was excluded from the linear regressions, no relation was found for  $\text{beta}_{\text{MineralSoil}}$  and MAT but for  $\text{beta}_{\text{MineralSoil}}$  and MAP, likely indicating a stronger impact of precipitation on the development of  $\delta^{13}\text{C}$  depth profiles in our study.

### 2.5.1 Temperature impact on $\delta^{13}\text{C}$ depth profiles

The litter layer (Oi horizon) of the warmer sites tended to have higher  $\delta^{13}\text{C}$  values (Tab. 2.3). The isotopic composition of C in litter partly reflects temperature conditions due to temperature impacts on plant physiological processes i.e., an air-to-leaf water vapor pressure deficit might force the stomata to be closed, the dark respiration could be enhanced, or temperature might lower the soil moisture through evapotranspiration. In the study of Wang et al. (2013), temperature and  $\delta^{13}\text{C}$  values of leaves were positively related along a 400 mm precipitation isoline corroborating our results. In contrast, Körner et al. (1991) found decreasing  $\delta^{13}\text{C}$  values in leaves with increasing temperature (decreasing latitude). But they emphasized the sampling of non water-stressed plants. Strong interrelations between temperature and humidity constrain the interpretation of sole temperature effects on litter  $\delta^{13}\text{C}$  values. Although we found a weak negative relation between altitude and litter  $\delta^{13}\text{C}$  values, the precipitation impact or the low altitudinal difference of 300 m might have diminished the isotopic fractionation effects leading to  $^{13}\text{C}$  enrichment with increasing altitude described by Körner et al. (1991). Furthermore, a potential altitude influence on the input signal ( $\delta^{13}\text{C}$  of the litter) was normalized by the regression used for calculating beta values.

Beta values were significantly lower in case of higher temperatures (Fig. 2.4). These findings contradict the interrelations of MAT and beta values of compiled data presented by Acton et al. (2013). If beta values are understood as proxy for C decomposition



(Acton et al., 2013; Garten, 2006), we can deduce decreasing decomposition of SOM under increasing temperatures. This is counterintuitive given the well-known relationship between temperature and reaction rates established by Van't Hoff (1884) that was corroborated by a positive relationship between temperature and carbon turnover (Amundson, 2001; Kirschbaum, 2000). The C:N ratio of the litter as an indicator for substrate decomposability was greater at sites with high temperatures as compared to sites with lower temperatures and might corroborate decreased litter decomposability in case of higher temperatures. Positive relationships between C:N ratios in litter and temperature were reviewed by Sardans et al. (2012) and typical for temperate ecosystems where high temperatures coincide with droughts.

As a result of high evapotranspiration at warmer sites in our study, soil moisture might have been reduced. Together with a low degradable litter (greater C:N ratios), the low soil moisture might have negatively affected microbial activity and the downward cycling of  $^{13}\text{C}$  enriched material. Therefore,  $\delta^{13}\text{C}$  depth profiles in SOM were less developed i.e., the  $^{13}\text{C}$  enrichment was distinctly smaller at the warmer sites. However, a sole temperature effect on  $\delta^{13}\text{C}$  depth profiles without a restriction on drought remains unclear.

### 2.5.2 Precipitation impact on $\delta^{13}\text{C}$ depth profiles

We found increasing beta values with increasing precipitation (Fig. 2.4). Higher decomposition under higher MAP was not consistently in line with literature. Precipitation increases were generally assumed to hamper decomposition, thus turning forest soils into C sinks (Amundson, 2001; Meier and Leuschner, 2010). Due to slope positions of our study sites, we presume no longer periods under saturated condition in soil matrix resulting in low microbial respiration. A higher decomposition under higher precipitation was supported by decreasing C: N ratios in mineral soil with increasing precipitation (Fig. 2.5) which may confirm the enhanced microbial decomposition due to better substrate decomposability or a relative accumulation of N. Higher water infiltration in soils under higher precipitation likely promoted conditions favorable for microbial activity in our study.

Vertical percolation of soil solution plays an important role in the translocation of  $^{13}\text{C}$  enriched DOC (Nakanishi et al., 2012). Dissolved organic carbon, originating from recent photosynthates, appeared to be more mobile and enriched in  $^{13}\text{C}$  as compared to

organic material with higher degradation status. Microbially altered or recycled materials are sorbed preferentially and depleted in  $^{13}\text{C}$  (Cleveland et al., 2004; Guggenberger and Kaiser, 2003; Nakanishi et al., 2012). The combination of the sorption of  $^{13}\text{C}$ -depleted products and the downward transport of  $^{13}\text{C}$  enriched material resulted in a distinct  $\delta^{13}\text{C}$  depth profile (Nakanishi et al., 2012). Optimal microbial activity in combination with high water fluxes and the sufficient input of plant material with specific litter quality likely guaranteed the release of overlaying SOM and enhanced the development of distinct  $\delta^{13}\text{C}$  depth profiles under higher precipitation.

Again, similar to temperature effects, we presume that precipitation effects on the  $^{13}\text{C}$  enrichment in soil profile were influenced by the interacting effects of (i) specific litter quality (e.g. changing C:N ratios), (ii) microbial respiration (e.g. degree of fractionation) and (iii) the physico-chemical sorption properties of the soils (e.g. amount of percolating soil solution), leading to a more pronounced  $^{13}\text{C}$  enrichment at sites with higher precipitation.

## 2.6 Conclusion

Temperature and precipitation impacts on vertical changes of SOC and  $\delta^{13}\text{C}$  values were investigated in 1-cm-intervals in SOM from Oi horizon down to the mineral soil at 10cm depth at 10 forest sites. With increasing soil depth we found decreasing SOC content while the  $\delta^{13}\text{C}$  values increased. Soils under higher temperatures exhibited a lower  $^{13}\text{C}$  enrichment compared to soils under higher precipitation. Therefore, these vertical depth profiles of  $\delta^{13}\text{C}$  values combined with C:N ratios in litter and in mineral soil indicated climate-driven decomposition trends. The results fit well to recent models and studies evidencing a combination of isotopic fractionation during microbial metabolism, of physical mixing processes during decomposition, and of downward transport of  $^{13}\text{C}$  enriched DOC inducing the vertical  $^{13}\text{C}$  enrichment in SOM.

However, uncertainties remained on temperature effects on  $\delta^{13}\text{C}$  depth profiles not affected by drought, the evidence of the decay continuum, interannual changes of depth profiles and on the time scale on which  $\delta^{13}\text{C}$  depth profiles develop and therefore, further studies on the dynamics and mechanisms of  $\delta^{13}\text{C}$  depth profiles are needed to fully explain climate impacts on vertical  $^{13}\text{C}$  enrichment in SOM and a supposed link to C decomposition and the physical accessibility of C.

## 2.7 Acknowledgement

We are grateful to the members of the Rhineland-Palatinate Centre of Excellence for Climate Change Impacts who provided extensive geodata committed by the Rhineland-Palatinate Forest Administration (Landesforsten RLP), the German Weather Service (DWD) and the Rhineland-Palatinate Geological Survey and Mining Authority (LGB RLP). Thanks to all the forest officials who kindly enabled the sampling. We extend our sincere thanks to Karina Traub and Ulli Bange (University of Koblenz) for collaboration and excellent assistance in the field and in the laboratory. Further special thanks go to Marc Ruppenthal (University of Tübingen) and Florian Brunn (University of Mainz) who valuably supported in analytical consultancy and solving problems. The research was funded by a grant of the Grant Foundation Rhineland-Palatinate (Stipendienstiftung RLP) and the Interdisciplinary Graduation Center (IPZ Koblenz) which we gratefully acknowledge.

## 2.8 References

- Accoe, F., Boeckx, P., Van Cleemput, O., Hofman, G., 2003. Relationship between soil organic C degradability and the evolution of the delta  $\delta^{13}\text{C}$  signature in profiles under permanent grassland. *Rapid Communications in Mass Spectrometry* 17(23), 2591-2596.
- Acton, P., Fox, J., Campbell, E., Rowe, H., Wilkinson, M., 2013. Carbon isotopes for estimating soil decomposition and physical mixing in well-drained forest soils. *Journal of Geophysical Research-Biogeosciences* 118(4), 1532-1545.
- Amundson, R., 2001. The carbon budget in soils. *Annual Review of Earth and Planetary Sciences* 29, 535-562.
- Badeck, F.W., Tcherkez, G., Nogues, S., Piel, C., Ghashghaie, J., 2005. Post-photosynthetic fractionation of stable carbon isotopes between plant organs - a widespread phenomenon. *Rapid Communications in Mass Spectrometry* 19(11), 1381-1391.
- Balesdent, J., Girardin, C., Mariotti, A., 1993. Site-related  $\delta^{13}\text{C}$  of tree leaves and soil organic matter in a temperate forest. *Ecology* 74(6), 1713-1721.
- Balesdent, J.M., A., 1996. Measurement of soil organic matter turnover using  $^{13}\text{C}$  natural abundance. In: T.W.Y. Boutton, S. I. (Ed.), *Mass spectrometry of soils*, New York, pp. 83-111
- Bird, M., Kracht, O., Derrien, D., Zhou, Y., 2003. The effect of soil texture and roots on the stable carbon isotope composition of soil organic carbon. *Australian Journal of Soil Research* 41(1), 77-94.
- Borken, W., Savage, K., Davidson, E.A., Trumbore, S.E., 2006. Effects of experimental drought on soil respiration and radiocarbon efflux from a temperate forest soil. *Global Change Biology* 12(2), 177-193.
- Boström, B., Comstedt, D., Ekblad, A., 2007. Isotope fractionation and  $^{13}\text{C}$  enrichment in soil profiles during the decomposition of soil organic matter. *Oecologia* 153(1), 89-98.
- Brüggemann, N., Gessler, A., Kayler, Z., Keel, S.G., Badeck, F., Barthel, M., Boeckx, P., Buchmann, N., Brugnoli, E., Esperschütz, J., Gavrichkova, O., Ghashghaie, J., Gomez-Casanovas, N., Keitel, C., Knohl, A., Kuptz, D., Palacio, S., Salmon, Y., Uchida, Y., Bahn, M., 2011. Carbon allocation and carbon isotope fluxes in the plant-soil-atmosphere continuum: a review. *Biogeosciences* 8(11), 3457-3489.
- Campbell, J.E., Fox, J.F., Davis, C.M., Rowe, H.D., Thompson, N., 2009. Carbon and Nitrogen Isotopic Measurements from Southern Appalachian Soils: Assessing Soil Carbon Sequestration under Climate and Land-Use Variation. *Journal of Environmental Engineering-Asce* 135(6), 439-448.

- Cleveland, C.C., Neff, J.C., Townsend, A.R., Hood, E., 2004. Composition, dynamics, and fate of leached dissolved organic matter in terrestrial ecosystems: Results from a decomposition experiment. *Ecosystems* 7(3), 275-285.
- Davidson, E.A., Janssens, I.A., 2006. Temperature sensitivity of soil carbon decomposition and feedbacks to climate change. *Nature* 440(7081), 165-173.
- Dümig, A., Rumpel, C., Dignac, M.F., Kögel-Knabner, I., 2013. The role of lignin for the  $\delta^{13}\text{C}$  signature in C-4 grassland and C-3 forest soils. *Soil Biology & Biochemistry* 57, 1-13.
- Ehleringer, J.R., Buchmann, N., Flanagan, L.B., 2000. Carbon isotope ratios in belowground carbon cycle processes. *Ecological Applications* 10(2), 412-422.
- Fang, C.M., Moncrieff, J.B., 2005. The variation of soil microbial respiration with depth in relation to soil carbon composition. *Plant and Soil* 268(1-2), 243-253.
- Francey, R.J., Allison, C.E., Etheridge, D.M., Trudinger, C.M., Enting, I.G., Leuenberger, M., Langenfelds, R.L., Michel, E., Steele, L.P., 1999. A 1000-year high precision record of  $\delta^{13}\text{C}$  in atmospheric  $\text{CO}_2$ . *Tellus Series B-Chemical and Physical Meteorology* 51(2), 170-193.
- Garten, C.T., 2006. Relationships among forest soil C isotopic composition, partitioning, and turnover times. *Canadian Journal of Forest Research-Revue Canadienne De Recherche Forestiere* 36(9), 2157-2167.
- Garten, C.T., 2011. Comparison of forest soil carbon dynamics at five sites along a latitudinal gradient. *Geoderma* 167-68, 30-40.
- Garten, C.T., Cooper, L.W., Post, W.M., Hanson, P.J., 2000. Climate controls on forest soil C isotope ratios in the Southern Appalachian Mountains. *Ecology* 81(4), 1108-1119.
- Garten, C.T., Taylor, G.E., 1992. Foliar  $\delta^{13}\text{C}$  within a temperate deciduous forest: spatial, temporal and species sources of variation. *Oecologia* 90(1), 1-7.
- Giardina, C.P., Ryan, M.G., 2000. Evidence that decomposition rates of organic carbon in mineral soil do not vary with temperature. *Nature* 404(6780), 858-861.
- Goebel, M.O., Bachmann, J., Reichstein, M., Janssens, I.A., Guggenberger, G., 2011. Soil water repellency and its implications for organic matter decomposition - is there a link to extreme climatic events? *Global Change Biology* 17(8), 2640-2656.
- Guggenberger, G., Kaiser, K., 2003. Dissolved organic matter in soil: challenging the paradigm of sorptive preservation. *Geoderma* 113(3-4), 293-310.
- Kaiser, K., Kalbitz, K., 2012. Cycling downwards - dissolved organic matter in soils. *Soil Biology & Biochemistry* 52, 29-32.
- Kammer, A., Schmidt, M.W.I., Hagedorn, F., 2012. Decomposition pathways of  $^{13}\text{C}$  depleted leaf litter in forest soils of the Swiss Jura. *Biogeochemistry* 108(1-3), 395-411.
- Keeling, C.D., Piper, S.C., Bacastow, R.B., Wahlen, M., Whorf, T.P., Heimann, M., Meijer, H.A., 2005. Atmospheric  $\text{CO}_2$  and ( $^{13}\text{CO}_2$ ) exchange with the terrestrial biosphere and oceans from 1978 to 2000: Observations and carbon cycle implications. In: J.R. Ehleringer, T.E. Cerling, M.D. Dearing (Eds.), *Ecological Studies. Ecological Studies : Analysis and Synthesis*. Springer, 233 Spring Street, New York, Ny 10013, United States, pp. 83-113.
- Kirschbaum, M.U.F., 2000. Will changes in soil organic carbon act as a positive or negative feedback on global warming? *Biogeochemistry* 48(1), 21-51.
- Körner, C., Farquhar, G.D., Wong, S.C., 1991. Carbon isotope discrimination by plants follows latitudinal and altitudinal trends. *Oecologia* 88(1), 30-40.
- Lerch, T.Z., Nunan, N., Dignac, M.F., Chenu, C., Mariotti, A., 2011. Variations in microbial isotopic fractionation during soil organic matter decomposition. *Biogeochemistry* 106(1), 5-21.
- Meier, I.C., Leuschner, C., 2010. Variation of soil and biomass carbon pools in beech forests across a precipitation gradient. *Global Change Biology* 16(3), 1035-1045.
- Moyano, F.E., Manzoni, S., Chenu, C., 2013. Responses of soil heterotrophic respiration to moisture availability: An exploration of processes and models. *Soil Biology & Biochemistry* 59, 72-85.
- Nadelhoffer, K.F., Fry, B., 1988. Controls on natural  $^{15}\text{N}$  and  $^{13}\text{C}$  abundances in forest soil organic matter. *Soil Science Society of America Journal* 52(6), 1633-1640.
- Nakanishi, T., Atarashi-Andoh, M., Koarashi, J., Saito-Kokubu, Y., Hirai, K., 2012. Carbon isotopes of water-extractable organic carbon in a depth profile of forest soil imply a dynamic relationship with soil carbon. *European Journal of Soil Science* 63(4), 495-500.
- Powers, J.S., Schlesinger, W.H., 2002. Geographic and vertical patterns of stable carbon isotopes in tropical rain forest soils of Costa Rica. *Geoderma* 109(1-2), 141-160.
- Sardans, J., Rivas-Ubach, A., Penuelas, J., 2012. The C:N:P stoichiometry of organisms and ecosystems in a changing world: A review and perspectives. *Perspectives in Plant Ecology Evolution and Systematics* 14(1), 33-47.

- Scharnweber, T., Manthey, M., Criegee, C., Bauwe, A., Schroder, C., Wilmking, M., 2011. Drought matters - Declining precipitation influences growth of *Fagus sylvatica* L. and *Quercus robur* L. in north-eastern Germany. *Forest Ecology and Management* 262(6), 947-961.
- Schindlbacher, A., Wunderlich, S., Borken, W., Kitzler, B., Zechmeister-Boltenstern, S., Jandl, R., 2012. Soil respiration under climate change: prolonged summer drought offsets soil warming effects. *Global Change Biology* 18(7), 2270-2279.
- Torn, M.S., Lapenis, A.G., Timofeev, A., Fischer, M.L., Babikov, B.V., Harden, J.W., 2002. Organic carbon and carbon isotopes in modern and 100-year-old-soil archives of the Russian steppe. *Global Change Biology* 8(10), 941-953.
- Unger, S., Maguas, C., Pereira, J.S., David, T.S., Werner, C., 2010. The influence of precipitation pulses on soil respiration - Assessing the "Birch effect" by stable carbon isotopes. *Soil Biology & Biochemistry* 42(10), 1800-1810.
- Wang, G.A., Li, J.Z., Liu, X.Z., Li, X.Y., 2013. Variations in carbon isotope ratios of plants across a temperature gradient along the 400 mm isoline of mean annual precipitation in north China and their relevance to paleovegetation reconstruction. *Quaternary Science Reviews* 63, 83-90.
- Werth, M., Kuzyakov, Y., 2010.  $^{13}\text{C}$  fractionation at the root-microorganisms-soil interface: A review and outlook for partitioning studies. *Soil Biology & Biochemistry* 42(9), 1372-1384.
- Wynn, J.G., Bird, M.I., Wong, V.N.L., 2005. Rayleigh distillation and the depth profile of  $^{13}\text{C}/^{12}\text{C}$  ratios of soil organic carbon from soils of disparate texture in Iron Range National Park, Far North Queensland, Australia. *Geochimica Et Cosmochimica Acta* 69(8), 1961-1973.

### 3 Three decades after afforestation are sufficient to yield decomposition-related vertical $\delta^{13}\text{C}$ depth profiles in soil

Melanie Brunn<sup>1</sup>, Steffi Brodbeck<sup>1</sup>, Yvonne Oelmann<sup>1</sup>

<sup>1</sup> Geoecology, University of Tübingen, Rümelinstraße 19-23, 72070 Tübingen, Germany

### 3.1 Abstract

Decomposition in soils is crucial in evaluating mitigation of rising atmospheric  $\text{CO}_2$  levels with vertical carbon (C) stable isotope distribution in topsoil serving as easily applicable method to investigate C dynamics in soil. Since many parameters affecting  $\delta^{13}\text{C}$  depth patterns can change fast and strongly during land-use changes, vegetation conversions provide valuable insights into C dynamics in soil.

We sampled 36 topsoil core profiles (0-10 cm) with sites under different land-use, i.e. arable sites and continuously forested sites as references for none or maximum development of vertical  $\delta^{13}\text{C}$  distribution, respectively and afforested sites to test for the time of  $\delta^{13}\text{C}$  depth profile formation in the Black Forest, Germany. Relations between the vertical decrease of C and the increase of  $\delta^{13}\text{C}$  values served to approximate decomposition and tested for relationships to potential soil respiration of a laboratory incubation study.

We found an accumulation of C with increasing time of forest cover and a development of  $\delta^{13}\text{C}$  depth profiles within decades. Carbon concentrations and decomposition were positively related, suggesting that C accumulation is not necessarily coupled with reduced decomposition. The Suess effect, increased belowground biomass production and related greater dissolved organic matter production as well as lower pH values may have accounted for greater isotopic differences in topsoil and increased potential soil respiration at afforested sites, leading to greater transport of  $^{13}\text{C}$  enriched microbial products. These parameters appeared to become further amplified at continuously forested sites. In contrast, soils under agricultural use showed near zero vertical enrichment in  $^{13}\text{C}$  but low measured potential soil respiration fits well to trends of increasing decomposition with time of forest cover.

Our results suggest a hampered applicability of vertical C stable isotope distribution to approximate low decomposition in soil, underpin the contribution of respiration to shape vertical C stable isotope patterns and provide evidence that short timescales of 30 yrs are sufficient to develop distinct  $\delta^{13}\text{C}$  depth profiles in topsoil.

### 3.2 Introduction

The vertical change in organic matter (OM) carbon (C) stable isotope ratios is a widely reported phenomenon across varieties of ecosystems and environmental gradi-

ents with OM becoming enriched in the heavier isotope  $^{13}\text{C}$ . The analyses of the vertical  $\delta^{13}\text{C}$  changes have been proven to be a useful tool investigating C processing, with linear regression slopes between logarithmized C concentrations and  $\delta^{13}\text{C}$  values in soil profiles serving to approximate decomposition of OM in soil (Brunn et al., 2016; Brunn et al., 2014). Assessing decomposition experiences significant attention owing to its strong relation to the C sequestration potential of soils and therefore, complements the evaluation of mitigating rising atmospheric  $\text{CO}_2$  concentrations (Lal, 2005; Wiesmeier et al., 2014). It remains an open question on what timescale OM pools react (Schmidt et al., 2011) and how fast  $\delta^{13}\text{C}$  depth profiles develop in soil.

Mechanistically, one main parameter shaping  $\delta^{13}\text{C}$  depth profiles appeared to be the accumulation of  $^{13}\text{C}$  enriched compounds from microbial C processing or microbial cells itself (Diachon and Kellman, 2008; Lerch et al., 2011). Lasting decades,  $^{13}\text{C}$  enriched microbial products might accumulate and facilitate greater enrichment in mineral soil. The atmospheric depletion of  $^{13}\text{CO}_2$  (Rubino et al., 2013) - known as Suess effect - during the past two centuries has often been discussed as another parameter shaping  $\delta^{13}\text{C}$  depth profiles (Acton et al., 2013; Boström et al., 2007; Menichetti et al., 2014). The incorporation of more depleted plant material in the upper parts of topsoil is supposed to enhance the isotopic difference of OM in soil profiles suggesting that the longer the site is exposed to the change of atmospheric  $\delta^{13}\text{CO}_2$ , the more pronounced the depth profile is.

During vegetation changes of ecosystems like the conversion from arable sites to forests, microbial processing and the impact of the Suess effect can profoundly change and therefore affect  $\delta^{13}\text{C}$  depth profiles. This might be attributed to shifted conditions for microbial activity and to time effects. For example, increased above- and below-ground biomass production and potential acidification induced by afforestation of arable sites can shift microbial community structures by promoting fungal abundance (Laganière et al., 2010; Pietri and Brookes, 2009), increase soil respiration (Hall and Silver, 2013) and increase dissolved organic matter production (Hansson et al., 2010) that are supposed to promote the development of distinct  $\delta^{13}\text{C}$  depth profiles (Kaiser and Kalbitz, 2012). While at arable sites, the removal of OM and disturbance by plowing may impede the development of  $\delta^{13}\text{C}$  depth profiles through hampered physical protection and aggregation of OM (Del Galdo et al., 2003; Six et al., 2002), afforested sites should experience a distinct vertical distribution of C stable isotopes. More pronounced  $\delta^{13}\text{C}$  depth profiles under afforested sites might be attributed to accumulated  $^{13}\text{C}$  en-



riched products originating from decomposition of OM, to greater OM inputs (above- and belowground) that can increase respiration, to the Suess effect and to undisturbed transport and sorption processes within the soil column. At continuously forested sites, the consequences of all these parameters should be amplified and facilitate a greater isotopic difference in topsoil and therefore more distinct  $\delta^{13}\text{C}$  depth profiles.

In our study, we focused on the time required for the development of vertical  $\delta^{13}\text{C}$  profiles in soils by comparing arable, afforested and continuously forested sites with different times of 0, < 50 and > 150 yrs grown with Norway spruce in the Black Forest, Germany. In addition, we elucidated decomposition inferred from vertical  $\delta^{13}\text{C}$  profiles patterns by measuring soil respiration in a laboratory incubation study. Our aim was to test whether  $\delta^{13}\text{C}$  depth profiles develop after afforestation of arable land. We hypothesized that  $\delta^{13}\text{C}$  depth profiles do not develop under arable land but vertical changes emerge within decades under afforested cropland and become further amplified at continuously forested sites.

### 3.3 Material and methods

#### 3.3.1 Sampling sites

We chose sites associated with different land-use forms and different times of forest cover (arable sites: 0 yrs, afforested sites: < 50 yrs and continuously forested sites: > 150 yrs) in the Black Forest, Germany (48°16'N, 8°15'E). This area in Southwestern Germany is prominent for a reforestation of former cropland that became unprofitable and thus, land-use change has established as a widely distributed practice within the last century. Arable sites were regularly plowed until a depth of 20 cm and grown with potato, rye and oat in crop rotation. Dominating species at afforested sites was *Picea abies* (L.) Karst. (Norway spruce) that has been cultivated c. 31 to 48 yr ago and has followed crop rotation (potato, rye and oat). Dominating species at continuously forest sites were *Picea abies* (L.) Karst. and *Abies alba* Mill. (Silver fir) which have persisted for  $\geq 150$  yrs. Silvicultural practice at the afforested and the continuously forested sites was selection cutting according to the local "Plenterwald" system. All sites were continuously grown with C3-vegetation and not exceeding a distance of 20 km. Cambisols with gneiss and granite as bedrock were sampled at steep slope positions within an altitudinal range between 385 and 680 meters above sea level. Mean annual temperature (1961-1990) at

Wolfach was 9.4 °C with mean annual precipitation of 1286 mm yr<sup>-1</sup> (German Weather Service).

### 3.3.2 Sampling and sample preparation

For each land-use type, we sampled soil cores in fourfold repetition at three different locations in October and November 2013, i.e. each type contains four pseudoreplicates (fourfold repetition at each site = variation at one site) multiplied by three (sampling at three different locations) resulting in 12 profile samples for each land-use and a total of 36 profile samples. In a quadratic pattern with 20 m distances between corners, we collected samples by a root auger (Eijkelkamp Agrisearch Equipment BV, Netherlands) to a depth of 10 cm in mineral soil and after removal, soil cores (diameter of 8 cm) were cut into 1 cm sections. The organic layers of the afforested and the continuously forested sites were collected as Oi (litter) horizon prior to cutting the mineral soil into sections. Arable sites were plowed and no organic horizon existed.

All samples were oven dried at 50°C until weight constancy. The dried organic layer was ground in a shredder (Retsch SM 2000). Dried mineral soil samples were sieved through a 2 mm sieve and root material was removed. Aliquots were ground and homogenized with a Planetary Ball Mill PM 200 (Retsch, Germany).

### 3.3.4 Laboratory analysis, statistics and calculations

#### 3.3.4.1 pH measurement

PH of soil samples was determined with  $\text{CaCl}_2$  solution and measured with a HI 1292 electrode (Sen Tix 81, WTW, Germany).

#### 3.3.4.2 Potential soil respiration

We determined the potential soil respiration in a two-day laboratory incubation experiment in order to relate them to beta values as an approximation of decomposition. Mineral soil samples were rewetted with deionized water to gain a soil moisture content of 30% and afterwards incubated at  $20 \pm 1$  °C in an airtight leach trap with KOH solution as  $\text{CO}_2$  absorbent (Macfayden, 1970). After 48 hours,  $\text{BaCl}_2$  mixed with a 2.5% phenolphthalein/thymophtalein tracer solution were added to the KOH solution. The released  $\text{CO}_2$  [ml h<sup>-1</sup>] during incubation was determined titrimetrically with HCl solution (Macfadyen 1970) and calculated as [Eq. 3.1]:

$$[3.1] \quad \text{CO}_2 = \frac{0.1 \times (\text{HCl}_b - \text{HCl}_s) \times f_t \times \frac{\text{KOH}_i}{\text{KOH}_t} \times 22.4}{h \times 2}$$

, where 0.1 is a factor for the concentration difference of  $1 \text{ mol l}^{-1}$  KOH and  $0.1 \text{ mol l}^{-1}$  HCl,  $\text{HCl}_b/\text{HCl}_s$  the HCl titration volume for the blank/sample,  $f_t$  the titration factor,  $\text{KOH}_i$  the total KOH volume incubated,  $\text{KOH}_t$  the KOH volume titrated, 22.4 is the molar gas volume [ $1 \text{ mol}^{-1}$ ] at  $20 \text{ }^\circ\text{C}$ ,  $h$  is the incubation period in hours and 2 is the reaction ratio factor. Produced  $\text{CO}_2$  was converted into  $\mu\text{g CO}_2$  per dry mass of soil per hour ( $\mu\text{g CO}_2 \text{ g soil}^{-1} \text{ h}^{-1}$ ) or into  $\mu\text{g CO}_2$  per mg C per hour ( $\mu\text{g CO}_2 \text{ mg C}^{-1} \text{ h}^{-1}$ ). Improper experimental setup was assumed when values exceeded  $7.7 \mu\text{g CO}_2 \text{ g soil}^{-1} \text{ h}^{-1}$  (mean plus twofold standard deviation) and therefore, soil respiration of two soil samples: afforested sites (A) and continuously forested sites (I) were excluded. By building means of values obtained from locations (pseudoreplicates), this exclusion of values did not affect data interpretation.

### 3.3.5 Elemental and isotopic measurements

Carbon concentrations were analyzed with an Elemental Analyzer (Isotope Cube, Elementar, Hanau, Germany). Since all pH values of soil samples were  $\leq 6.3$  and free of carbonate (tested with hydrochloric acid on properly ground samples), the measured total C concentration was equivalent to the organic C concentration. Stable isotope ratios were analyzed by a coupled isotope ratio mass spectrometry (IRMS) (Isoprime 100, Isoprime, Manchester, England). Results are given in delta notation as  $\delta^{13}\text{C}$  [Eq. 3.2]:

$$[3.2] \quad \delta^{13}\text{C} = \left[ \frac{R_{\text{sample}} - R_{\text{standard}}}{R_{\text{standard}}} \right] \times 1000$$

where R is the  $^{13}\text{C}/^{12}\text{C}$  ratio. We used IAEA-CH-6, IAEA-CH-7 and EMA-P2 for normalization of measured  $\delta^{13}\text{C}$  values [in  $\text{‰}_{\text{VPDB}}$ ]. Measurement accuracy of IRMS analyses based on routine measurements of interspersed samples per 15 samples of EMA-P2 during the measurement period was  $\leq \pm 0.01\text{‰}$  ( $n = 31$ ) and for sulfanilic acid  $\pm 0.02\text{‰}$  ( $n = 18$ ).

### 3.3.6 Calculations and statistical analyses

Linear regression analyses were used to determine the patterns of isotopic changes within the soil profile. We regressed  $\log_{10}$ -transformed carbon concentrations [ $\log_{10}(\text{g}\cdot\text{C}\cdot\text{kg}^{-1})$ ] (= x) and their respective stable isotope values [ $\delta^{13}\text{C} \text{ ‰}$ ] (= y) of the depth intervals (organic layers and of the mineral soil) (Brunn et al., 2016; Brunn et al., 2014; Garten, 2006). Absolute values of regression slopes were termed beta values, so that higher beta values approximate higher decomposition and vice versa. We defined beta values as beta = 0 at sites with formerly positive regression slopes ( $n = 2$ ; 6% of all cases) (Fig. S3.1), corresponding to a vertical isotopic depletion. To omit bias, beta values of all non-significant linear regressions ( $n = 11$ ; 31% of all cases) were included into analyses.

In addition to beta values, we used  $\Delta$  values to describe vertical changes in C concentrations (=  $\Delta\text{C}$ ) and in  $\delta^{13}\text{C}$  values (=  $\Delta^{13}\text{C}$ ) of soil profiles. Due to spatial variation in the depth and thickness of soil horizons between sampling sites, e.g. a soil horizon at 10 cm soil depth of a given location does correspond to a slightly deeper or shallower depth as compared to the neighboring sampling site, we used maximum difference in profiles instead of the difference between topmost and lowermost sampled soil depth to best represent the vertical changes. At afforested and continuously forested sites,  $\Delta$  values equal the difference in C concentration between mineral soil (low C concentrations) and litter (high C concentrations) and the isotopic difference between mineral soil (maximum  $\delta^{13}\text{C}$  value) and litter (minimum  $\delta^{13}\text{C}$  value). No distinct vertical decrease in C concentrations and isotopic enrichment in  $^{13}\text{C}$  were found at arable sites. I.e. in half of these soil profiles, OM decreased in C concentrations with depth with average depth of minimum C concentrations at -5.8 cm and average depth of maximum C concentrations at -5.7 cm depth. Similarly, in 7 out of 12 soil profiles, minimum  $\delta^{13}\text{C}$  value were deeper (average depth = -6.4 cm) in soil profile than maximum  $\delta^{13}\text{C}$  values (average depth = -5.7) contradicting an isotopic enrichment. Therefore,  $\Delta$  values on arable sites rather refer to a maximum variation of C concentrations and  $\delta^{13}\text{C}$  values in soil profiles more than to the general vertical decrease of C concentrations and the isotopic enrichment of  $^{13}\text{C}$ . Relative standard deviation (%RSD= relative standard deviation calculated by dividing the standard deviation by the mean) are given for averaged values.

We employed one-way ANOVA post hoc tests to quantify vertical changes on variables or different land-use forms. In case of homogeneity of variances we used a post hoc Tukey test whereas in case of heteroscedasticity, the Games Howell test was conducted.

We applied paired t-tests (in case of homogeneity of variances) or Welch's t-tests (in case of heteroscedasticity) to compare two values. In addition, we tested for relations between values by linear regression analysis. Significance was determined at  $p \leq 0.05$  in all tests. Normal distribution was tested by a Kolmogorov-Smirnov test.

### 3.4 Results

Carbon concentrations as mean of the total depth profile were *c.* one quarter lower on arable sites compared to continuously forested sites ( $F(2,6) = 25.7$ ;  $P = 0.001$ ) with no significant change in C concentrations between afforestation and continuous forest (Tab. 3.1). In mineral soil only, mean C concentrations of arable sites did not significantly differ from afforested sites but from continuously forested sites ( $F(2,6) = 11.0$ ;  $P = 0.010$ ) (Tab. 3.1) pointing to (i) times of  $> 50$  yrs of forest cover are required for distinct C accumulation in mineral soil and (ii) the importance of the organic layer in affecting total profile C concentrations.  $\delta^{13}\text{C}$  values in mineral soil OM were by 1‰ lower on arable sites compared to the continuously forested sites ( $F(2,6) = 6.07$ ;  $P = 0.036$ ) (Tab. 3.1). While continuously forested sites were characterized by significantly greatest C concentrations in mineral soil compared to arable and afforested sites, they also featured highest  $\delta^{13}\text{C}$  values in mineral soil OM compared to arable sites.

No organic layer existed on arable sites. On continuously forested sites, we observed a greater accumulation of organic material with a mean litter layer thickness of  $2.9 \pm 0.1$  cm compared to afforested sites where organic layers were  $1.8 \pm 0.2$  cm thick ( $F(22) = 1.1$ ;  $P = 0.000$ ). We found no significant differences in litter layer C concentrations and C isotopic signature between sites. However, litter at continuously forested sites had slightly lower C concentrations ( $409.4 \pm 35.6 \text{ g}\cdot\text{C}\cdot\text{kg}^{-1}$ ) compared to afforested sites ( $421.4 \pm 9.2 \text{ g}\cdot\text{C}\cdot\text{kg}^{-1}$ ) and was by *c.* 1‰ depleted in  $^{13}\text{C}$  compared to the afforested sites. Litter C: N ratios did not differ between afforestation ( $29.7 \pm 1.4$ ) and continuously forested sites ( $29.4 \pm 0.8$ ).

Table 3.1 Mean  $\pm$  SE values of parameters at sites of different land-use with letters representing significant differences between land-uses.  $n = 9$ , except litter  $\delta^{13}\text{C}$  values  $n = 6$  owing to the missing organic layer at arable sites.

Land-use	Soil respiration on $[\mu\text{g}\cdot\text{CO}_2\cdot$	beta	$\Delta^{13}\text{C}$ [‰VPDB]	$\Delta\text{C}$ [g·C·kg <sup>-1</sup> ]	pH	$\text{C}_{\text{soil profile}}$ [g·C·kg <sup>-1</sup> ]	$\text{C}_{\text{mineral soil}}$ [g·C·kg <sup>-1</sup> ]	$\delta^{13}\text{C}_{\text{mineral soil}}$ [‰VPDB]	$\delta^{13}\text{C}_{\text{litter}}$ [‰VPDB]
Arable sites	3.4 $\pm$ 0.3 b	1.6 $\pm$ 0.6	0.3 $\pm$ 0.1 c	4.7 $\pm$ 1.2 b	4.5	24.8 $\pm$ 4.9 b	24.8 $\pm$ 4.9 b	-27.9 $\pm$ 0.1 b	
Afforested sites	3.9 $\pm$ 0.1 ab	1.4 $\pm$ 0.3	1.8 $\pm$ 0.3 b	394.1 $\pm$ 10.7 a	4.1	71.1 $\pm$ 5.5 a	36.1 $\pm$ 5.9 b	-27.4 $\pm$ 0.2 ab	-28.7 $\pm$ 0.3
Continuous forest	5.1 $\pm$ 0.5 a	3.1 $\pm$ 0.5	3.0 $\pm$ 0.3 a	362.9 $\pm$ 36.7 a	3.7	99.0 $\pm$ 10.5 a	67.9 $\pm$ 8.8 a	-26.9 $\pm$ 0.3 a	-29.6 $\pm$ 0.5

We found lowest vertical changes of C concentrations on arable sites compared to afforested and continuously forested sites ( $F(2,6) = 96.2$ ;  $P = 0.000$ ) (Tab. 3.1). This nearly missing vertical variation in C concentrations on arable sites was also present in the vertical variation of OM  $\delta^{13}\text{C}$  values, resulting in low  $\Delta^{13}\text{C}$  values (Tab. 3.1). We found lowest isotopic difference on arable sites, with greater isotopic difference at afforested and highest isotopic difference at continuously forested sites ( $F(2,6) = 31.9$ ;  $P = 0.001$ ) (Tab. 3.1).

Absolute values of the linear regression slopes (= beta) between  $\log_{10}$ -transformed C concentration and the corresponding  $\delta^{13}\text{C}$  values served to approximate decomposition. Linear regressions were in 58% ( $n = 21$ ) highly significant ( $P \leq 0.001$ ), while in 28% ( $n = 10$ ) of all profiles non-significant linear regressions were found; mainly attributed to arable sites (Fig. S3.1). Beta ranged between 0.6 and 4.1 with a mean of  $2.1 \pm 0.4$  (RSD = 53%) and  $r$  between -0.42 and -0.99. On arable sites, beta values were significant in only two out of 12 depth profiles and had a low mean coefficient of determination of  $R^2 = 0.16 \pm 0.0$ . Nevertheless, non-significant beta values were included into analysis. We found more significant relationships and higher coefficients of determination at the continuously forested sites (afforestation:  $R^2 = 0.78 \pm 0.0$ ; continuously forested sites:  $R^2 = 0.91 \pm 0.0$ ) with only one non-significant linear regression at afforested sites (Fig. S3.1). Beta values did not significantly differ between land-uses. Low significance of linear regressions (Fig. S3.1) and high RSD of 60% of beta values on arable sites might have hampered distinct differences. However, a trend of higher beta values with time of forest cover was visible (Fig. 3.1c & Tab. 3.1).

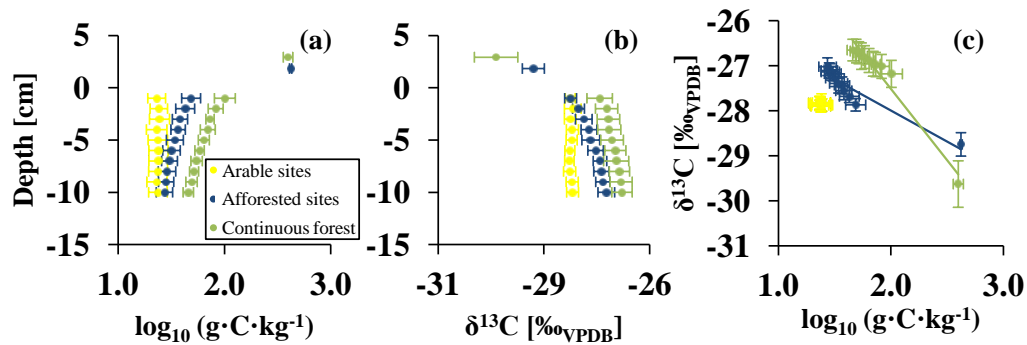


Figure 3.1 Mean  $\pm$  SE changes of logarithmized C concentrations [ $\log_{10}(\text{g}\cdot\text{C}\cdot\text{kg}^{-1})$ ] with depth (a), of OM  $\delta^{13}\text{C}$  values [‰<sub>VPDB</sub>] with depth (b) and  $\log_{10}(\text{g}\cdot\text{C}\cdot\text{kg}^{-1})$  plotted against  $\delta^{13}\text{C}$  values (c) for sites under different land-use: arable sites (yellow), afforested sites (blue) and continuously forested sites (green).  $n = 3$  for each data point. Error bars represent two standard errors.

Among land-uses, we found trends of decreasing pH values with time of forest cover. Although insignificant, arable sites had highest pH values (4.5) compared to afforested sites (4.1) and continuously forested sites (3.7).

Potential soil respiration per g soil measured during the two-day laboratory study ranged between 2.7 and 5.8  $\mu\text{g CO}_2 \text{ h}^{-1}$  with mean soil respiration of  $4.1 \pm 0.3 \mu\text{g CO}_2 \text{ h}^{-1}$ . Values differed between arable and continuously forested sites ( $F(2,6) = 7.3$ ;  $P = 0.025$ ) with lowest soil respiration on arable sites, intermediate soil respiration at the afforested sites and highest soil respiration at the continuously forested sites (Tab. 3.1). Soil respiration was significantly and positively related to beta values and to the isotopic difference  $\Delta^{13}\text{C}$ , while it was negatively related to litter  $\delta^{13}\text{C}$  values (Tab. 3.2). In addition, beta values were positively related to  $\Delta^{13}\text{C}$  and C concentrations in mineral soil. Similarly, we found a negative relation of beta and litter  $\delta^{13}\text{C}$  values (Tab. 3.2). No relations of any value with pH values of soil were observed. Similarly, C: N ratios of litter were not related to any parameter investigated in this study. All other observed relations with correlation coefficients and significance are given in Tab. 2.

Table 3.2 Correlation coefficients between variables. Bold numbers represent significant relations with \*,  $P \leq 0.05$ ; \*\*,  $P \leq 0.01$ ; \*\*\*,  $P \leq 0.001$ .  $n = 9$ , except litter  $\delta^{13}\text{C}$  values  $n = 6$  owing to the missing organic layer on arable sites with 0 yrs of forest cover.

	Soil respiration	beta	$\Delta^{13}\text{C}$	$\Delta\text{C}$	pH	$\text{C}_{\text{soil profile}}$	$\text{C}_{\text{mineral soil}}$
beta	<b>0.767**</b>						
$\Delta^{13}\text{C}$	<b>0.895***</b>	<b>0.670*</b>					
$\Delta\text{C}$	0.483	0.170	<b>0.765*</b>				
pH	-0.308	-0.292	-0.309	0.254			
$\text{C}_{\text{soil profile}}$	0.637	0.511	<b>0.873**</b>	<b>0.871**</b>	-0.357		
$\text{C}_{\text{mineral soil}}$	0.631	<b>0.682*</b>	<b>0.789*</b>	0.600	-0.378	<b>0.915***</b>	
$\delta^{13}\text{C}_{\text{litter}}$	<b>-0.954**</b>	<b>-0.909*</b>	<b>-0.877*</b>	<b>0.829*</b>	-0.043	-0.189	-0.338

### 3.5 Discussion

With changing land-use, we found distinct variations of vertical isotopic differences ( $\Delta^{13}\text{C}$ ) in topsoil. At arable sites,  $\delta^{13}\text{C}$  depth profiles were least developed, while we found most pronounced  $\delta^{13}\text{C}$  depth profiles at continuously forested sites, i.e. the longer the time of forest cover, the greater the vertical enrichment in  $^{13}\text{C}$ , which approves our hypothesis. Values of the isotopic difference close to zero on arable sites may be attributed to a missing organic layer on top of soils - assumed to set the isotopic baseline (Shilenkova and Tiunov, 2013) - and recent plowing, and therefore mixing and disturbance of OM in soil profiles. However, despite an assumed strong impact of the organic layer, Menichetti et al. (2014) observed a small but present vertical isotopic enrichment of  $^{13}\text{C}$  in soils of different bare-fallow experimental sites kept without any OM inputs. This finding is in line with the observations of small  $\Delta^{13}\text{C}$  values on arable sites in our study. We discuss several parameters that have accounted for isotopic differences in topsoil under different land-use; (i) the Suess effect, (ii) litter  $\delta^{13}\text{C}$  values, (iii) microbial processing, (iv) roots and (v) transport and sorption processes in soil profiles (Fig. 3.2).



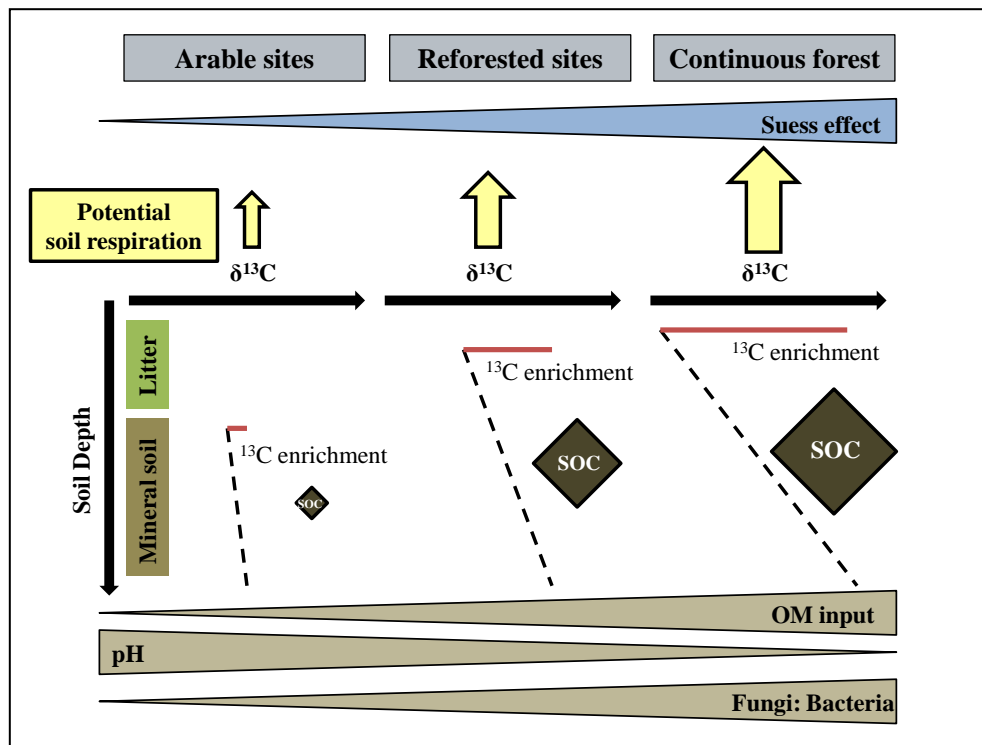


Figure 3.2 Conceptual figure showing parameters that appeared to affect  $\delta^{13}\text{C}$  depth profiles for sites exposed to different land-use (arable sites, afforested sites, and continuously forested sites) in this study. Potential soil respiration,  $^{13}\text{C}$  enrichment, soil organic carbon (SOC) concentration and pH were determined in this study. Other parameters are based on literature data.

It remains challenging to what extent the Suess effect can serve to explain vertical trends of  $\delta^{13}\text{C}$  in OM. Presuming that the isotopic dilution of atmospheric  $\text{CO}_2$  with  $^{13}\text{C}$  of *c.* 2‰ is first, fully transferred into plants and litter during the total observed time span of our study and is second, the only parameter affecting the vertical isotopic difference in topsoil, the isotopic difference from litter to mineral soil at sites with plant cover > 150 yrs should equal the decrease in  $\delta^{13}\text{CO}_2$  of 2‰. In our study, sites with forest cover > 150 yrs (continuously forested sites) had mean  $\Delta^{13}\text{C}$  of  $3.0 \pm 0.3\text{‰}$  which was greater than the expected impact of the atmospheric depletion. Even sites with forest cover < 50 yrs (afforested sites) had an isotopic difference of  $1.8 \pm 0.3\text{‰}$ ; exceeding the expectations of the Suess effect being the only driver of  $\delta^{13}\text{C}$  depth profiles, since the atmospheric depletion is approximated to have *c.* 1.5‰ within the past 50 yrs (Rubino et al., 2013). The other way, the Suess effect as single driver of  $\delta^{13}\text{C}$  depth profiles would result in a difference of 0.5‰ in  $\Delta^{13}\text{C}$  values between afforested and continuously forested sites, but we observed a difference more than twice as high. Conforming to other studies, we assume that besides the Suess effect, additional processes must exist to contribute to the vertical  $\delta^{13}\text{C}$  distribution.

Litter as the uppermost isotopic signal was slightly depleted in  $^{13}\text{C}$  at continuously forested sites compared to afforested sites (Tab. 3.1). Since needle litter experiences turnover times within a decadal range (Czimczik and Trumbore, 2007), we can exclude a pure effect of the atmospheric depletion in  $^{13}\text{C}$  on litter  $\delta^{13}\text{C}$  values in our study. Trends of lower litter  $\delta^{13}\text{C}$  values at continuously forested sites might be linked with greater fungal abundance, probably related to slightly lower pH values. Lower pH values could affect microbial community structures by promoting fungi (Pietri and Brookes, 2009). Since fungi were found to be depleted in  $^{13}\text{C}$  (Kohl et al., 2015; Wallander et al., 2009), the spatial separation of fungi and bacteria in soil profiles can increase the isotopic difference in soil profiles. A potential increasing abundance of fungi in the litter layer could therefore result in more depleted litter at continuously forested sites. However, the isotopic signature of litter lacks in explaining the greater enrichment in  $^{13}\text{C}$  of OM in mineral soil at sites with longer times of forest cover (Tab. 3.1 & Fig. 3.1).

The positive relations between beta values,  $\Delta^{13}\text{C}$  and potential soil respiration (Tab. 3.2) suggest a contribution of microbial processing in shaping  $\delta^{13}\text{C}$  depth profiles. The idea behind relations of the isotopic enrichment and decomposition refers to kinetic fractionation during the respiration process, resulting in respiration of the lighter  $^{12}\text{C}$  and accumulation of the heavier  $^{13}\text{C}$  isotope in soil OM (Diochon and Kellman, 2008; Lerch et al., 2011; Wynn et al., 2005). Given that the loss pathway of C is determined via soil respiration, OM should become enriched in  $^{13}\text{C}$ , resulting in positive relations between soil respiration and beta values. The results of our study show a significant relation between the vertical distribution of  $\delta^{13}\text{C}$  values and potential soil respiration (Tab. 3.2) and therefore clearly suggest the evidence of beta values being an approximation of microbial C processing in soil. Beta values did not significantly distinguish between sites exposed to different land-uses (Tab. 3.1). However, we found trends of higher beta values, higher potential soil respiration and a significantly more pronounced vertical isotopic difference ( $\Delta^{13}\text{C}$ ) in topsoil of afforested sites that further increased at continuously forested sites (Tab. 3.1). The accuracy of beta values as approximation for decomposition at sites with low decomposition appeared to be debatable since linear regressions at arable sites had low coefficients of determination and were predominantly non-significant. The generally very good curve fitting of linear regressions to calculate beta values of previous and other studies (Acton et al., 2013; Brunn et al., 2016; Brunn et al., 2014; Powers and Schlesinger, 2002) suggest a limited applicability of beta val-

ues on plowed arable sites. Though, the significant relation between beta values and potential soil respiration (Tab. 3.2) indicates the good approximation of beta values as a measure for C processing and therefore suggests lower decomposition on arable sites owing to lower beta values and lower soil respiration, supporting trends of greater decomposition at afforested and continuously forested sites.

Considering respired  $\text{CO}_2$  is composed of heterotrophic (microorganisms decomposing OM) and autotrophic (roots and associated microorganisms) components (Brüggemann et al., 2011; Hanson et al., 2000), greater rooting density and biomass production (Bahn et al., 2008; Peri et al., 2015) at sites longer exposed to forest cover might induce greater respiration. Since roots have higher  $\delta^{13}\text{C}$  values compared to leaves (Badeck et al., 2005; Hobbie et al., 2004), the greater enrichment in  $^{13}\text{C}$  in mineral soil of continuously forested sites in our study (Tab. 3.1 & Fig. 3.1) suggests a greater rooting and contributes to explain increased potential soil respiration. As a result of crop harvesting, low root abundance at arable sites likely reduced respiration rates.

In addition to root impacts, transport and sorption processes may have contributed to trends of more pronounced  $\delta^{13}\text{C}$  depth profiles with time of forest cover. Hansson et al. (2010) underlined the contribution of roots in creating dissolved organic matter (DOM), which were attributed to play an important role in shaping  $\delta^{13}\text{C}$  depth profiles (Kaiser and Kalbitz, 2012). They found DOM produced from root litter at later stages of decomposition more strongly sorbed in mineral soil compared to DOM from fresh litter types, suggesting that the greater length of tree colonization at continuously forested sites compared to afforested sites in our study likely induced accumulating effects through more continuous input of decomposition products from litter and roots. In addition, lower pH values were found to increase dissolved organic C and increase microbial respiration (Hall and Silver, 2013) and could therefore also enhance  $\delta^{13}\text{C}$  depth profiles through greater transport of  $^{13}\text{C}$  enriched products.

### 3.6 Conclusion

We could show that land-use affected vertical  $\delta^{13}\text{C}$  distribution with significantly less distinct  $\delta^{13}\text{C}$  depth profiles at arable sites compared to continuously forested sites. Three decades after conversion,  $\delta^{13}\text{C}$  depth profiles developed with isotopic differences in topsoil in between those of arable sites and continuously forested sites. Absolute values of slopes of linear regression lines (= beta) between  $\log_{10}$ -transformed C concentra-

tion and  $\delta^{13}\text{C}$  values were used to approximate decomposition. Beta values were positively related to potential soil respiration suggesting microbial processing as a component to explain vertical C stable isotope distribution. In addition, depletion of atmospheric  $\text{CO}_2$  in  $^{13}\text{C}$ , accumulation of  $^{13}\text{C}$  enriched microbial products, increasing fungal:bacterial ratios, greater root biomass, decreasing pH, as well as increased transport and sorption processes in soil profiles are proposed to enhance  $\delta^{13}\text{C}$  depth trends. However, greater potential soil respiration and greater beta values under continuously forested sites contradict expectations of forest soils offering a mitigation strategy to reduce global warming by acting as a C sink and suggest a low C sequestration potential of forest soils. This might demand a reconsideration of the role of soils afforested with spruce in regard to its postulated function within the global change.

### 3.7 Acknowledgement

We thank A. Mestrot and D. Fischer (University of Berne, Switzerland) for providing isotopic analysis, S. Flaiz and L. Funke (University of Tuebingen, Germany) for laboratory assistance and F. Brunn (University of Mainz, Germany) for facilitating this work. This research did not receive any specific grant from funding agencies in the public, commercial, or not-for-profit sectors.

### 3.8 References

- Acton, P., Fox, J., Campbell, E., Rowe, H., Wilkinson, M., 2013. Carbon isotopes for estimating soil decomposition and physical mixing in well-drained forest soils. *Journal of Geophysical Research-Biogeosciences* 118, 1532-1545.
- Badeck, F.W., Tcherkez, G., Nogues, S., Piel, C., Ghashghaie, J., 2005. Post-photosynthetic fractionation of stable carbon isotopes between plant organs - a widespread phenomenon. *Rapid Communications in Mass Spectrometry* 19, 1381-1391.
- Bahn, M., Rodeghiero, M., Anderson-Dunn, M., Dore, S., Gimeno, C., Drosler, M., Williams, M., Ammann, C., Berninger, F., Flechard, C., Jones, S., Balzarolo, M., Kumar, S., Newesely, C., Priwitzer, T., Raschi, A., Siegwolf, R., Susiluoto, S., Tenhunen, J., Wohlfahrt, G., Cernusca, A., 2008. Soil Respiration in European Grasslands in Relation to Climate and Assimilate Supply. *Ecosystems* 11, 1352-1367.
- Boström, B., Comstedt, D., Ekblad, A., 2007. Isotope fractionation and C-13 enrichment in soil profiles during the decomposition of soil organic matter. *Oecologia* 153, 89-98.
- Brüggemann, N., Gessler, A., Kayler, Z., Keel, S.G., Badeck, F., Barthel, M., Boeckx, P., Buchmann, N., Brugnoli, E., Esperschütz, J., Gavrichkova, O., Ghashghaie, J., Gomez-Casanovas, N., Keitel, C., Knohl, A., Kuptz, D., Palacio, S., Salmon, Y., Uchida, Y., Bahn, M., 2011. Carbon allocation and carbon isotope fluxes in the plant-soil-atmosphere continuum: a review. *Biogeosciences* 8, 3457-3489.

- Brunn, M., Condrón, L., Wells, A., Spielvogel, S., Oelmann, Y., 2016. Vertical distribution of carbon and nitrogen stable isotope ratios in topsoil across a temperate rainforest dune chronosequence in New Zealand. *Biogeochemistry*, 1-15.
- Brunn, M., Spielvogel, S., Sauer, T., Oelmann, Y., 2014. Temperature and precipitation effects on delta C-13 depth profiles in SOM under temperate beech forests. *Geoderma* 235, 146-153.
- Czimczik, C.I., Trumbore, S.E., 2007. Short-term controls on the age of microbial carbon sources in boreal forest soils. *Journal of Geophysical Research-Biogeosciences* 112.
- Del Galdo, I., Six, J., Peressotti, A., Cotrufo, M.F., 2003. Assessing the impact of land-use change on soil C sequestration in agricultural soils by means of organic matter fractionation and stable C isotopes. *Global Change Biology* 9, 1204-1213.
- Diochon, A., Kellman, L., 2008. Natural abundance measurements of  $(^{13}\text{C})$  indicate increased deep soil carbon mineralization after forest disturbance. *Geophysical Research Letters* 35, 1-5.
- Garten, C.T., 2006. Relationships among forest soil C isotopic composition, partitioning, and turnover times. *Canadian Journal of Forest Research-Revue Canadienne De Recherche Forestiere* 36, 2157-2167.
- Hall, S.J., Silver, W.L., 2013. Iron oxidation stimulates organic matter decomposition in humid tropical forest soils. *Global Change Biology* 19, 2804-2813.
- Hanson, P.J., Edwards, N.T., Garten, C.T., Andrews, J.A., 2000. Separating root and soil microbial contributions to soil respiration: A review of methods and observations. *Biogeochemistry* 48, 115-146.
- Hansson, K., Kleja, D.B., Kalbitz, K., Larsson, H., 2010. Amounts of carbon mineralised and leached as DOC during decomposition of Norway spruce needles and fine roots. *Soil Biology & Biochemistry* 42, 178-185.
- Hobbie, E.A., Johnson, M.G., Rygielwicz, P.T., Tingey, D.T., Olszyk, D.M., 2004. Isotopic estimates of new carbon inputs into litter and soils in a four-year climate change experiment with Douglas-fir. *Plant and Soil* 259, 331-343.
- Kaiser, K., Kalbitz, K., 2012. Cycling downwards - dissolved organic matter in soils. *Soil Biology & Biochemistry* 52, 29-32.
- Kohl, L., Laganier, J., Edwards, K.A., Billings, S.A., Morrill, P.L., Van Biesen, G., Ziegler, S.E., 2015. Distinct fungal and bacterial delta C-13 signatures as potential drivers of increasing delta C-13 of soil organic matter with depth. *Biogeochemistry* 124, 13-26.
- Laganier, J., Angers, D.A., Paré, D., 2010. Carbon accumulation in agricultural soils after afforestation: a meta-analysis. *Global Change Biology* 16, 439-453.
- Lal, R., 2005. Forest soils and carbon sequestration. *Forest Ecology and Management* 220, 242-258.
- Lerch, T.Z., Nunan, N., Dignac, M.F., Chenu, C., Mariotti, A., 2011. Variations in microbial isotopic fractionation during soil organic matter decomposition. *Biogeochemistry* 106, 5-21.
- Macfayden, A., 1970. Simple methods for measuring and maintaining the proportion of carbon dioxide in air for use in ecological studies of soil respiration. *Soil Biology and Biochemistry* 2, 9-18.
- Menichetti, L., Houot, S., van Oort, F., Kätterer, T., Christensen, B., Chenu, C., Barré, P., Vasilyeva, N., Ekblad, A., 2014. Increase in soil stable carbon isotope ratio relates to loss of organic carbon: results from five long-term bare fallow experiments. *Oecologia*, 1-11.
- Peri, P.L., Bahamonde, H., Christiansen, R., 2015. Soil respiration in Patagonian semiarid grasslands under contrasting environmental and use conditions. *Journal of Arid Environments* 119, 1-8.
- Pietri, J.C.A., Brookes, P.C., 2009. Substrate inputs and pH as factors controlling microbial biomass, activity and community structure in an arable soil. *Soil Biology & Biochemistry* 41, 1396-1405.
- Powers, J.S., Schlesinger, W.H., 2002. Geographic and vertical patterns of stable carbon isotopes in tropical rain forest soils of Costa Rica. *Geoderma* 109, 141-160.
- Rubino, M., Etheridge, D.M., Trudinger, C.M., Allison, C.E., Battle, M.O., Langenfelds, R.L., Steele, L.P., Curran, M., Bender, M., White, J.W.C., Jenk, T.M., Blunier, T., Francey, R.J., 2013. A revised 1000 year atmospheric delta C-13-CO<sub>2</sub> record from Law Dome and South Pole, Antarctica. *Journal of Geophysical Research-Atmospheres* 118, 8482-8499.
- Schmidt, M.W.I., Torn, M.S., Abiven, S., Dittmar, T., Guggenberger, G., Janssens, I.A., Kleber, M., Kögel-Knabner, I., Lehmann, J., Manning, D.A.C., Nannipieri, P., Rasse, D.P., Weiner, S., Trumbore, S.E., 2011. Persistence of soil organic matter as an ecosystem property. *Nature* 478, 49-56.
- Shilenkova, O.L., Tiunov, A.V., 2013. Soil-litter nitrogen transfer and changes in delta C-13 and delta N-15 values in decomposing leaf litter during laboratory incubation. *Pedobiologia* 56, 147-152.
- Six, J., Callewaert, P., Lenders, S., De Gryze, S., Morris, S.J., Gregorich, E.G., Paul, E.A., Paustian, K., 2002. Measuring and understanding carbon storage in afforested soils by physical fractionation. *Soil Science Society of America Journal* 66, 1981-1987.

- Wallander, H., Morth, C.M., Giesler, R., 2009. Increasing abundance of soil fungi is a driver for N-15 enrichment in soil profiles along a chronosequence undergoing isostatic rebound in northern Sweden. *Oecologia* 160, 87-96.
- Wiesmeier, M., Hubner, R., Sporlein, P., Geuss, U., Hangen, E., Reischl, A., Schilling, B., von Lutzow, M., Kogel-Knabner, I., 2014. Carbon sequestration potential of soils in southeast Germany derived from stable soil organic carbon saturation. *Global Change Biology* 20, 653-665.
- Wynn, J.G., Bird, M.I., Wong, V.N.L., 2005. Rayleigh distillation and the depth profile of C-13/C-12 ratios of soil organic carbon from soils of disparate texture in Iron Range National Park, Far North Queensland, Australia. *Geochimica Et Cosmochimica Acta* 69, 1961-1973.

3.9 Supplementary material

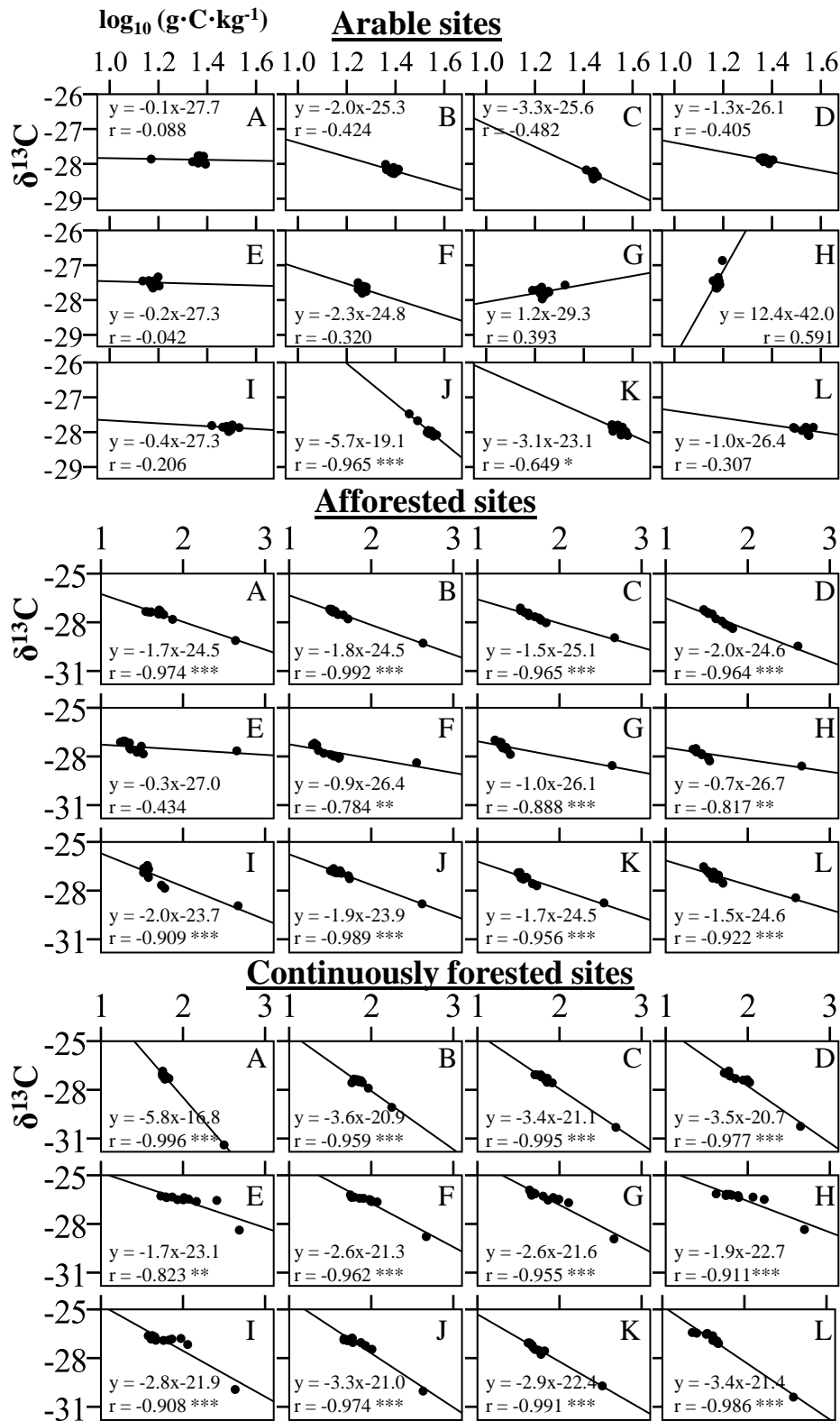


Figure S3.1 Linear regressions between carbon concentrations [ $\log_{10}(\text{g}\cdot\text{C}\cdot\text{kg}^{-1})$ ] and corresponding  $\delta^{13}\text{C}$  values [ $\text{‰}_{\text{VPDB}}$ ] with linear regression lines and regression equation of arable sites, afforested sites and continuously forested sites. Plots in one line represent fourfold pseudoreplicates at one location. \*,  $P < 0.05$ ; \*\*,  $P < 0.01$ ; \*\*\*,  $P < 0.001$ .

## 4 Vertical distribution of carbon and nitrogen stable isotope ratios in topsoil across a temperate rainforest dune chronosequence in New Zealand

Melanie Brunn<sup>1</sup>, Leo Condrón<sup>2</sup>, Andrew Wells<sup>2</sup>, Sandra Spielvogel<sup>3</sup>, Yvonne Oelmann<sup>1</sup>

<sup>1</sup> Geocology, University of Tuebingen, Ruemelinstraße 19-23, 72070 Tuebingen, Germany

<sup>2</sup> Faculty of Agriculture and Life Sciences, Lincoln University, Lincoln, New Zealand

<sup>3</sup> Institute of Geography, University of Bern, Bern, Switzerland

Biogeochemistry (2016) 129:37-51 (accepted 11.05.2016)

DOI 10.1007/s10533-016-0218-4

The final publication is available at [link.springer.com](http://link.springer.com)



## 4.1 Abstract

Chronosequences can provide valuable insights into carbon (C) and nitrogen (N) dynamics across natural gradients with C and N stable isotopes serving as powerful tool investigating these dynamics.

We studied changes in  $\delta^{13}\text{C}$  and  $\delta^{15}\text{N}$  values in litter, organic layer and mineral soil on dunes across the Haast chronosequence (New Zealand), which spans 120 to 2,870 yrs of pedogenesis beneath a temperate rainforest. Decomposition was approximated from linear regression slopes between C concentrations and  $\delta^{13}\text{C}$  values and termed  $\text{beta}_\text{C}$ . Similarly we calculated  $\text{beta}_\text{N}$  values to test the relationship between vertical N decrease and  $\delta^{15}\text{N}$  increase.

Decreasing  $\delta^{13}\text{C}$  values of litter with age suggests a physiological response of plants to decreased litter N concentrations. A decrease of litter  $\delta^{15}\text{N}$  in the early succession stages and a second decline after 1,300 yrs indicates reduced  $\text{N}_2$  fixation.  $\text{Beta}_\text{C}$  values increased during early ecosystem development and at old sites, and were lowest at the intermediate stages (1,500 yrs), which suggests decomposition did not decrease constantly with time.  $\text{Beta}_\text{N}$  values were lowest at the youngest site and increased within the first 200 yrs, likely because litter as the uppermost part of the vertical depth profile reflected an increased supply of N depleted in  $^{15}\text{N}$  provided by fungi. We found relations between  $\text{beta}_\text{C}$  and  $\text{beta}_\text{N}$  values suggesting that there might be shared processes shaping  $\delta^{13}\text{C}$  and  $\delta^{15}\text{N}$  vertical depth profiles, e.g. microbial cycling, transport or sorption.

## 4.2 Introduction

Chronosequences provide unique opportunities to investigate carbon (C) and nitrogen (N) dynamics in natural ecosystems. Environmental and biological changes during ecosystem development are considered an important driver of C stabilization in soils (Jones et al., 2015; Schmidt et al., 2011) which profoundly affects atmospheric carbon dioxide concentrations (Stockmann et al., 2013). For example, in boreal systems with slow decomposition, old soils sequestered more C than younger soils, caused by the accumulation of an organic layer (Clemmensen et al., 2013). Stable isotopes of carbon ( $\delta^{13}\text{C}$ ) and nitrogen ( $\delta^{15}\text{N}$ ) can be used as indirect indicators of biogeochemical patterns and processes across chronosequences (Craine et al., 2015; Högberg, 1997). During biogeochemical reactions, isotopic fractionation occurs, i.e. a discrimination of heavier

isotopes that leave the reactant enriched and the product isotopically depleted (Hobbie and Högberg, 2012). For instance, isotopic ratios served to assess plant N nutrition (Hyodo et al., 2013; Unkovich, 2013), C and N transfer to and by mycorrhizal fungi (Clemmensen et al., 2013; Hobbie and Högberg, 2012), decomposition (Acton et al., 2013; Brunn et al., 2014; Garten, 2006; Guillaume et al., 2015) or interrelations between above and belowground processes (Hobbie and Ouimette, 2009; Hyodo and Wardle, 2009; Menge et al., 2011). Despite the complexity of the C and N cycle, interpretation of C and N isotopes in plants, soil and depth profiles can help to elucidate key aspects and processes that dominate the C and N cycle in particular ecosystems.

Ecosystem and soil development across chronosequences can be defined in a progressive phase after initial disturbance, in a phase of maximal biomass in which the ecosystem stabilizes and in a retrogressive phase, where the ecosystem undergoes declines in productivity and nutrient cycling; trends that have been observed along chronosequences around the world (Peltzer et al., 2010; Wardle et al., 2004). Early in primary succession, primary production is commonly limited by N availability (Vitousek, 2004; Vitousek and Howarth, 1991), which may progress to phosphorus (P) limitation in extremely old and/or highly weathered soils (Vitousek and Farrington, 1997; Walker and Syers, 1976). Changes in C and N stocks and cycling accompany these biogeochemical shifts, and may influence the isotopic signatures of plants and soils (Martinelli et al., 1999).

For example, litter  $\delta^{13}\text{C}$  values in boreal forest chronosequences in Sweden increased with proceeding time (Hyodo et al., 2013; Hyodo and Wardle, 2009). Foliar morphological adaption to lower nutrient availability at late stages of pedogenesis, i.e. increased internal resistance of  $\text{CO}_2$  diffusion through the development of thicker and smaller leaves was supposed. This adaption is comparable to water stress effects on plants that equally reduces the stomatal conductance and results in higher  $\delta^{13}\text{C}$  values due to closed stomata (Farquhar et al., 1989). Similarly, according to positive relations between foliar N concentrations and  $\delta^{13}\text{C}$  values (Guehl et al., 1995; Körner and Diemer, 1987; Vitousek et al., 1990),  $\delta^{13}\text{C}$  values should increase with increasing N and therefore with time across chronosequences.

In contrast to foliar and litter  $\delta^{13}\text{C}$  values, which typically is interpreted as an integrator of water stress,  $\delta^{15}\text{N}$  values have been used to infer N input and loss pathways, as well as overall N availability (Craine et al., 2015; Högberg, 1997). Specifically,  $\delta^{15}\text{N}$  of litter reflects the fraction of N incorporated from dinitrogen ( $\text{N}_2$ ) fixation, as well as

isotopic enrichment of the available soil N pool due to fractionating losses that preferentially remove  $^{14}\text{N}$  (e.g. denitrification) (Houlton and Bai, 2009; Houlton et al., 2006). Due to the negligible fractionation during nutrient retranslocation before leaf abscission (Garten et al., 2011; Menge et al., 2011),  $\delta^{15}\text{N}$  values in litter layer of soils can reflect N sources and their transformation by N cycling processes. Across chronosequences, deposition or bedrock material are comparable and should not affect variations in litter  $\delta^{15}\text{N}$  values, while N loss and all other forms of N input may change. However, to compare chronosequences from different sites with each other, all N input values have to be considered, making chronosequences of each site specific in its isotopic signature. For example, low N deposition and less N from bedrock in early phases of ecosystem development can generate systems with strong dependence on  $\text{N}_2$  fixation (Menge and Hedin, 2009; Vitousek and Howarth, 1991). The high energy costs of  $\text{N}_2$  fixation make it unlikely to persist if soil N availability is high compared to the utilization of other N forms (Andrews et al., 2011; Vitousek and Howarth, 1991). However, contrasting trends with a decoupling of  $\text{N}_2$  fixation and N availability in soil were also documented (Menge and Hedin, 2009; Reed et al., 2011). Since litter  $\delta^{15}\text{N}$  values converge to atmospheric isotopic signatures at sites where biological  $\text{N}_2$  fixation dominates (Unkovich, 2013) and e.g., N supplied by fungi results in  $^{15}\text{N}$  depleted litter (Hobbie and Ouimette, 2009), litter  $\delta^{15}\text{N}$  values can help to indicate the dominating N source used by plants.

The uppermost litter layer contains more C and N than mineral soil below and this vertical decrease in C and N concentrations is associated with an increase in  $\delta^{13}\text{C}$  and  $\delta^{15}\text{N}$  values, i.e. organic matter (OM) becomes enriched lower in the soil (Billings and Richter, 2006; Brunn et al., 2014; Hobbie and Ouimette, 2009; Nadelhoffer and Fry, 1988a). In addition to several mechanisms and processes driving vertical isotopic changes, the accumulation of  $^{13}\text{C}$  and  $^{15}\text{N}$  enriched compounds from microbial products or microbial cells itself are supposed as important parameters (Billings and Richter, 2006; Dijkstra et al., 2006; Lerch et al., 2011). Vertical isotopic patterns in soils have been described by enrichment factors corresponding to the isotopic difference from litter to mineral soil (Krull et al., 2002) or by plotting logarithmized ( $\log_{10}x$ ) element concentration in OM against its isotopic signature (Acton et al., 2013; Brunn et al., 2014; Garten, 2006; Guillaume et al., 2015). In the latter, slopes of linear regressions (indicated as  $\beta_{\text{C}}$  values) between logarithmized C concentrations and the according isotopic ratios served to approximate decomposition.  $\beta_{\text{C}}$  values could therefore be a valuable tool to assess changes of C processing during ecosystem and soil development.

In addition to the vertical enrichment of  $^{13}\text{C}$ , a similar enrichment of  $^{15}\text{N}$  can develop in topsoil (Craine et al., 2015; Hobbie and Ouimette, 2009; Wallander et al., 2009). Likewise,  $\beta_{\text{N}}$  values can be calculated by means of linear regressions between logarithmized N concentrations and according  $\delta^{15}\text{N}$  values. Similar relations were compiled by Hobbie and Ouimette (2009) and the authors emphasized the importance of mycorrhizal fungi in controlling vertical  $\delta^{15}\text{N}$  depth trends. Fractionation against  $^{15}\text{N}$  during N transfer by mycorrhizal fungi to host plants is suggested, resulting in  $^{15}\text{N}$  depleted litter and  $^{15}\text{N}$  enriched OM in mineral soil (Hobbie and Ouimette, 2009). The vertical enrichment in  $^{15}\text{N}$  between litter and mineral soil was found to vary strongly, with ectomycorrhizal (EM) systems *c.* doubling the enrichment in  $^{15}\text{N}$  compared to systems dominated by arbuscular mycorrhiza (AM) (Hobbie and Ouimette, 2009). Mycorrhizal associations inconstantly shifted with time across chronosequences (Dickie et al., 2013) with strong host specificity (Martinez-Garcia et al., 2015). For example, while boreal chronosequences are supposed to lack a stage with AM, EM plants are absent across sequences in Hawaii (Dickie et al., 2013). Chronosequences in New Zealand are potentially able to host both mycorrhiza types. However, the Franz Josef chronosequence (*c.* 200 km north of Haast) does not harbor EM plant species (Dickie et al. 2013) that are present at the late stages of the Haast chronosequence (Turner et al., 2012b).

In this study, we aimed to contribute to a better understanding of C and N dynamics with providing stable C and N isotope data in high resolution of topsoil during pedogenesis and ecosystem development. We investigated *c.* 2,870 yrs across the well established Haast chronosequence (Eger et al., 2011; Jangid et al., 2013; Turner et al., 2012a; Turner et al., 2012b; Turner et al., 2014) located on a well drained sandy dune substrate with fast podzolisation (Turner et al., 2012b) on New Zealand's South Island. Our objectives were to unravel whether (i)  $\delta^{13}\text{C}$  and  $\delta^{15}\text{N}$  values in litter and (ii) vertical shifts of  $\delta^{13}\text{C}$  and  $\delta^{15}\text{N}$  values with soil depth change with soil age across a soil chronosequence under superhumid climate conditions.

Previous studies showed increasing nutrient limitation across the Haast chronosequence (Turner et al., 2012a) and abundances of bacterial taxa closely related to heterotrophic diazotrophs (Jangid et al., 2013). Therefore, we hypothesized (1) that litter  $\delta^{13}\text{C}$  values increase with proceeding ecosystem development and pedogenesis, similarly to  $\delta^{13}\text{C}$  values in boreal chronosequences and (2) that  $\delta^{15}\text{N}$  values of litter are close to the isotopic signature of atmospheric  $\text{N}_2$  due to the high contribution of biologi-

cal N<sub>2</sub> fixation at Haast. Conforming to the retrogressive model which suggests declines in ecosystem productivity, decomposition and nutrient cycling (Peltzer et al., 2010), we hypothesized (3) that  $\beta_C$  values, as a measure of decomposition, decrease with proceeding time. According to the possible shift in mycorrhizal communities with time, i.e. AM to EM due to host specificity inferred from shifts in tree species (Turner et al., 2012b), we hypothesized (4) that differences between  $\delta^{15}\text{N}$  values of litter and mineral soil OM increase with time resulting in increasing  $\beta_N$  values.

### 4.3 Material and methods

#### 4.3.1 Sampling site

The Haast coastal foredune progradation dune ridge system has formed under temperate humid climate (mean annual temperature = 11.3 °C, mean annual precipitation = 3455 mm) at the West Coast of New Zealand's South Island (43°53'S, 169°3'E). The chronosequence features comparable parent material with  $88.7 \pm 2.8\%$  sand,  $8.0 \pm 2.1\%$  silt and  $3.5 \pm 0.5\%$  clay content (Turner et al., 2012a), negligible human disturbance and low atmospheric N deposition ( $0.9$  to  $1.5 \text{ kg N}\cdot\text{ha}^{-1}\cdot\text{yr}^{-1}$ ) (Galloway et al., 2004; Menge et al., 2011). Dune ridges form a slightly undulating topography (< 5 m to 20 m a.s.l.) with overall extension *c.* 5 km inland and soils developing from Arenosol to Podzol (Turner et al., 2012a). The whole formation covers a time of *c.* 6,000 yrs and was extensively described by Wells and Goff (2007) and Turner et al. (2012a).

#### 4.3.2 Sampling and sample preparation

We collected five replicate samples from litter, organic layer and mineral soil on 11 dune ridges (landward direction) in March 2013, resulting in 55 profiles covering a time span from *c.* 120 to *c.* 2,870 yrs (Tab. 4.1). Soil samples were collected by a root auger (Eijkelkamp Agrisearch Equipment BV, Netherlands) to a depth of 10 cm of the mineral soil. After removal of soil cores (diameter of 8 cm), we cut mineral soil into 1 cm depth sections. Organic layers were collected as litter (Oi horizon) and organic (Oe and Oa horizons) layers. At some sites, thick roots restricted the depth which could be sampled, resulting in a sampling depth of 7 cm at dune stage 0 (B), 8 cm at dune stages 0 (A and D), 3 (A), 4 (B) and 5 (B) and 9 cm for two replicates of the dune stage 0 (C and E).

Table 4.1 Sampling sites description with dune age [B.P.], dating method, depth of the organic horizons [cm] (= Oi, Oe and Oa horizons) with standard errors and letters across the Haast dune chronosequence, New Zealand

Dune stage	Dune age [years B.P.] <sup>a</sup>	Dating method	Depth of the organic horizons [cm]
0 <sup>b</sup>	120	Estimated	1.4 ± 0.5 c
1 <sup>b</sup>	187	Tree rings	1.0 ± 0.3 c
2	296	Tree rings	3.8 ± 1.4 bc
3	398	Tree rings	4.6 ± 0.5 b
4	523	Tree rings	2.4 ± 0.2 bc
5	603	Tree rings	3.4 ± 1.2 bc
6 <sup>b</sup>	793	Tree rings	3.0 ± 0.9 bc
7	1,310	Estimated	11.6 ± 2.5 abc
8	1,830	Estimated	26.2 ± 8.6 abc
9	2,350	Estimated	29.2 ± 3.8 a
10	2,870	Estimated	18.2 ± 3.3 abc

<sup>a</sup> Dates from year of sampling (2013); ages of dune stages 1–6 from Wells and Goff (2007) and Turner et al. (2012), and stages 7–10 estimated by assuming an equal number of years (*c.* 520 yr) between each dune stage.

<sup>b</sup> Dunes for these stages were less pronounced on the north side of the river therefore, dunes occurring on a parallel system on the south side of the river were sampled.

All samples were oven dried at 60°C and visible roots and parts of green moss that survived drying procedure were carefully removed. The dried litter and organic layer samples were ground in a shredder (Retsch SM 2000). Dried mineral soil samples were sieved < 2 mm. Aliquots and those of the shredded litter and organic layer samples were ground and homogenized using a Planetary Ball Mill PM 200 (Retsch, Germany).

#### 4.3.3 Laboratory analysis, calculations and statistics

##### 4.3.3.1 Elemental and isotopic measurements

Carbon and nitrogen concentrations were determined with an Elemental Analyzer (Isotope Cube, Elementar, Hanau, Germany). Since all soil samples were strongly acidic (Turner et al., 2012a) and free of carbonate (verified by means of hydrochloric acid addition to finely ground mineral soil samples), measured total C concentration equals the organic C concentration. Stable isotope ratios were analyzed by coupled isotope ratio

mass spectrometry (IRMS) (Isoprime 100, Isoprime, Manchester, England). Results are given in delta notation as  $\delta^{13}\text{C}$  for C and  $\delta^{15}\text{N}$  for N stable isotopes in ‰: [Eq. 4.1]

$$[4.1] \quad \delta^{13}\text{C}, \delta^{15}\text{N} [\text{‰}] = \left[ \frac{R_{\text{sample}}}{R_{\text{standard}}} - 1 \right] \times 1000$$

, where R represents the  $^{13}\text{C}/^{12}\text{C}$  or the  $^{15}\text{N}/^{14}\text{N}$  ratio, respectively. We used IAEA-CH-3, IAEA-CH-6 and IAEA-600 for normalization of measured  $\delta^{13}\text{C}$  values [in ‰<sub>VPDB</sub>] and USGS25, IAEA-N-1 and IAEA-N-2 for normalization of measured  $\delta^{15}\text{N}$  values [in ‰<sub>Air</sub>]. Measurement precision of IRMS analyses based on routine measurements of interspersed samples per 15 samples of sulfanilic acid (Merck KGaA, Germany) during the measurement period was  $\pm 0.1\text{‰}$  ( $n = 53$ ) for  $\delta^{13}\text{C}$  and  $\pm 0.2\text{‰}$  ( $n = 52$ ) for  $\delta^{15}\text{N}$ . This analytical uncertainty was less than the expected natural variability. Mean difference of duplicate measurement for  $\delta^{13}\text{C}$  values ( $n = 112$ ) of the organic horizons and mineral soil samples was  $0.08\text{‰}$  and for  $\delta^{15}\text{N}$  values ( $n = 53$ )  $0.07\text{‰}$ .

#### 4.3.3.2 Calculations and statistical analysis

Linear regression analyses determined the patterns of isotopic changes within soil profiles. We regressed  $\log_{10}x$ -transformed element concentrations [ $\log_{10}(\text{g}\cdot\text{C}\cdot\text{kg}^{-1})$ ] or [ $\log_{10}(10^{-1}\text{g}\cdot\text{N}\cdot\text{kg}^{-1})$ ] (= x) and their according stable isotope values [ $\delta^{13}\text{C}$ ] or [ $\delta^{15}\text{N}$ ] (= y) of the depth intervals (organic layers and mineral soil) (Acton et al., 2013; Brunn et al., 2014; Garten, 2006). Different units for the logarithmized C and N concentrations resulted in positive values on the x-axis. The absolute values of the slopes were termed beta and referred to as  $\beta_{\text{C}}$  and  $\beta_{\text{N}}$ , respectively.

In addition to beta values, we used vertical isotopic differences to describe vertical changes in C ( $\Delta^{13}\text{C}$ ) and N stable isotopes ( $\Delta^{15}\text{N}$ ) from litter to mineral soil. There was spatial variation in the depth and thickness of soil horizons between dune stages, e.g. a soil horizon at 10 cm soil depth of a given location corresponds to a slightly deeper or shallower depth as compared to the neighboring sampling site. We tried to account for this by using maximum difference in profiles instead of the difference between the litter layer and mineral soil at 10 cm soil depth to best represent the vertical changes in  $\delta^{13}\text{C}$  and  $\delta^{15}\text{N}$  values. The difference between maximum  $\delta^{13}\text{C}_{\text{Max}}$  or  $\delta^{15}\text{N}_{\text{Max}}$  (isotopic signature of the mineral soil) and minimum values  $\delta^{13}\text{C}_{\text{Min}}$  or  $\delta^{15}\text{N}_{\text{Min}}$  (isotopic signature of the litter) of each profile was calculated using equation [4.2] for C and [4.3] for N values:

$$[4.2] \quad \Delta^{13}\text{C} = \delta^{13}\text{C}_{\text{Max}} - \delta^{13}\text{C}_{\text{Min}}$$

$$[4.3] \quad \Delta^{15}\text{N} = \delta^{15}\text{N}_{Max} - \delta^{15}\text{N}_{Min}$$

Linear regression analyses were used to quantify the impact of soil age on variables. We assessed trends across the overall chronosequence as well as in singles phases, i.e. the early phase (stages 0-2), the intermediate phase (stages 3-6) and the late phase (stages 7-10). Since these phases potentially do not cover the changes of variables with time in between these phases, we additionally provide two tables containing mean  $\pm$  SE values of variables in the supplemental material with results from one-way ANOVA post-hoc tests showing differences between the stages (Tab. S4.1 and Tab. S4.2). In case of homogeneous variances, we used a post-hoc Tukey test. In case of heteroscedasticity, a Games-Howell test was conducted. In addition to this we applied matched pairs t tests (in case of homogeneity of variances) or Welch's t tests (in case of heteroscedasticity) for the comparison of beta values, proportions of explained variations and  $\Delta^{13}\text{C}$  or  $\Delta^{15}\text{N}$  values. Autocorrelation of data was tested by the Durbin-Watson Test and reconciled with critical values for the Durbin-Watson Test provided by Savin and White (1977). Only non-autocorrelated data were evaluated. The level of significance was set to  $P \leq 0.05$  in all tests. Probability of fit to normal distribution was tested by Kolmogorov-Smirnov tests.

## 4.4 Results

### 4.4.1 Element concentrations, C: N ratios and isotopic signatures in litter, organic layer and mineral soil with proceeding pedogenesis

With increasing soil depth, average C concentration in OM decreased from  $338.2 \pm \text{SE } 41.4 \text{ g}\cdot\text{C}\cdot\text{kg}^{-1}$  in litter to  $21.9 \pm 1.2 \text{ g}\cdot\text{C}\cdot\text{kg}^{-1}$  in mineral soil, while  $\delta^{13}\text{C}$  values increased from  $-29.9 \pm 0.9\text{‰}_{\text{VPDB}}$  to  $-28.2 \pm 0.6\text{‰}$  (Fig. 4.1). Similarly, average N concentration decreased vertically from  $12.3 \pm 1.3 \text{ g}\cdot\text{N}\cdot\text{kg}^{-1}$  to  $1.3 \pm 0.1 \text{ g}\cdot\text{N}\cdot\text{kg}^{-1}$ , while  $\delta^{15}\text{N}$  values increased from  $-2.4 \pm 1.5\text{‰}_{\text{Air}}$  to  $3.2 \pm 2.7\text{‰}$  (Fig. 4.1). Litter and organic layer thickness (Oi, Oe and Oa horizon) increased with time across the chronosequence ( $P < 0.001$ ;  $r = 0.745$ ) with development of a distinguishable organic layer (Oe and Oa horizon) from stage 7 onwards. Mean thickness of the Oi, Oa and Oe layers until stage 6 was  $2.8 \pm 0.4 \text{ cm}$  while from stage 7 average thickness increased to  $22.1 \pm 3.0 \text{ cm}$ .



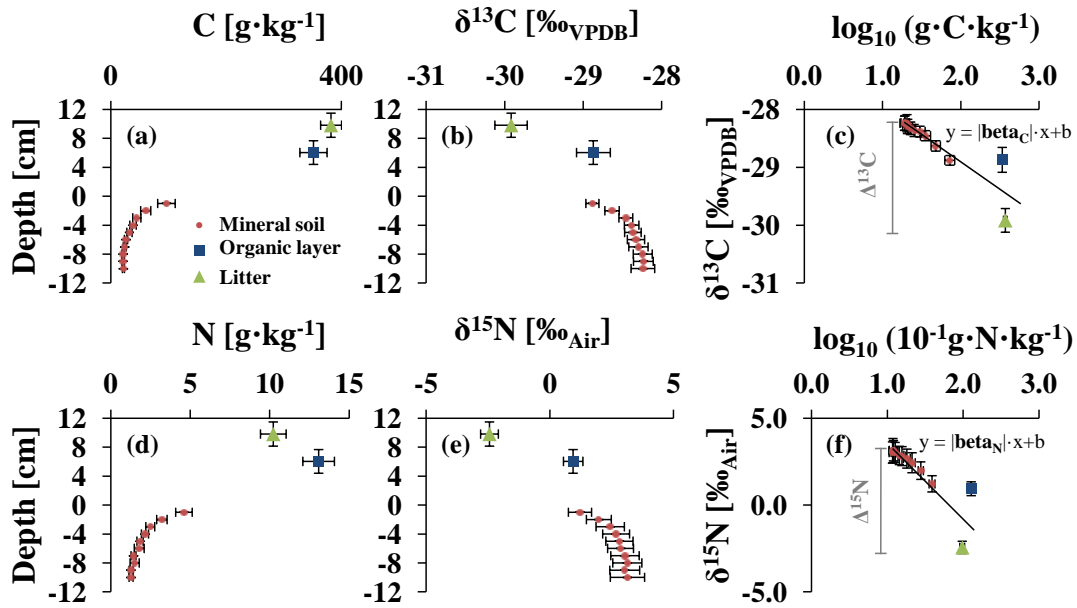


Figure 4.1 Mean  $\pm$  SE C (a) and N concentrations [g·kg<sup>-1</sup>] (d) and δ<sup>13</sup>C [‰<sub>VPDB</sub>] and (b) δ<sup>15</sup>N values [‰<sub>Air</sub>] (e) with depth [cm] across all dune stages ( $n = 11$ , except the organic layer:  $n = 4$ ) showing a vertical decrease in C and N concentrations and an increase in δ<sup>13</sup>C and δ<sup>15</sup>N values. Figures on the right represent relations between log<sub>10</sub> (g·C·kg<sup>-1</sup>) and δ<sup>13</sup>C values (c) or log<sub>10</sub> (10<sup>-1</sup>·g·N·kg<sup>-1</sup>) and δ<sup>15</sup>N values (f) of which beta values can be derived. Litter layer (Oi layer) values depicted as triangles ( $n = 11$ ), organic layers (Oe and Oa layer) as squares ( $n = 4$ ). Organic layers occur from stage 7 on (soil age > 1,300 yrs) and are not present in the stages before. Depths of litter and organic layers as mean  $\pm$  SE in cm. Error bars represent two standard errors.

Litter (Oi layer) C concentrations increased with time across the overall chronosequence ( $P < 0.001$ ;  $r = 0.594$ ), while N concentrations in litter decreased ( $P = 0.006$ ;  $r = -0.37$ ) and C: N ratios increased with time ( $P < 0.001$ ;  $r = 0.73$ ) (Fig. 4.2). Litter δ<sup>13</sup>C values ranged between -33.1‰ and -28.4‰ and significantly decreased by  $c. 2‰$  ( $P < 0.001$ ;  $r = -0.61$ ) across the chronosequence (Fig. 4.3a). δ<sup>15</sup>N values in litter varied in a much wider range between -4.8‰ and 1.3‰ but we could not find an overall trend across the chronosequence, rather two declines in litter δ<sup>15</sup>N values. The organic layer (Oe and Oa layer) was characterized by decreasing δ<sup>13</sup>C values ( $P = 0.024$ ;  $r = -0.60$ ) with time (Fig. 4.3a). In mineral soil, we found an overall increase in C: N ratios ( $P < 0.001$ ;  $r = 0.75$ ) and in δ<sup>15</sup>N values ( $P < 0.001$ ;  $r = 0.75$ ).

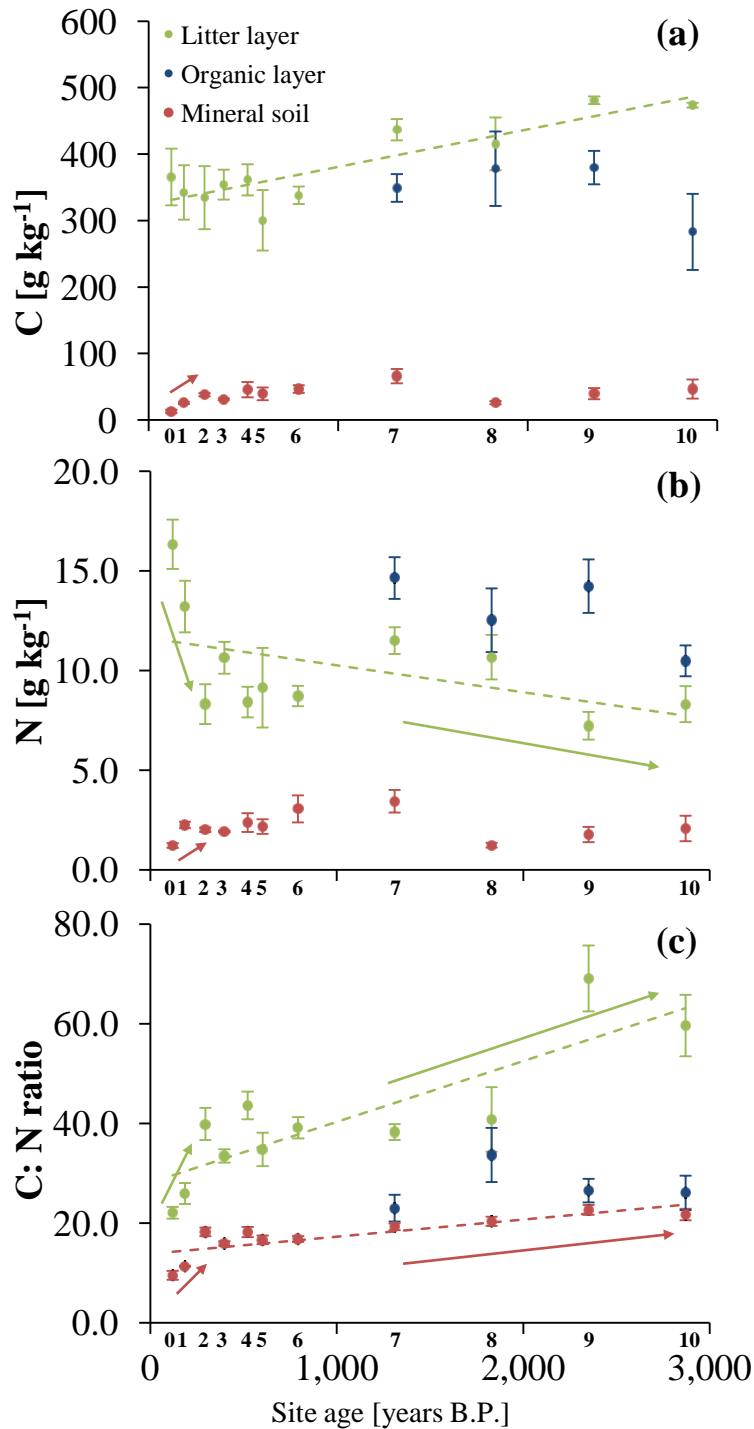


Figure 4.2 Mean  $\pm$  SE C (a) and N concentrations [g·kg<sup>-1</sup>] (b) and C: N ratios (c) in litter (Oi horizon), organic layers (Oe and Oa horizons) and mineral soil as functions of site age in years before present [yrs B.P.]. Dotted lines depict significant linear trends across the overall chronosequence, while arrows depict linear trends during the early (stages 0-2), the intermediate (stages 3-6) or the late (stages 7-10) phase of ecosystem development. Numbers at the *x* axis represent the dune stages referring to Tab. 4.1. Error bars are two standard errors and represent variation on one dune with *n* = 5.

We found significant linear changes with time in element concentrations, C: N ratios and isotopic signatures in litter and mineral soil during the early (stages 0-2) and the late

phase (stages 7-10), while the intermediate phase (stages 3-6) was lacking significant trends. Early ecosystem development was characterized by a strong increase in mineral soil C concentrations ( $P < 0.001$ ;  $r = 0.91$ ), a decrease in litter N concentrations ( $P < 0.001$ ;  $r = -0.81$ ) and an increase in mineral soil N concentrations ( $P = 0.038$ ;  $r = 0.54$ ), an increase in litter and mineral soil C: N ratios ( $P < 0.001$ ;  $r = 0.84$  and  $r = 0.91$ ) (Fig. 4.2) and decreasing  $\delta^{13}\text{C}$  ( $P = 0.016$ ;  $r = -0.61$ ) and  $\delta^{15}\text{N}$  values ( $P < 0.001$ ;  $r = -0.93$ ) (Fig. 4.3).

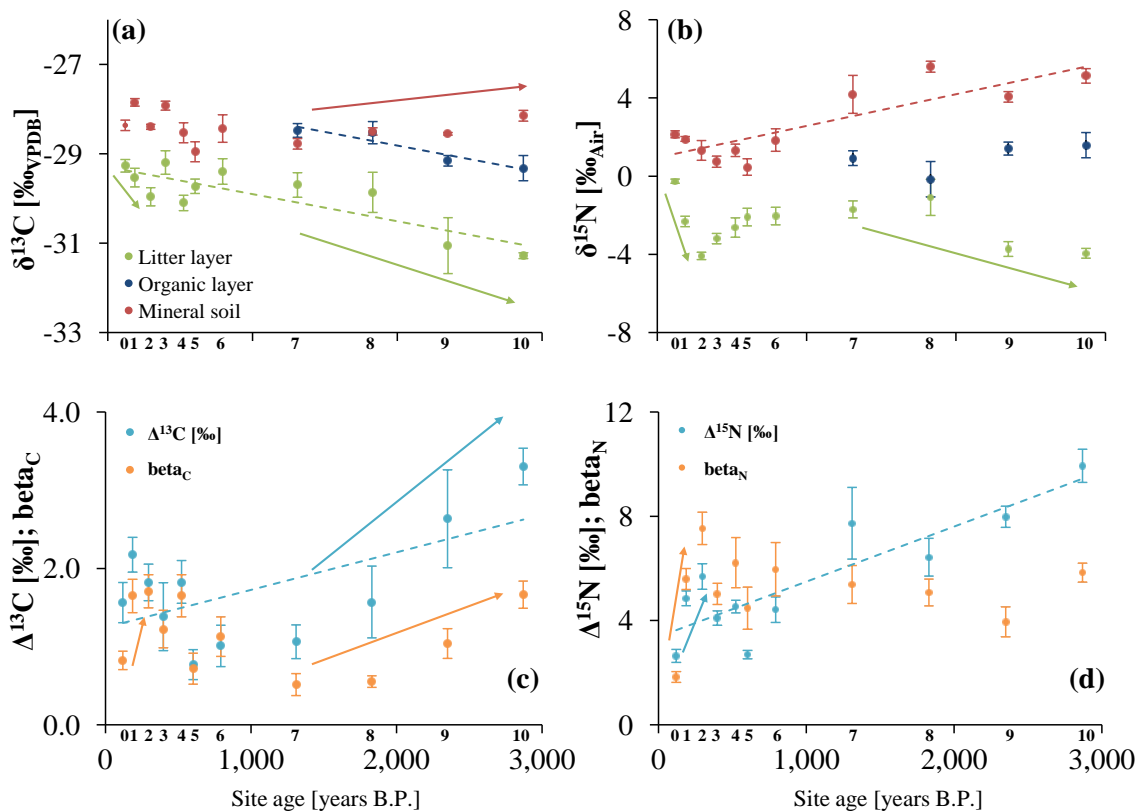


Figure 4.3 Mean  $\pm$  SE  $\delta^{13}\text{C}$  [‰<sub>VPDB</sub>] (a) and  $\delta^{15}\text{N}$  [‰<sub>Air</sub>] values (b) in the litter layer (Oi horizon), the organic layers (Oe and Oa horizons) and in the mineral soil. Maximum isotopic difference from litter to mineral soil in  $^{13}\text{C}$  (c) and  $^{15}\text{N}$  (d) is given as  $\Delta^{13}\text{C}$  and  $\Delta^{15}\text{N}$ .  $\text{Beta}_\text{C}$  (c) and  $\text{beta}_\text{N}$  (d) values represent absolute values of regression slopes between  $\log_{10}x$  element concentrations and isotopic signatures. All values as functions of site age in years before present [yrs B.P.]. Dotted lines depict significant linear trends across the overall chronosequence, while arrows depict linear trends during the early (stages 0-2), the intermediate (stages 3-6) or the late (stages 7-10) phase of ecosystem development. Numbers at the x-axis represent the dune stages referred to Tab. 4.1. Error bars are two standard errors and represent variation on one dune with  $n = 5$ .

During the late ecosystem development, we found similar trends in litter as compared to the early ecosystem development, i.e. a second decrease in litter N concentrations ( $P = 0.006$ ;  $r = -0.60$ ), an increase in litter C: N ratios ( $P = 0.005$ ;  $r = 0.60$ ) (Fig. 4.2) and

decreasing  $\delta^{13}\text{C}$  ( $P = 0.004$ ;  $r = -0.62$ ) and  $\delta^{15}\text{N}$  values ( $P = 0.003$ ;  $r = -0.63$ ) (Fig. 4.3) with time. Stages 4 to 8 featured mean  $\delta^{15}\text{N}$  values with  $-2.1 \pm 0.2\text{‰}$  but wide ranges in litter  $\delta^{15}\text{N}$  values, always with maximum values converging to the atmospheric signature (0‰). In addition, C: N ratios ( $P = 0.011$ ;  $r = 0.55$ ) and  $\delta^{13}\text{C}$  values ( $P = 0.003$ ;  $r = 0.64$ ) increased in mineral soil during the late phase.

#### 4.4.2 Vertical differences in $\delta^{13}\text{C}$ and $\delta^{15}\text{N}$ values and beta values with proceeding pedogenesis

We found a mean enrichment in  $^{13}\text{C}$  of  $\Delta^{13}\text{C} = 1.9 \pm 0.1\text{‰}$  and a three times greater enrichment in  $^{15}\text{N}$  of  $\Delta^{15}\text{N} = 6.0 \pm 0.3\text{‰}$  in profiles from litter to mineral soil. In 40% of the profiles, mineral soil C concentrations and  $\delta^{13}\text{C}$  values at 10 cm depth matched with the observed minimum C concentration and maximum  $\delta^{13}\text{C}$  values. In the other profiles ( $n = 32$ ), we found  $2.5 \pm 0.6 \text{ g}\cdot\text{kg}^{-1}$  higher C concentrations and  $0.2 \pm 0.3\text{‰}$  lower  $\delta^{13}\text{C}$  values in the mineral soil at 10 cm depth, corresponding to 11.4% and 0.7% variation, respectively. The variation was less pronounced for N concentrations. In 33% of the profiles ( $n = 18$ ), N concentrations were higher by  $0.2 \pm 0.0 \text{ g}\cdot\text{N}\cdot\text{kg}^{-1}$  as compared to minimum N, while in 70% of the profiles ( $n = 38$ )  $\delta^{15}\text{N}$  values in the mineral soil at 10 cm depth deviated by  $0.7 \pm 0.1\text{‰}$  from maximum  $\delta^{15}\text{N}$  values corresponding to 15.4% and 21.9% variation, respectively. In total, the vertical variation from a continuous C and N decrease and an isotopic enrichment of  $^{13}\text{C}$  and  $^{15}\text{N}$  was considered negligible.

Absolute values of linear regression slopes (=  $\beta_{\text{C}}$ ) between  $\log_{10}(\text{g}\cdot\text{C}\cdot\text{kg}^{-1})$  and according  $\delta^{13}\text{C}$  values served to describe vertical isotopic patterns with mean  $\beta_{\text{C}}$  value of  $1.2 \pm 0.1$ . Linear regressions were significant in 90% of the profiles ( $n = 51$ ). Non-significant regressions ( $P > 0.05$ ) were observed at sites 0B, 5B, 6D, 7E and 8D (Fig. S4.1). To omit bias,  $\beta_{\text{C}}$  values of these regressions were included in further analyses. Mean  $R^2$  was  $0.67 \pm 0.0$ . In 95% of the profiles ( $n = 52$ )  $\beta_{\text{N}}$  values resulted from significant linear regressions between  $\log_{10}(10^{-1}\text{g}\cdot\text{N}\cdot\text{kg}^{-1})$  and according  $\delta^{15}\text{N}$ . Non-significant regressions ( $P \geq 0.05$ ) were observed at sites 5B, 6A and 9B (Fig. S4.2). Mean  $\beta_{\text{N}}$  value was  $5.0 \pm 0.3$  with  $R^2 = 0.77 \pm 0.0$ . Residuals were normally distributed in either case both for regressions of C and N. Sites with a distinguishable accumulated organic layer (soil age  $\geq 1,300 \text{ yrs B.P.}$ ) featured a lower proportion of explained variation of 20%. Thus,  $R^2$  at sites with an accumulated organic layer (stages 0 to 6:  $R^2 = 0.75 \pm 0.0$ ; stages 7 to 10:  $R^2 = 0.54 \pm 0.0$ ) were significantly lower for relations be-

tween  $\log_{10}(\text{g}\cdot\text{C}\cdot\text{kg}^{-1})$  and  $\delta^{13}\text{C}$  values ( $P = 0.008$ ) and for relations between  $\log_{10}(10^1\text{g}\cdot\text{N}\cdot\text{kg}^{-1})$  and  $\delta^{15}\text{N}$  values (stages 0 to 6:  $R^2 = 0.83 \pm 0.0$ ; stages 7 to 10:  $R^2 = 0.54 \pm 0.0$ ) ( $P = 0.015$ ).

$\Delta^{13}\text{C}$  ( $P = 0.001$ ;  $r = 0.49$ ) and  $\Delta^{15}\text{N}$  ( $P < 0.001$ ;  $r = 0.77$ ) linearly increased with time across the overall chronosequence. In contrast,  $\text{beta}_{\text{C}}$  and  $\text{beta}_{\text{N}}$  values did not show significant linear trends (Fig. 4.3c and 4.3d). For every one per mill increase in  $^{13}\text{C}$ , OM increased by  $3.1 \pm 0.2\%$  in  $^{15}\text{N}$ .  $\text{Beta}_{\text{C}}$  and  $\Delta^{13}\text{C}$  values were significantly related ( $P < 0.001$ ;  $r = 0.65$ ), similarly to  $\text{beta}_{\text{N}}$  and  $\Delta^{15}\text{N}$  values ( $P = 0.007$ ;  $r = 0.36$ ). In addition,  $\Delta^{13}\text{C}$  and  $\Delta^{15}\text{N}$  were significantly related ( $P < 0.001$ ;  $r = 0.52$ ), similarly to  $\text{beta}_{\text{C}}$  and  $\text{beta}_{\text{N}}$  ( $P < 0.001$ ;  $r = 0.47$ ). During the early phase, we found increasing trends of  $\Delta^{15}\text{N}$  values ( $P < 0.001$ ;  $r = 0.81$ ),  $\text{beta}_{\text{C}}$  values ( $P = 0.018$ ;  $r = 0.60$ ) and  $\text{beta}_{\text{N}}$  values ( $P < 0.001$ ;  $r = 0.89$ ). Slight but not significantly higher  $\text{beta}_{\text{N}}$  values ( $5.0 \pm 0.4$ ) compared to  $\Delta^{15}\text{N}$  ( $4.1 \pm 0.2\%$ ) during the early and the intermediate phase disclose the deviation of vertical  $^{15}\text{N}$  enrichment with depth. Those effects were obscured by stronger impacts of litter and organic layers on the regression slopes at the later stages. We found no linear trends of isotopic differences and beta values during the intermediate phase. However,  $\Delta^{13}\text{C}$  was lowest in this phase of the chronosequence ( $1.2 \pm 0.2\%$ ) as compared to the early ( $1.9 \pm 0.1\%$ ) and the late phase ( $2.1 \pm 0.3\%$ ) ( $P < 0.025$ ). The late phase featured increasing  $\Delta^{13}\text{C}$  values ( $P < 0.001$ ;  $r = 0.72$ ) and increasing  $\text{beta}_{\text{C}}$  values ( $P < 0.001$ ;  $r = 0.79$ ). There were no linear trends of  $\Delta^{15}\text{N}$  values in the late phase, but these values were with mean  $\Delta^{15}\text{N}$  of  $8.0 \pm 0.5\%$  significantly higher at the late phase as compared to the early ( $4.4 \pm 0.4\%$ ) and the intermediate ( $3.9 \pm 0.2\%$ ) phase ( $P < 0.001$ ).

## 4.5 Discussion

### 4.5.1 $\delta^{13}\text{C}$ and $\delta^{15}\text{N}$ values in litter with proceeding pedogenesis

As a result of a possible morphological adaption to decreasing nutrient availability with time, we hypothesized that litter  $\delta^{13}\text{C}$  values increase with proceeding ecosystem development and pedogenesis. However, we observed a decrease in litter  $\delta^{13}\text{C}$  values with site age (Fig. 4.3a) which was contrary to findings across boreal chronosequences (Clemmensen et al., 2013; Hyodo et al., 2013; Hyodo and Wardle, 2009) and therefore falsifies our first hypothesis. The following parameters might be involved in explaining the decreased  $\delta^{13}\text{C}$  values of litter (i) soil respiration, (ii) irradiance, (iii) nutrient limita-

tion. At Haast, there is an increasing abundance of moss, understory species and seedlings with site age (Turner et al., 2012b) which utilize a greater proportion of  $^{13}\text{C}$  depleted  $\text{CO}_2$  respired from soil (Hyodo and Wardle, 2009) and are exposed to a lower irradiance which would both result in lower  $\delta^{13}\text{C}$  values in litter (Fotelli et al., 2003; Hyodo and Wardle, 2009) and could therefore induce a decrease in litter  $\delta^{13}\text{C}$  with time. On the other hand, root respired  $\text{CO}_2$  of woody species or of species associated with mycorrhiza was found to be  $^{13}\text{C}$  enriched (Ghashghaie and Badeck, 2014). Therefore, respiration impacts on plants remain indistinct and cannot clearly be related to changed litter  $\delta^{13}\text{C}$  values. Due to the close distance of the dunes (< 5 km), we exclude spatial variations in humidity, since the humid climate would not cause differences on stomatal conductance.

Nutrient limitation provides another explanation for lower litter  $\delta^{13}\text{C}$  values as it is shown by decreasing N concentrations of litter and increasing C: N ratios across the chronosequence (Fig. 4.2). Nutrient limitation promotes plant stress which could either force plants to adapt morphologically, resulting in increased  $\delta^{13}\text{C}$  values as it was found in boreal systems (Hyodo et al., 2013; Hyodo and Wardle, 2009), or nutrient limitation can induce increased stomatal conductivity and therefore a higher photosynthetic fractionation (Cernusak et al., 2013; Farquhar et al., 1989; Peltzer et al., 2010). Although P is typically thought to limit primary production on older surfaces (Vitousek and Farrington, 1997; Walker and Syers, 1976), we observed decreasing litter N concentrations and decreasing  $\delta^{13}\text{C}$  values, similar to results from other studies (Guehl et al. 1995; Vitousek et al. 1990). Thus, it is possible that nutrient limitation may have driven the depletion of  $^{13}\text{C}$  in litter. In contrast to findings across chronosequences in boreal ecosystems, decreasing  $\delta^{13}\text{C}$  values of litter suggest a physiological response rather than a morphological adaption to changes in nutrient dynamics in this temperate rainforest system.

Our second hypothesis assuming that litter  $\delta^{15}\text{N}$  values are close to the atmospheric signature due to the contribution of N via biological  $\text{N}_2$  fixation across the overall Haast chronosequence cannot be fully verified. The  $\delta^{15}\text{N}$  signature of litter suggests biological  $\text{N}_2$  fixation occurring in the early stages of ecosystem development with a decline at c. 300 yrs and a subsequent increase of  $\text{N}_2$  fixation again at stages 4-8, but at this time rather related to free-living than symbiotic pathways of  $\text{N}_2$  fixation. Immediately after dune formation, we found  $\delta^{15}\text{N}$  values in litter of  $-0.3 \pm 0.1\text{‰}$  (Fig. 4.3b). Atmospheric  $\text{N}_2$  fixing legumes, e.g. the visibly dominant species broom (*Cytisus Scoparius*) that

colonized the beachfront dune likely converged litter  $\delta^{15}\text{N}$  values to the atmospheric value and raised C and N concentrations in mineral soil in the following development (Fig. 4.2b). According to the visible abundance of legumes and litter  $\delta^{15}\text{N}$  values close to zero, biological  $\text{N}_2$  fixation appears to be important during ecosystem establishment at Haast which supports the outstanding role in N supply by biological  $\text{N}_2$  fixation during early succession (Menge and Hedin, 2009; Vitousek et al., 2013).

The subsequent decrease of litter  $\delta^{15}\text{N}$  values within the first *c.* 300 yrs of ecosystem development (Fig. 4.3b) suggests a reduced  $\text{N}_2$  fixation rate. Reduced  $\text{N}_2$  fixation during the early phase might be related to the growing overstory vegetation, since  $\text{N}_2$  fixers were found to be shade-intolerant (Vitousek et al., 2013) or to species replacement as it was found for a symbiotic  $\text{N}_2$  fixing plant at the Franz Josef chronosequence (Menge and Hedin, 2009). While it is accepted that a higher N availability reduces  $\text{N}_2$  fixation (DeLuca et al., 2008; Menge and Hedin, 2009), which could additionally well explain a reduction of  $\text{N}_2$  fixation, we found that N concentrations of litter decreased in the early phase, that rather argues for a reduced N availability. This decreased N availability during the early phase at Haast is linked with a decrease in litter  $\delta^{15}\text{N}$  values and therefore in line with literature data where positive relations between N availability and litter  $\delta^{15}\text{N}$  values were widely presented (Craine et al., 2015). In addition, different  $\text{N}_2$  fixation strategies (Menge et al., 2015; Reed et al., 2011) may exist at Haast and could be decoupled from N availability. However, reduced  $\text{N}_2$  fixation combined with reduced N availability raises the importance of other N nutrition forms to maintain N acquisition. Utilization of nitrate ( $\text{NO}_3^-$ ) (Templer et al., 2007) or N supply by mycorrhizal fungi (Hobbie et al., 1999; Hyodo et al., 2013) would both result in distinct depletion of  $^{15}\text{N}$  in litter. On the other hand, readily available mineral forms of N were found to induce a reduction of biological  $\text{N}_2$  fixation (Reed et al., 2011) calling for further studies on function, species composition and possible switch off of  $\text{N}_2$  fixers to clarify our findings.

Between stages 4 to 8 (*c.* 523 to *c.* 1,830 yrs),  $\delta^{15}\text{N}$  values of litter converging closer to zero suggest  $\text{N}_2$  fixation, while lower  $\delta^{15}\text{N}$  values of litter rather argue for a supply with other N forms, e.g. through fungi or mycorrhiza (Hobbie and Högberg, 2012). Dinitrogen fixation during the intermediate stages could confirm the activity of diazotrophic  $\text{N}_2$  fixers, since abundances of  $\text{N}_2$  fixing bacterial rRNA genes were observed at Haast (Jangid et al., 2013). In addition, the role of  $\text{N}_2$  fixing bryophytes and lichens colonizing the more diverse and tall habitats during the intermediate stages

could have been increased. Menge and Hedin (2009) proposed a possible decoupling of  $N_2$  fixation and N availability in soil, with these species possibly serving as a positive feedback to ecosystem N availability. Again, full documentation of  $N_2$  fixing species composition might clarify the functioning of biological  $N_2$  fixation at Haast. However, we assume that the intermediate phase featured mixed impacts of atmospheric  $N_2$  fixation, i.e. symbiotic and free living  $N_2$  fixation and supply with other recycled N forms, which might parallel the supposed heterogeneity associated with patches (Pickett and White, 1985).

During the late phase (stages 7-10), we found a decline in litter  $\delta^{15}N$  values (Fig. 4.3b) together with decreasing litter N concentrations and increasing C: N ratios (Fig. 4.2), similarly to the early phase. In the same manner, greater N availability as reduction of  $N_2$  fixation could be excluded. Increasing mycorrhizal abundance with supply of  $^{15}N$  depleted N,  $^{15}N$  depleted N provided by litter decomposition (Menge et al., 2011) or a potential decrease of  $N_2$  fixation under increasing P limitation (Vitousek and Howarth, 1991) might serve as alternative explanations for decreasing  $\delta^{15}N$  values of litter.

In summary,  $\delta^{15}N$  values of litter converged to the atmospheric isotopic signature in the early succession and in the intermediate stages. However, under several conditions, e.g. changes in species composition, structural changes of the canopy or as a result of increasing P limitation,  $N_2$  fixation seems to be replaced by other N nutrition forms and appeared to be not constantly dominant across the Haast chronosequence.

#### 4.5.2 Vertical patterns of $\delta^{13}C$ values with proceeding pedogenesis

Thirdly, we hypothesized a continuous decrease in decomposition with time. However,  $\beta_{aC}$  values as approximation of decomposition (Acton et al., 2013; Brunn et al., 2014; Diochon and Kellman, 2008; Garten, 2006; Guillaume et al., 2015; Marty et al., 2015) increased during early ecosystem development and at old sites, while they were lowest at the intermediate stages (1,500 yrs) which falsifies our third hypothesis. Vertical  $\delta^{13}C$  patterns described by  $\beta_{aC}$  values ( $1.2 \pm 0.1$ ) and  $\Delta^{13}C$  ( $1.9 \pm 0.1\text{‰}$ ) were at the lower end of data reported in the literature (Brunn et al., 2014; Garten, 2006; Guillaume et al., 2015; Powers and Schlesinger, 2002). This was possibly affected by the coarse soil texture at Haast that has been shown to influence isotope fractionation on mineral soil  $\delta^{13}C$  values (Bird et al., 2003). Low vertical enrichment in  $^{13}C$  might be exacerbated with root removal during our sample preparation. In systems where fungi



are abundant, root removal could increase the amount of fungal remains (Hobbie and Ouimette, 2009). Since fungi are  $^{13}\text{C}$  depleted (Kohl et al., 2015) their contribution could lower  $\delta^{13}\text{C}$  values in mineral soil samples and therefore the isotopic difference between litter and mineral soil OM. Impacts of a continuous decrease of atmospheric  $\delta^{13}\text{CO}_2$  by 1.5‰ during the last two centuries (Francey et al., 1999; Keeling et al., 2005) might explain the observed average vertical change in  $\delta^{13}\text{C}$ . However, this Suess effect would result in  $\Delta^{13}\text{C}$  values distinctly lower than 1.5‰ at the youngest site (<120 yrs) that contained no C before its formation. In addition, the Suess effect lacks in explaining variations in  $\Delta^{13}\text{C}$  between dune stages > 300 yrs, i.e. the atmospheric change as single driver of  $\delta^{13}\text{C}$  depth profiles would result in more constant  $\Delta^{13}\text{C}$  values. Together with findings from other studies (Acton et al., 2013; Guillaume et al., 2015), we infer that the Suess effect alone is not able to fully explain the vertical enrichment of  $^{13}\text{C}$  in OM in soil profiles.

Increasing  $\text{beta}_\text{C}$  values during the early phase of ecosystem development (Fig. 4.3c) suggest enhanced decomposition, probably stimulated through plant communities containing low abundances of woody species (Turner et al., 2012b). At stage 7 and 8, we observed lowest  $\text{beta}_\text{C}$  values (Fig. 4.3c & Tab. S4.2). First generation trees collapsed after stage 6 and a distinguishable organic layer started to accumulate from stage 7 on (Tab. 4.1). Fungi preferably colonize the organic horizon below the fresh litter layer (Lindahl et al., 2007) and the accumulated organic layer could therefore promote fungal colonization. Fungi and mycorrhiza are supposed to reduce decomposition rates (Clemmensen et al., 2015; Gadgil and Gadgil, 1971; Langley and Hungate, 2003) and could lower  $\text{beta}_\text{C}$  values. Low  $\text{beta}_\text{C}$  values were associated with relatively low  $\delta^{13}\text{C}$  values in mineral soil (Tab. S4.1 & Fig. 4.3a) probably governed by decreased microbial cycling and therefore a lower accumulation of  $^{13}\text{C}$  enriched microbial products. In addition, Kramer et al. (2003) observed no vertical trends in  $\delta^{13}\text{C}$  if OM is recycled from the structurally and chemically altered organic layer.

While we can mechanistically explain a possible reduction in decomposition rates from early to the intermediate stages, we lack an explanation for the increase of  $\text{beta}_\text{C}$  values at the later stages. Stimulated decomposition probably owing to a reduced canopy closure after the collapse of first generation trees likely lowered organic layer thickness at stage 10 as compared to stages 8 and 9 (Tab. 4.1). However, increasing decomposition is against our third hypothesis that decomposition declines constantly across the chronosequence according to the retrogressive model (Peltzer et al., 2010). And in-

creasing decomposition contradicts the reduced N concentrations in litter attributed to a lower N availability (Fig. 4.2). This implies that the later stages do not belong to the retrogressive phase and could be better described as transition time characterized by an elevated decomposition, e.g. related to canopy opening. Higher decomposition results in elevated  $^{13}\text{C}$  enriched decomposition products (Billings and Richter, 2006) and together with a shift to slightly finer soil texture (Turner et al., 2012a) that facilitate a better sorption capacity of enriched microbial products (Bird et al., 2003), higher decomposition results in increased  $\delta^{13}\text{C}$  values in mineral soil at the late stages. Alternatively,  $\text{beta}_\text{C}$  values could be insufficient to describe decomposition at sites with an accumulated organic layer. Including the organic layer (Oe and Oa layer) with high C concentrations but strong  $^{13}\text{C}$  enrichment (Fig. 4.1) into linear regressions between  $\log_{10}(\text{g}\cdot\text{C}\cdot\text{kg}^{-1})$  and  $\delta^{13}\text{C}$  values results in less steep regression lines, visible in diverging  $\Delta^{13}\text{C}$  and  $\text{beta}_\text{C}$  values as soils age (Fig. 4.3c). Lower  $\delta^{13}\text{C}$  values of litter at later stages might suggest that litter layers control the vertical isotopic gradients. In dependence of a decomposition continuum from less decomposed litter to more decomposed OM in the mineral soil (Melillo et al., 1989),  $\delta^{13}\text{C}$  values of litter form part of the vertical patterns in isotopic enrichment and should therefore not control vertical isotopic gradients. This decomposition continuum can be underpinned by manganese (Mn) concentrations in litter (unpublished data). Manganese concentrations in litter were found to be positively related to litter decomposition (Berg et al., 2007; Keiluweit et al., 2015). Significant linear relations between litter Mn concentrations and  $\text{beta}_\text{C}$  values at Haast ( $r = 0.41$ ;  $P = 0.002$ ) suggest the applicability for beta values as an indicator of decomposition. However, the falsification of our third hypothesis merits further detailed studies of the quality of  $\text{beta}_\text{C}$  values and the interplay between the accumulation of an organic layer, decomposition rates, and the translocation of organic compounds to deeper spodic horizons (not considered in our study) at older sites.

#### 4.5.3 Vertical patterns in $\delta^{15}\text{N}$ values with proceeding pedogenesis

Our fourth hypothesis was that differences between  $\delta^{15}\text{N}$  values of litter and mineral soil OM increase with time resulting in increasing  $\text{beta}_\text{N}$  values. Average  $\text{beta}_\text{N}$  ( $5.0 \pm 0.3$ ) and  $\Delta^{15}\text{N}$  values ( $6.0 \pm 0.4\text{‰}$ ) were in line with literature data reviewed by Hobbie and Ouimette (2009). The wide range of observed data ( $\text{beta}_\text{N}$  between 1.3 and 9.3;  $\Delta^{15}\text{N}$  between 1.7‰ and 13.0‰) suggests a diversity of dominant fractionation processes.

es across the chronosequence, e.g. mineralization in soil (Dijkstra et al., 2006) or changes in mycorrhizal fungal association (Hobbie and Ouimette, 2009).  $\delta^{15}\text{N}$  values in soil as one component of the difference between litter and soil increased continuously with proceeding dune age (Fig. 4.3). This might be caused by “stripping”: During mineralization, the dynamic exchange of microbially derived hydrophilic and plant derived hydrophobic OM and subsequent continuous stripping throughout the soil profile (Kusliene et al., 2015). This concept relies on the most abundant forms of transported N, being dissolved organic N (DON) combined with  $\text{NH}_4^+$  in unpolluted areas (Perakis and Hedin, 2002). Since  $\text{NH}_4^+$  and microbial biomass are enriched in  $^{15}\text{N}$  (Dijkstra et al., 2006; Templer et al., 2007), the mixing of microbial vs. plant derived OM result in stripping of charged OM that is retained in soil, whereas non-charged compounds will be transported downwards. This stripping is controlled by sorption sites and thus, soil texture. In our chronosequence, the shift to soils with slightly finer textures (Turner et al., 2012a) together with increased aggregate formation and stabilization by fungal hyphae (Rillig et al., 2015) might feature greater sorption capacity through organo-mineral-complexes with increased site age and therefore probably amplify the  $\delta^{15}\text{N}$  increase in mineral soil with time.

If combined with litter  $\delta^{15}\text{N}$  values, during early succession,  $\Delta^{15}\text{N}$  and  $\text{beta}_\text{N}$  values strongly increased, supporting the assumption of fungal colonization in this time owing to fractionation against  $^{15}\text{N}$  and thus,  $^{15}\text{N}$ -depleted N transferred to plants. As a result, low  $\delta^{15}\text{N}$  values of litter further increase the difference between litter and mineral soil and thus, also vertical patterns. In addition, microbial recycling of OM originating from the structurally and compositionally altered organic layer rather than from fresh litter (Kramer et al., 2003) or greater proportions of  $^{15}\text{N}$ -enriched fungal remains (Hobbie and Högberg, 2012) could explain elevated  $\delta^{15}\text{N}$  values in mineral soil from stage 7 on. In line, arbuscular mycorrhiza that were host specific for kamahi (*Weinmannia racemosa*) at the nearby Franz-Josef chronosequence (Martinez-Garcia et al., 2015) could also be dominant at Haast, where kamahi regenerates in tree-fall gaps (Turner et al., 2012b). However, mean isotopic enrichment during the late phase ( $\Delta^{15}\text{N}$ ) of  $8.0 \pm 0.5\text{‰}$  was greater than gradients observed in AM-dominated systems (Hobbie and Ouimette, 2009). At stage 10, we observed an isotopic enrichment ( $\Delta^{15}\text{N}$ ) of  $9.9 \pm 0.6\text{‰}$  that is in line with  $^{15}\text{N}$  enrichment found in EM-dominated systems (Hobbie and Ouimette, 2009). Thus, the increasing abundance of ectomycorrhizal Silver beech (*Nothofagus*

*menziesii*) (Turner et al., 2012b) might also explain elevated mineral soil  $\delta^{15}\text{N}$  values at the late stages.

The contribution of denitrification to the enrichment of  $^{15}\text{N}$  in soils, as it has been widely observed (Craine et al., 2015; Houlton and Bai, 2009; Houlton et al., 2006) was found to not occur or being not expressed at the nearby Franz Josef chronosequence (Menge et al., 2011). Although waterlogging was excluded at Haast (Turner et al., 2012a), we are unable to exclude impacts on gaseous N losses on isotopic signatures in soil profiles that may also account for greater  $\delta^{15}\text{N}$  values in mineral soil and therefore to more distinct depth profiles. However, a possible increase of  $\delta^{15}\text{N}$  values in mineral soil induced by denitrification contradicts the decrease of  $\delta^{15}\text{N}$  values of litter during the late phase (Fig. 4.3).

Analogous to relations between  $\beta_{\text{C}}$  and  $\Delta^{13}\text{C}$ , we found  $\beta_{\text{N}}$  and  $\Delta^{15}\text{N}$  values diverging as soils aged (Fig. 4.3d). Similarly, the accumulated organic layer seems to contribute to this trend, i.e. including the organic layer, containing even higher N concentrations but being strongly  $^{15}\text{N}$  enriched compared to the litter layer (Fig. 4.1), into linear regressions between  $\log_{10}(10^{-1}\text{g}\cdot\text{N}\cdot\text{kg}^{-1})$  and  $\delta^{15}\text{N}$  values results in less steep regression lines. Our fourth hypothesis that  $\beta_{\text{N}}$  values increase with site age cannot fully be verified, since only  $\Delta^{15}\text{N}$  increased across the chronosequence but not  $\beta_{\text{N}}$  values, probably indicating that despite effects of mycorrhizal fractionation other processes affect  $\delta^{15}\text{N}$  depth profiles during ecosystem development and pedogenesis.

## 4.6 Conclusion

The findings of this study provided new information on C and N dynamics occurring during *c.* 2,870 yrs of soil and ecosystem development across the temperate rainforest Haast dune chronosequence. In contrast to findings across boreal chronosequences, we found  $\delta^{13}\text{C}$  values in litter decreasing with time, probably indicating a physiological rather than a morphological adaptation to changes in nutrient dynamics. Litter  $\delta^{15}\text{N}$  values suggested  $\text{N}_2$  fixation that might be attributable to the activity of diazotrophs identified at Haast. However, other N nutrition forms, e.g. utilization of  $\text{NO}_3^-$  or N supply by mycorrhizal fungi likely contributed to two declines in litter  $\delta^{15}\text{N}$  values, one in the early phase (between 120 and 296 yrs) and a second decline in the late phase (between 1,300 and 2,870 yrs). Against our hypothesis, decomposition (approximated with linear regression slopes between  $\log_{10}(\text{g}\cdot\text{C}\cdot\text{kg}^{-1})$  and  $\delta^{13}\text{C}$  values) did not constantly decrease

with time. Instead, we found an increase of decomposition at the beginning of ecosystem development and a second increase in the late phase. Lowest decomposition during the intermediate phase matched with the accumulation of the organic layer. Increasing decomposition during the late phase might indicate dynamics linked with canopy opening after the collapse of first generation trees. While we have indications that  $\delta^{15}\text{N}$  depth profiles are related to mycorrhizal fractionation as it is reported in the literature, additional processes might affect  $\delta^{15}\text{N}$  depth profiles during ecosystem development. Interestingly, we found relations between  $\beta_{\text{C}}$  and  $\beta_{\text{N}}$  values, similarly to  $\Delta^{13}\text{C}$  and  $\Delta^{15}\text{N}$ , suggesting that there might be shared processes shaping  $\delta^{13}\text{C}$  and  $\delta^{15}\text{N}$  depth profiles, e.g. microbial cycling, transport or sorption. However, further manipulative experiments and measurements of different  $\text{N}_2$  fixation pathways are needed to underpin the assumed mechanisms and causal connections, particularly the role of mycorrhizal associations and forms of  $\text{N}_2$  fixation, vertical transport and sorption processes and the functioning of the organic layer.

#### 4.7 Acknowledgment

We thank G. Guggenberger, L. Sauheitl and S. Bokeloh (Leibniz University Hannover, Germany) for providing isotopic analysis, U. Bange, M. Kraft and A. Bell (University of Koblenz-Landau, Germany) for laboratory assistance, A. Torkey and N. Franks (Lincoln University, New Zealand) for organizing the sample transport and W. Wilcke (Karlsruhe Institute of Technology, Germany) and F. Brunn (University of Mainz, Germany) for facilitating this work. We gratefully acknowledge research funding by the German Academic Exchange Service (DAAD Grant D/12/45516).

#### 4.8 Literature

- Acton P, Fox J, Campbell E, Rowe H, Wilkinson M (2013) Carbon isotopes for estimating soil decomposition and physical mixing in well-drained forest soils. *Journal of Geophysical Research-Biogeosciences* 118(4): 1532-1545
- Andrews M, James EK, Sprent JI, Boddey RM, Gross E, dos Reis FB (2011) Nitrogen fixation in legumes and actinorhizal plants in natural ecosystems: values obtained using N-15 natural abundance. *Plant Ecol. Divers.* 4(2-3): 131-140
- Berg B, Steffen KT, McLaugherty C (2007) Litter decomposition rate is dependent on litter Mn concentrations. *Biogeochemistry* 82(1): 29-39
- Billings SA, Richter DD (2006) Changes in stable isotopic signatures of soil nitrogen and carbon during 40 years of forest development. *Oecologia* 148(2): 325-333

- Bird M, Kracht O, Derrien D, Zhou Y (2003) The effect of soil texture and roots on the stable carbon isotope composition of soil organic carbon. *Australian Journal of Soil Research* 41(1): 77-94
- Brunn M, Spielvogel S, Sauer T, Oelmann Y (2014) Temperature and precipitation effects on delta C-13 depth profiles in SOM under temperate beech forests. *Geoderma* 235: 146-153
- Cernusak LA, Ubierna N, Winter K, Holtum JAM, Marshall JD, Farquhar GD (2013) Environmental and physiological determinants of carbon isotope discrimination in terrestrial plants. *New Phytol.* 200(4): 950-965
- Clemmensen KE, Bahr A, Ovaskainen O, Dahlberg A, Ekblad A, Wallander H, Stenlid J, Finlay RD, Wardle DA, Lindahl BD (2013) Roots and Associated Fungi Drive Long-Term Carbon Sequestration in Boreal Forest. *Science* 339(6127): 1615-1618
- Clemmensen KE, Finlay RD, Dahlberg A, Stenlid J, Wardle DA, Lindahl BD (2015) Carbon sequestration is related to mycorrhizal fungal community shifts during long-term succession in boreal forests. *New Phytol.* 205(4): 1525-1536
- Craine JM, Brookshire ENJ, Cramer MD, Hasselquist NJ, Koba K, Marin-Spiotta E, Wang LX (2015) Ecological interpretations of nitrogen isotope ratios of terrestrial plants and soils. *Plant Soil* 396(1-2): 1-26
- DeLuca TH, Zackrisson O, Gundale MJ, Nilsson MC (2008) Ecosystem feedbacks and nitrogen fixation in boreal forests. *Science* 320(5880): 1181-1181
- Dickie IA, Martinez-Garcia LB, Koele N, Grelet GA, Tylianakis JM, Peltzer DA, Richardson SJ (2013) Mycorrhizas and mycorrhizal fungal communities throughout ecosystem development. *Plant Soil* 367(1-2): 11-39
- Dijkstra P, Ishizu A, Doucet R, Hart SC, Schwartz E, Menyailo OV, Hungate BA (2006) C-13 and N-15 natural abundance of the soil microbial biomass. *Soil Biol. Biochem.* 38(11): 3257-3266
- Diochon A, Kellman L (2008) Natural abundance measurements of (13)C indicate increased deep soil carbon mineralization after forest disturbance. *Geophys. Res. Lett.* 35(14): 1-5
- Eger A, Almond PC, Condron LM (2011) Pedogenesis, soil mass balance, phosphorus dynamics and vegetation communities across a Holocene soil chronosequence in a super-humid climate, South Westland, New Zealand. *Geoderma* 163(3-4): 185-196
- Farquhar GD, Ehleringer JR, Hubick KT (1989) Carbon isotope discrimination and photosynthesis. *Annu. Rev. Plant Physiol. Plant Molec. Biol.* 40: 503-537
- Fotelli MN, Rennenberg H, Holst T, Mayer H, Gessler A (2003) Carbon isotope composition of various tissues of beech (*Fagus sylvatica*) regeneration is indicative of recent environmental conditions within the forest understorey. *New Phytol.* 159(1): 229-244
- Francey RJ, Allison CE, Etheridge DM, Trudinger CM, Enting IG, Leuenberger M, Langenfelds RL, Michel E, Steele LP (1999) A 1000-year high precision record of delta C-13 in atmospheric CO<sub>2</sub>. *Tellus Series B-Chemical and Physical Meteorology* 51(2): 170-193
- Gadgil RL, Gadgil PD (1971) Mycorrhiza and litter decomposition. *Nature* 233(5315): 133-+
- Galloway JN, Dentener FJ, Capone DG, Boyer EW, Howarth RW, Seitzinger SP, Asner GP, Cleveland CC, Green PA, Holland EA, Karl DM, Michaels AF, Porter JH, Townsend AR, Vorosmarty CJ (2004) Nitrogen cycles: past, present, and future. *Biogeochemistry* 70(2): 153-226
- Garten CT (2006) Relationships among forest soil C isotopic composition, partitioning, and turnover times. *Canadian Journal of Forest Research-Revue Canadienne De Recherche Forestiere* 36(9): 2157-2167
- Garten CT, Iversen CM, Norby RJ (2011) Litterfall N-15 abundance indicates declining soil nitrogen availability in a free-air CO<sub>2</sub> enrichment experiment. *Ecology* 92(1): 133-139
- Ghashghaie J, Badeck FW (2014) Opposite carbon isotope discrimination during dark respiration in leaves versus roots - a review. *New Phytol.* 201(3): 751-769
- Guehl JM, Fort C, Ferhi A (1995) Differential response of leaf conductance, carbon isotope discrimination and water-use efficiency to nitrogen deficiency in maritime pine and pedunculate oak plants. *New Phytol.* 131(2): 149-157
- Guillaume T, Damris M, Kuzyakov Y (2015) Losses of soil carbon by converting tropical forest to plantations: erosion and decomposition estimated by delta C-13. *Glob. Change Biol.* 21(9): 3548-3560
- Hobbie EA, Högberg P (2012) Nitrogen isotopes link mycorrhizal fungi and plants to nitrogen dynamics. *New Phytol.* 196(2): 367-382
- Hobbie EA, Macko SA, Shugart HH (1999) Insights into nitrogen and carbon dynamics of ectomycorrhizal and saprotrophic fungi from isotopic evidence. *Oecologia* 118(3): 353-360
- Hobbie EA, Ouimette AP (2009) Controls of nitrogen isotope patterns in soil profiles. *Biogeochemistry* 95(2-3): 355-371
- Högberg P (1997) Tansley review No 95 - N-15 natural abundance in soil-plant systems. *New Phytol.* 137(2): 179-203

- Houlton BZ, Bai E (2009) Imprint of denitrifying bacteria on the global terrestrial biosphere. *Proc. Natl. Acad. Sci. U. S. A.* 106(51): 21713-21716
- Houlton BZ, Sigman DM, Hedin LO (2006) Isotopic evidence for large gaseous nitrogen losses from tropical rainforests. *Proc. Natl. Acad. Sci. U. S. A.* 103(23): 8745-8750
- Hyodo F, Kusaka S, Wardle DA, Nilsson MC (2013) Changes in stable nitrogen and carbon isotope ratios of plants and soil across a boreal forest fire chronosequence. *Plant Soil* 367(1-2): 111-119
- Hyodo F, Wardle DA (2009) Effect of ecosystem retrogression on stable nitrogen and carbon isotopes of plants, soils and consumer organisms in boreal forest islands. *Rapid Commun. Mass Spectrom.* 23(13): 1892-1898
- Jangid K, Whitman WB, Condrón LM, Turner BL, Williams MA (2013) Progressive and retrogressive ecosystem development coincide with soil bacterial community change in a dune system under lowland temperate rainforest in New Zealand. *Plant Soil* 367(1-2): 235-247
- Jones AR, Sanderman J, Allen D, Dalal R, Schmidt S (2015) Subtropical giant podzol chronosequence reveals that soil carbon stabilisation is not governed by litter quality. *Biogeochemistry* 124(1-3): 205-217
- Keeling CD, Piper SC, Bacastow RB, Wahlen M, Whorf TP, Heimann M, Meijer HA (2005) Atmospheric CO<sub>2</sub> and (CO<sub>2</sub>)-C-13 exchange with the terrestrial biosphere and oceans from 1978 to 2000: Observations and carbon cycle implications. In: Ehleringer JR, Cerling TE & Dearing MD (eds) *Ecological Studies: Analysis and Synthesis*. Springer, 233 Spring Street, New York, NY 10013, United States. p 83-113
- Keiluweit M, Nico P, Harmon ME, Mao JD, Pett-Ridge J, Kleber M (2015) Long-term litter decomposition controlled by manganese redox cycling. *Proc. Natl. Acad. Sci. U. S. A.* 112(38): E5253-E5260
- Kohl L, Laganier J, Edwards KA, Billings SA, Morrill PL, Van Biesen G, Ziegler SE (2015) Distinct fungal and bacterial delta C-13 signatures as potential drivers of increasing delta C-13 of soil organic matter with depth. *Biogeochemistry* 124(1-3): 13-26
- Körner C, Diemer M (1987) In situ photosynthetic responses to light, temperature and carbon dioxide in herbaceous plants from low and high altitude. *Functional Ecology* 1(3): 179-194
- Kramer MG, Sollins P, Sletten RS, Swart PK (2003) N isotope fractionation and measures of organic matter alteration during decomposition. *Ecology* 84(8): 2021-2025
- Krull ES, Bestland EA, Gates WP (2002) Soil organic matter decomposition and turnover in a tropical Ultisol: Evidence from delta C-13, delta N-15 and geochemistry. *Radiocarbon* 44(1): 93-112
- Kusliene G, Eriksen J, Rasmussen J (2015) Leaching of dissolved organic and inorganic nitrogen from legume-based grasslands. *Biol. Fertil. Soils* 51(2): 217-230
- Langley JA, Hungate BA (2003) Mycorrhizal controls on belowground litter quality. *Ecology* 84(9): 2302-2312
- Lerch TZ, Nunan N, Dignac MF, Chenu C, Mariotti A (2011) Variations in microbial isotopic fractionation during soil organic matter decomposition. *Biogeochemistry* 106(1): 5-21
- Lindahl BD, Ihrmark K, Boberg J, Trumbore SE, Hogberg P, Stenlid J, Finlay RD (2007) Spatial separation of litter decomposition and mycorrhizal nitrogen uptake in a boreal forest. *New Phytol.* 173(3): 611-620
- Martinelli LA, Piccolo MC, Townsend AR, Vitousek PM, Cuevas E, McDowell W, Robertson GP, Santos OC, Treseder K (1999) Nitrogen stable isotopic composition of leaves and soil: Tropical versus temperate forests. *Biogeochemistry* 46(1-3): 45-65
- Martinez-García LB, Richardson SJ, Tylianakis JM, Peltzer DA, Dickie IA (2015) Host identity is a dominant driver of mycorrhizal fungal community composition during ecosystem development. *New Phytol.* 205(4): 1565-1576
- Marty C, Houle D, Gagnon C (2015) Effect of the Relative Abundance of Conifers Versus Hardwoods on Soil delta C-13 Enrichment with Soil Depth in Eastern Canadian forests. *Ecosystems* 18(4): 629-642
- Melillo JM, Aber JD, Linkins AE, Ricca A, Fry B, Nadelhoffer KJ (1989) Carbon and nitrogen dynamics along the decay continuum - plant litter to soil organic-matter. *Plant Soil* 115(2): 189-198
- Menge DNL, Baisden WT, Richardson SJ, Peltzer DA, Barbour MM (2011) Declining foliar and litter delta 15N diverge from soil, epiphyte and input delta 15N along a 120 000 yr temperate rainforest chronosequence. *New Phytol.* 190(4): 941-952
- Menge DNL, Hedin LO (2009) Nitrogen fixation in different biogeochemical niches along a 120 000-year chronosequence in New Zealand. *Ecology* 90(8): 2190-2201
- Menge DNL, Wolf AA, Funk JL (2015) Diversity of nitrogen fixation strategies in Mediterranean legumes. *Nat. Plants* 1(6): 1-5
- Nadelhoffer KF, Fry B (1988) Controls on natural N-15 and C-13 abundances in forest soil organic-matter. *Soil Sci. Soc. Am. J.* 52(6): 1633-1640

- Peltzer DA, Wardle DA, Allison VJ, Baisden WT, Bardgett RD, Chadwick OA, Condrón LM, Parfitt RL, Porder S, Richardson SJ, Turner BL, Vitousek PM, Walker J, Walker LR (2010) Understanding ecosystem retrogression. *Ecol. Monogr.* 80(4): 509-529
- Perakis SS, Hedin LO (2002) Nitrogen loss from unpolluted South American forests mainly via dissolved organic compounds. *Nature* 415(6870): 416-419
- Pickett STA, White PS (1985) *The Ecology of Natural Disturbance and Patch Dynamics*. Academic Press. Orlando, Fla.: 472 pp
- Powers JS, Schlesinger WH (2002) Geographic and vertical patterns of stable carbon isotopes in tropical rain forest soils of Costa Rica. *Geoderma* 109(1-2): 141-160
- Reed SC, Cleveland CC, Townsend AR (2011) Functional Ecology of Free-Living Nitrogen Fixation: A Contemporary Perspective. In: Futuyama DJ, Shaffer HB & Simberloff D (eds) *Annual Review of Ecology, Evolution, and Systematics*, Vol 42. *Annual Review of Ecology Evolution and Systematics*. Annual Reviews, Palo Alto. p 489-512
- Rillig MC, Aguilar-Trigueros CA, Bergmann J, Verbruggen E, Veresoglou SD, Lehmann A (2015) Plant root and mycorrhizal fungal traits for understanding soil aggregation. *New Phytol.* 205(4): 1385-1388
- Savin NE, White KJ (1977) Durbin-Watson Test for serial -correlation with extreme sample sizes or many regressors. *Econometrica* 45(8): 1989-1996
- Schmidt MWI, Torn MS, Abiven S, Dittmar T, Guggenberger G, Janssens IA, Kleber M, Kögel-Knabner I, Lehmann J, Manning DAC, Nannipieri P, Rasse DP, Weiner S, Trumbore SE (2011) Persistence of soil organic matter as an ecosystem property. *Nature* 478(7367): 49-56
- Stockmann U, Adams MA, Crawford JW, Field DJ, Henakaarchchi N, Jenkins M, Minasny B, McBratney AB, de Courcelles VD, Singh K, Wheeler I, Abbott L, Angers DA, Baldock J, Bird M, Brookes PC, Chenu C, Jastrow JD, Lal R, Lehmann J, O'Donnell AG, Parton WJ, Whitehead D, Zimmermann M (2013) The knowns, known unknowns and unknowns of sequestration of soil organic carbon. *Agriculture Ecosystems & Environment* 164: 80-99
- Templer PH, Arthur MA, Lovett GM, Weathers KC (2007) Plant and soil natural abundance delta N-15: indicators of relative rates of nitrogen cycling in temperate forest ecosystems. *Oecologia* 153(2): 399-406
- Turner BL, Condrón LM, Wells A, Andersen KM (2012a) Soil nutrient dynamics during podzol development under lowland temperate rain forest in New Zealand. *Catena* 97: 50-62
- Turner BL, Wells A, Andersen KM, Condrón LM (2012b) Patterns of tree community composition along a coastal dune chronosequence in lowland temperate rain forest in New Zealand. *Plant Ecol.* 213(10): 1525-1541
- Turner BL, Wells A, Condrón LM (2014) Soil organic phosphorus transformations along a coastal dune chronosequence under New Zealand temperate rain forest. *Biogeochemistry* 121(3): 595-611
- Unkovich M (2013) Isotope discrimination provides new insight into biological nitrogen fixation. *New Phytol.* 198(3): 643-646
- Vitousek P (2004) *Nutrient cycling and limitation: Hawai'i as a model system*. Princeton University Press, Princeton
- Vitousek PM, Farrington H (1997) Nutrient limitation and soil development: Experimental test of a biogeochemical theory. *Biogeochemistry* 37(1): 63-75
- Vitousek PM, Field CB, Matson PA (1990) Variation in foliar  $\delta^{13}\text{C}$  in Hawaiian *Metrosideros polymorpha*: a case of internal resistance? *Oecologia* 84(3): 362-370
- Vitousek PM, Howarth RW (1991) Nitrogen limitation on land and in the sea: How it can occur? *Biogeochemistry* 13(2): 87-115
- Vitousek PM, Menge DNL, Reed SC, Cleveland CC (2013) Biological nitrogen fixation: rates, patterns and ecological controls in terrestrial ecosystems. *Philosophical transactions of the Royal Society of London. Series B, Biological sciences* 368(1621): 20130119
- Walker TW, Syers JK (1976) The fate of phosphorus during pedogenesis. *Geoderma* 15(1): 1-19
- Wallander H, Morth CM, Giesler R (2009) Increasing abundance of soil fungi is a driver for N-15 enrichment in soil profiles along a chronosequence undergoing isostatic rebound in northern Sweden. *Oecologia* 160(1): 87-96
- Wardle DA, Walker LR, Bardgett RD (2004) Ecosystem properties and forest decline in contrasting long-term chronosequences. *Science* 305(5683): 509-513
- Wells A, Goff J (2007) Coastal dunes in Westland, New Zealand, provide a record of paleoseismic activity on the Alpine fault. *Geology* 35(8): 731-734



4.9 Supplementary material

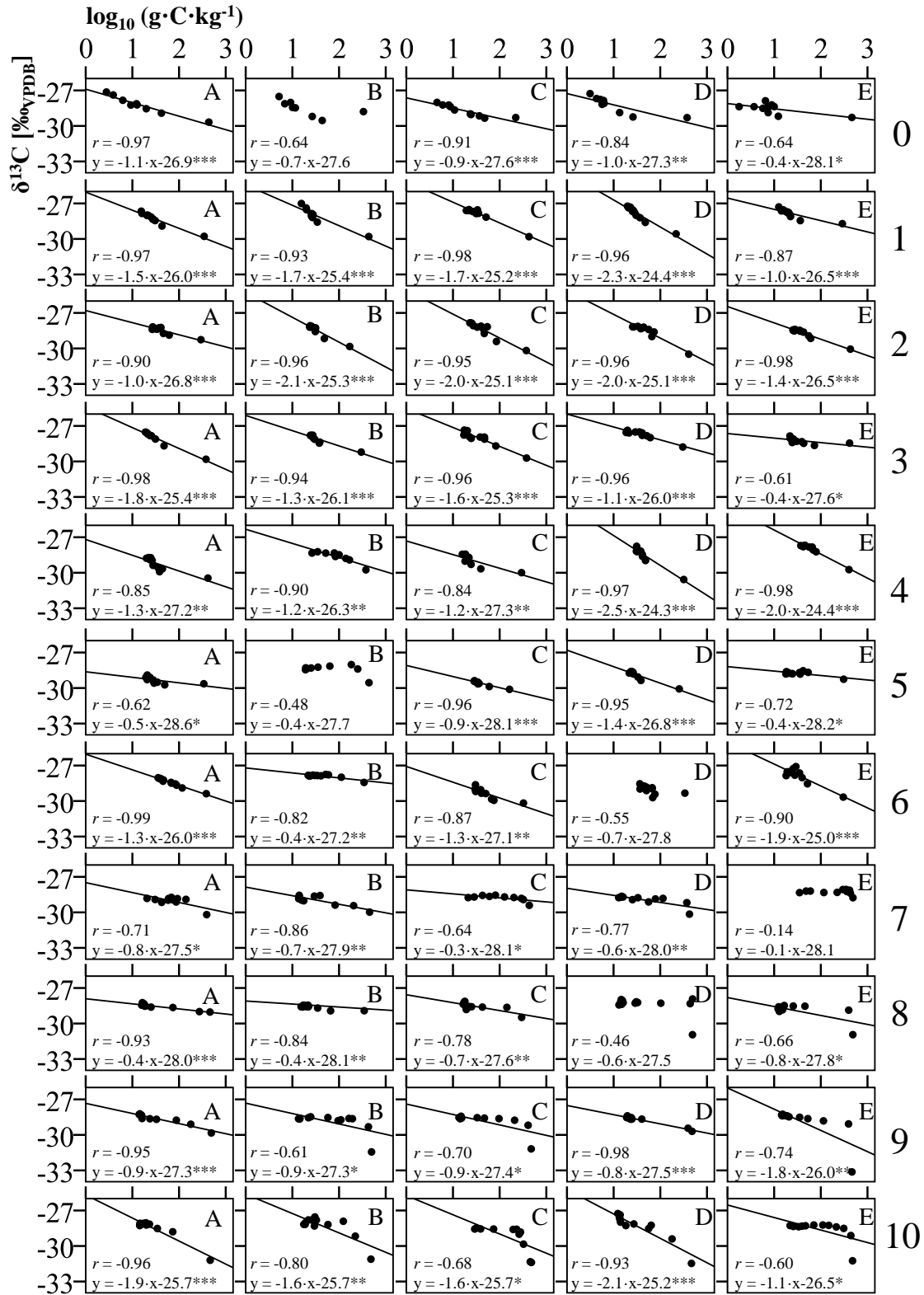


Figure S4.1 Linear regressions between logarithmized carbon concentrations  $\log_{10}(\text{g}\cdot\text{C}\cdot\text{kg}^{-1})$  and corresponding  $\delta^{13}\text{C}$  values [ $\text{‰VPDB}$ ] for dune stages (0-10) with five replicates each (A-E) and linear regression lines including regression equation. No regression lines at sites with insignificant linear regressions. \*,  $P < 0.05$ ; \*\*,  $P < 0.01$ ; \*\*\*,  $P < 0.001$ .

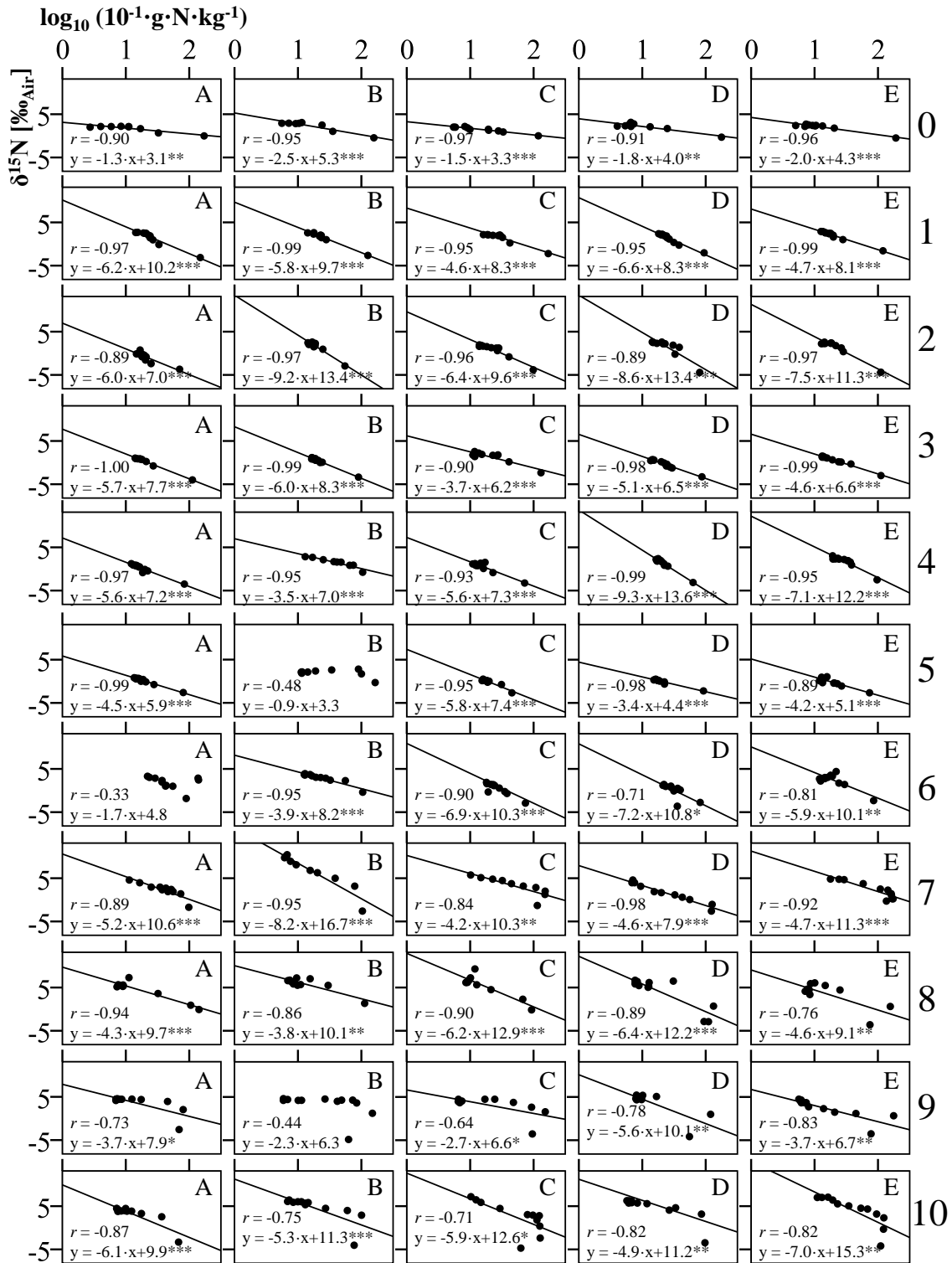


Figure S4.2 Linear regressions between logarithmized nitrogen concentrations  $\log_{10}(10^{-1} \cdot \text{g} \cdot \text{N} \cdot \text{kg}^{-1})$  and corresponding  $\delta^{15}\text{N}$  values [ $\text{‰}_{\text{Air}}$ ] for dune stages (0-10) with five replicates each (A-E) and linear regression lines including regression equation. No regression lines at sites with insignificant linear regressions.

\*,  $P < 0.05$ ; \*\*,  $P < 0.01$ ; \*\*\*,  $P < 0.001$ .

Table S4.1 Mean  $\pm$  SE element concentrations and isotopic signatures in litter (Oi layer), organic layers (Oe and Oa layer) and in mineral soil of dune stages. Letters represent significant differences between dune stages. In case of homogeneous variances we used a post-hoc Tukey test. In case of heteroscedasticity, a Games-Howell test was conducted.  $P \leq 0.05$ ;  $n = 5$

Pool	Dune stage	C [g·kg <sup>-1</sup> ]	N [g·kg <sup>-1</sup> ]	C: N ratio	$\delta^{13}\text{C}$ [‰ <sub>VPDB</sub> ]	$\delta^{15}\text{N}$ [‰ <sub>Air</sub> ]
Litter	0	365.5 $\pm$ 42.5 abc	16.3 $\pm$ 1.2 a	22.1 $\pm$ 1.2 c	-29.3 $\pm$ 0.1 a	-0.3 $\pm$ 0.1 a
	1	342.4 $\pm$ 41.0 abc	13.2 $\pm$ 1.3 ab	25.9 $\pm$ 2.1 bc	-29.5 $\pm$ 0.2 a	-2.3 $\pm$ 0.3 b
	2	334.5 $\pm$ 47.2 abc	8.3 $\pm$ 1.0 bc	39.9 $\pm$ 3.2 ab	-30.0 $\pm$ 0.2 a	-3.8 $\pm$ 0.3 bc
	3	354.0 $\pm$ 22.6 ab	10.6 $\pm$ 0.8 bc	33.5 $\pm$ 1.3 ab	-29.2 $\pm$ 0.3 a	-3.2 $\pm$ 0.3 bc
	4	361.1 $\pm$ 23.5 abc	8.4 $\pm$ 0.8 bc	43.6 $\pm$ 2.8 a	-30.1 $\pm$ 0.2 a	-2.6 $\pm$ 0.5 abc
	5	300.5 $\pm$ 45.6 abc	9.1 $\pm$ 2.0 bc	34.8 $\pm$ 3.4 abc	-29.7 $\pm$ 0.2 a	-2.1 $\pm$ 0.5 abc
	6	338.1 $\pm$ 13.3 c	8.7 $\pm$ 0.5 bc	39.1 $\pm$ 2.2 a	-29.4 $\pm$ 0.3 a	-2.0 $\pm$ 0.5 abc
	7	436.7 $\pm$ 16.1 ab	11.5 $\pm$ 0.7 abc	38.2 $\pm$ 1.6 a	-29.7 $\pm$ 0.3 a	-1.7 $\pm$ 0.4 abc
	8	415.5 $\pm$ 39.8 abc	10.7 $\pm$ 1.1 bc	40.8 $\pm$ 6.5 abc	-29.9 $\pm$ 0.5 ab	-1.1 $\pm$ 0.9 abc
	9	481.0 $\pm$ 5.8 a	7.2 $\pm$ 0.7 c	69.1 $\pm$ 6.6 a	-31.1 $\pm$ 0.6 ab	-3.7 $\pm$ 0.4 bc
Organic layer	10	473.7 $\pm$ 3.8 ab	8.3 $\pm$ 0.9 bc	59.6 $\pm$ 6.2 a	-31.3 $\pm$ 0.1 b	-3.9 $\pm$ 0.3 c
	7	349.0 $\pm$ 20.8 a	14.6 $\pm$ 1.0 a	24.1 $\pm$ 2.7 a	-28.7 $\pm$ 0.3 a	0.5 $\pm$ 0.8 a
	8	377.9 $\pm$ 56.1 a	12.5 $\pm$ 1.6 a	31.0 $\pm$ 5.4 a	-28.7 $\pm$ 0.3 a	0.1 $\pm$ 0.6 a
	9	379.8 $\pm$ 25.2 a	14.2 $\pm$ 1.3 a	27.0 $\pm$ 2.4 a	-29.2 $\pm$ 0.1 a	1.2 $\pm$ 0.3 a
Mineral soil	10	283.1 $\pm$ 57.2 a	10.5 $\pm$ 0.8 a	26.2 $\pm$ 3.4 a	-29.3 $\pm$ 0.1 a	1.8 $\pm$ 0.8 a
	0	12.9 $\pm$ 2.2 b	1.2 $\pm$ 0.1 bc	9.6 $\pm$ 0.9 d	-28.4 $\pm$ 0.1 abc	2.2 $\pm$ 0.2 bc
	1	25.7 $\pm$ 1.8 a	2.2 $\pm$ 0.2 a	11.3 $\pm$ 0.1 d	-27.8 $\pm$ 0.1 a	1.9 $\pm$ 0.1 c
	2	37.7 $\pm$ 2.4 a	2.0 $\pm$ 0.1 a	18.2 $\pm$ 0.9 bc	-28.4 $\pm$ 0.1 bc	1.3 $\pm$ 0.5 c
	3	31.1 $\pm$ 1.4 a	1.9 $\pm$ 0.0 a	15.8 $\pm$ 0.5 c	-27.9 $\pm$ 0.1 ab	0.7 $\pm$ 0.3 c
	4	45.5 $\pm$ 11.4 ab	2.4 $\pm$ 0.5 ab	18.3 $\pm$ 1.0 bc	-28.5 $\pm$ 0.2 abc	1.3 $\pm$ 0.3 c
	5	39.1 $\pm$ 9.6 ab	2.2 $\pm$ 0.4 ab	16.7 $\pm$ 0.9 bc	-28.9 $\pm$ 0.2 abc	0.5 $\pm$ 0.4 c
	6	46.5 $\pm$ 5.7 a	3.1 $\pm$ 0.7 ab	16.8 $\pm$ 0.6 bc	-28.4 $\pm$ 0.3 abc	1.8 $\pm$ 0.6 c
	7	65.9 $\pm$ 10.6 ab	3.4 $\pm$ 0.6 ab	19.1 $\pm$ 0.7 abc	-28.7 $\pm$ 0.1 c	4.2 $\pm$ 1.0 ab
	8	25.9 $\pm$ 2.5 ab	1.2 $\pm$ 0.1 b	20.3 $\pm$ 0.9 ab	-28.5 $\pm$ 0.1 c	5.7 $\pm$ 0.3 a
9	39.4 $\pm$ 8.3 ab	1.8 $\pm$ 0.4 ab	22.6 $\pm$ 1.0 a	-28.5 $\pm$ 0.0 c	4.1 $\pm$ 0.3 ab	
10	46.4 $\pm$ 14.4 ab	2.1 $\pm$ 0.6 ab	22.3 $\pm$ 1.1 a	-28.2 $\pm$ 0.1 abc	5.3 $\pm$ 0.4 a	

Table S4.2 Mean  $\pm$  SE beta values and maximum isotopic difference as  $\Delta^{13}\text{C}$  or  $\Delta^{15}\text{N}$  in soil profiles of dune stages. Letters represent significant differences between dune stages. In case of homogeneous variances we used a post-hoc Tukey test. In case of heteroscedasticity, a Games-Howell test was conducted.  $P \leq 0.05$ ;  $n = 5$ .

Dune stage	betaC	beta <sub>N</sub>	$\Delta^{13}\text{C}$ [‰ <sub>VPDB</sub> ]	$\Delta^{15}\text{N}$ [‰ <sub>Air</sub> ]
<b>0</b>	0.8 $\pm$ 0.1 abc	1.8 $\pm$ 0.2 c	1.6 $\pm$ 0.3 bc	2.6 $\pm$ 0.2 d
<b>1</b>	1.6 $\pm$ 0.2 ab	5.6 $\pm$ 0.4 ab	2.2 $\pm$ 0.2 abc	4.9 $\pm$ 0.3 c
<b>2</b>	1.7 $\pm$ 0.2 a	7.5 $\pm$ 0.6 a	1.8 $\pm$ 0.2 abc	5.7 $\pm$ 0.5 bc
<b>3</b>	1.2 $\pm$ 0.2 abc	5.0 $\pm$ 0.4 ab	1.4 $\pm$ 0.4 bc	4.1 $\pm$ 0.3 bcd
<b>4</b>	1.6 $\pm$ 0.3 ab	6.2 $\pm$ 1.0 ab	1.8 $\pm$ 0.3 abc	4.5 $\pm$ 0.2 bc
<b>5</b>	0.7 $\pm$ 0.2 bc	3.8 $\pm$ 0.8 bc	0.8 $\pm$ 0.2 c	2.7 $\pm$ 0.2 d
<b>6</b>	1.1 $\pm$ 0.3 abc	5.1 $\pm$ 1.0 ab	1.0 $\pm$ 0.3 c	4.4 $\pm$ 0.5 bcd
<b>7</b>	0.5 $\pm$ 0.1 c	5.4 $\pm$ 0.7 ab	1.1 $\pm$ 0.2 bc	7.7 $\pm$ 1.4 abcd
<b>8</b>	0.6 $\pm$ 0.1 c	5.1 $\pm$ 0.5 ab	1.6 $\pm$ 0.5 bc	6.4 $\pm$ 0.7 abcd
<b>9</b>	1.0 $\pm$ 0.2 abc	3.6 $\pm$ 0.6 bc	2.6 $\pm$ 0.6 ab	8.0 $\pm$ 0.4 ab
<b>10</b>	1.7 $\pm$ 0.2 a	5.8 $\pm$ 0.4 ab	3.3 $\pm$ 0.2 a	9.9 $\pm$ 0.6 a

